Volume 25, Number 1, 2025 ISSN 1562-8353

NONLINEAR DYNAMICS AND SYSTEMS THEORY
An International Journal of Research and Surveys

Volume 25 Number 1 2025

CONTENTS

The Dynamics and Stability of Prey -Predator Model of Migration with Holling Type -III Response Function and Interspecific Competition for Prey 1
Syamsul Agus, Syamsuddin Toaha, Kasbawati and Khaeruddin

Φ-Hilfer Proportional Fractional Differential System: Uniqueness and Stability Result 13
Ahmad Alhabahbeh, Ma'mon Abu Hammad, Oualid Zentar, Mohamed Ziane, Shameseddin Alshorm and Ali Ateiwi

Simulation of Tsunami Wave Propagation Using the Finite Difference Method for Disaster Early Warning System 27
Ahmad Zaenal Arifin, Sriwulan, Marita Ika Joesidawati, Teguh Herlambang, Saeful Mizan and Andik Adi Suryanto

On Neumann Systems with Singularity Applied in Quenching Phenomena in Museilack Spaces.....37
A. Elouardani, A. Aberqi and M. Elmassoudi

Existence and Uniqueness of Solution for Stochastic Nonlocal Random Functional Integral Equation 53
A. Ferrag, A. Aoufi and M. Tadjine

Estimation of Amphibious Aircraft Trajectory Using Particle Filter and Square Root Ensemble Kalman Filter 59
T. Herlambang, Syamsuar, R.S. Marianto, N.I. Gutami, H. Arof, F.S. Puriningsih, A. Roschyntawati, H. Hendrato, M. Muhammad, I. Ansori, Y.F. Kusuma and K. Oktafiant

Study of the Existence of Extremal Solutions for Differential Inclusions with Nonlocal Integral Boundary Conditions 68
Y. Khouni and M. Denche

General Stability Result for a Nonlinear Viscoelastic Wave Equation With Boundary Dissipation 78
B. Madjour and A. Boudiaf

Efficient Descent Direction of a Conjugate Gradient Algorithm for Nonlinear Optimization.....91
Mohamed Lamine Ouaoua and Samia Khelladi

Theoretical and Numerical Results for Nonlinear Optimization Problems 101
C. Souli and A. Leulmi

© 2025, InforMath Publishing Group ISSN 1562-8353 Printed in Ukraine
To receive contents and abstracts by e-mail, visit our Website at: **http://www.e-ndst.kiev.ua**

NONLINEAR DYNAMICS & SYSTEMS THEORY
Volume 25, No. 1, 2025

Nonlinear Dynamics and Systems Theory

An International Journal of Research and Surveys

EDITOR-IN-CHIEF A.A.MARTYNYUK
S.P.Timoshenko Institute of Mechanics
National Academy of Sciences of Ukraine, Kiev, Ukraine

MANAGING EDITOR I.P.STAVROULAKIS
Department of Mathematics, University of Ioannina, Greece

REGIONAL EDITORS

S.G. GEORGIEV, Paris, France
A.OKNIŃSKI, Kielce, Poland
Europe

M.BOHNER, Rolla, USA
HAO WANG, Edmonton, Canada
USA and Canada

T.A.BURTON, Port Angeles, USA
C.CRUZ-HERNANDEZ, Ensenada, Mexico
Central and South America

M.ALQURAN, Irbid, Jordan
Jordan and Middle East

T.HERLAMBANG, Surabaya, Indonesia
Indonesia and New Zealand

InforMath Publishing Group
http://www.e-ndst.kiev.ua

Nonlinear Dynamics and Systems Theory
An International Journal of Research and Surveys

EDITOR-IN-CHIEF A.A.MARTYNYUK
The S.P. Timoshenko Institute of Mechanics, National Academy of Sciences of Ukraine,
Nesterov Str. 3, 03057, Kyiv-57, UKRAINE / e-mail: journalndst@gmail.com

MANAGING EDITOR I.P.STAVROULAKIS
Department of Mathematics, University of Ioannina
451 10 Ioannina, HELLAS (GREECE) / e-mail: ipstav@cc.uoi.gr

ADVISORY EDITOR A.G.MAZKO,
Institute of Mathematics of NAS of Ukraine, Kiev (Ukraine)
e-mail: mazko@imath.kiev.ua

REGIONAL EDITORS
S.G. GEORGIEV, France, e-mail: svetlingeorgiev1@gmail.com
A. OKNINSKI, Poland, e-mail: fizao@tu.kielce.pl
M. BOHNER, USA, e-mail: bohner@mst.edu
HAO WANG, Edmonton, Canada, e-mail: hao8@ualberta.ca
T.A. BURTON, USA, e-mail: taburton@olypen.com
C. CRUZ-HERNANDEZ, Mexico, e-mail: ccruz@cicese.mx
M. ALQURAN, Jordan, e-mail: marwan04@just.edu.jo
T. HERLAMBANG, Indonesia, e-mail: teguh@unusa.ac.id

EDITORIAL BOARD

Adzkiya, D. (Indonesia)
Artstein, Z. (Israel)
Awrejcewicz, J. (Poland)
Braiek, N. B. (Tunisia)
Chen Ye-Hwa (USA)
De Angelis, M. (Italy)
Denton, Z. (USA)
Djemai, M. (France)
Dshalalow, J. H. (USA)
Gajic Z. (USA)
Georgiou, G. (Cyprus)
Honglei Xu (Australia)
Jafari, H. (South African Republic)
Khusainov, D. Ya. (Ukraine)
Kloeden, P. (Germany)
Kokologiannaki, C. (Greece)
Kouzou A. (Algeria)
Krishnan, E. V. (Oman)
Kryzhevich, S. (Poland)
Limarchenko, O. S. (Ukraine)
Lopez Gutierrez R. M. (Mexico)
Lozi, R. (France)
Peterson, A. (USA)
Radziszewski, B. (Poland)
Shi Yan (Japan)
Sivasundaram, S. (USA)
Staicu V. (Portugal)
Vatsala, A. (USA)

ADVISORY COMPUTER SCIENCE EDITORS
A.N.CHERNIENKO and A.S.KHOROSHUN, Kiev, Ukraine

ADVISORY LINGUISTIC EDITOR
S.N.RASSHYVALOVA, Kiev, Ukraine

© 2025, InforMath Publishing Group, ISSN 1562-8353 print, ISSN 1813-7385 online, Printed in Ukraine
No part of this Journal may be reproduced or transmitted in any form or by any means without permission from InforMath Publishing Group.

INSTRUCTIONS FOR CONTRIBUTORS

(1) General. Nonlinear Dynamics and Systems Theory (ND&ST) is an international journal devoted to publishing peer-refereed, high quality, original papers, brief notes and review articles focusing on nonlinear dynamics and systems theory and their practical applications in engineering, physical and life sciences. Submission of a manuscript is a representation that the submission has been approved by all of the authors and by the institution where the work was carried out. It also represents that the manuscript has not been previously published, has not been copyrighted, is not being submitted for publication elsewhere, and that the authors have agreed that the copyright in the article shall be assigned exclusively to InforMath Publishing Group by signing a transfer of copyright form. Before submission, the authors should visit the website:

http://www.e-ndst.kiev.ua

for information on the preparation of accepted manuscripts. Please download the archive Sample_NDST.zip containing example of article file (you can edit only the file Samplefilename.tex).

(2) Manuscript and Correspondence. Manuscripts should be in English and must meet common standards of usage and grammar. To submit a paper, send by e-mail a file in PDF format directly to

Professor A.A. Martynyuk, Institute of Mechanics,
Nesterov str.3, 03057, Kiev-57, Ukraine
e-mail: journalndst@gmail.com

or to one of the Regional Editors or to a member of the Editorial Board. Final version of the manuscript must typeset using LaTex program which is prepared in accordance with the style file of the Journal. Manuscript texts should contain the title of the article, name(s) of the author(s) and complete affiliations. Each article requires an abstract not exceeding 150 words. Formulas and citations should not be included in the abstract. AMS subject classifications and key words must be included in all accepted papers. Each article requires a running head (abbreviated form of the title) of no more than 30 characters. The sizes for regular papers, survey articles, brief notes, letters to editors and book reviews are: (i) 10-14 pages for regular papers, (ii) up to 24 pages for survey articles, and (iii) 2-3 pages for brief notes, letters to the editor and book reviews.

(3) Tables, Graphs and Illustrations. Each figure must be of a quality suitable for direct reproduction and must include a caption. Drawings should include all relevant details and should be drawn professionally in black ink on plain white drawing paper. In addition to a hard copy of the artwork, it is necessary to attach the electronic file of the artwork (preferably in PCX format).

(4) References. Each entry must be cited in the text by author(s) and number or by number alone. All references should be listed in their alphabetic order. Use please the following style:

Journal: [1] H. Poincare, Title of the article. *Title of the Journal* **volume** (issue) (year) pages. [Language]

Book: [2] A.M. Lyapunov, *Title of the Book.* Name of the Publishers, Town, year.

Proceeding: [3] R. Bellman, Title of the article. In: *Title of the Book.* (Eds.). Name of the Publishers, Town, year, pages. [Language]

(5) Proofs and Sample Copy. Proofs sent to authors should be returned to the Editorial Office with corrections within three days after receipt. The corresponding author will receive a sample copy of the issue of the Journal for which his/her paper is published.

(6) Editorial Policy. Every submission will undergo a stringent peer review process. An editor will be assigned to handle the review process of the paper. He/she will secure at least two reviewers' reports. The decision on acceptance, rejection or acceptance subject to revision will be made based on these reviewers' reports and the editor's own reading of the paper.

NONLINEAR DYNAMICS AND SYSTEMS THEORY
An International Journal of Research and Surveys
Published by InforMath Publishing Group since 2001

Volume 25 Number 1 2025

CONTENTS

The Dynamics and Stability of Prey-Predator Model of Migration with Holling Type-III Response Function and Interspecific Competition for Prey 1
Syamsul Agus, Syamsuddin Toaha, Kasbawati and Khaeruddin

Φ-Hilfer Proportional Fractional Differential System: Uniqueness and Stability Result 13
Ahmad Alhabahbeh, Ma'mon Abu Hammad, Oualid Zentar, Mohamed Ziane, Shameseddin Alshorm and Ali Ateiwi

Simulation of Tsunami Wave Propagation Using the Finite Difference Method for Disaster Early Warning System 27
Ahmad Zaenal Arifin, Sriwulan, Marita Ika Joesidawati, Teguh Herlambang, Saeful Mizan and Andik Adi Suryanto

On Neumann Systems with Singularity Applied in Quenching Phenomena in Museilack Spaces 37
A. Elouardani, A. Aberqi and M. Elmassoudi

Existence and Uniqueness of Solution for Stochastic Nonlocal Random Functional Integral Equation 53
A. Ferrag, A. Aoufi and M. Tadjine

Estimation of Amphibious Aircraft Trajectory Using Particle Filter and Square Root Ensemble Kalman Filter 59
T. Herlambang, Syamsuar, R.S. Marianto, N.I. Gutami, H. Arof, F.S. Puriningsih, A. Roschyntawati, H. Hendrato, M. Muhammad, I. Ansori, Y.F. Kusuma and K. Oktafiant

Study of the Existence of Extremal Solutions for Differential Inclusions with Nonlocal Integral Boundary Conditions 68
Y. Khouni and M. Denche

General Stability Result for a Nonlinear Viscoelastic Wave Equation With Boundary Dissipation 78
B. Madjour and A. Boudiaf

Efficient Descent Direction of a Conjugate Gradient Algorithm for Nonlinear Optimization 91
Mohamed Lamine Ouaoua and Samia Khelladi

Theoretical and Numerical Results for Nonlinear Optimization Problems 101
C. Souli and A. Leulmi

Founded by A.A. Martynyuk in 2001.
Registered in Ukraine Number: KB No 5267 / 04.07.2001.

NONLINEAR DYNAMICS AND SYSTEMS THEORY

An International Journal of Research and Surveys

Impact Factor from SCOPUS for 2023: SJR – 0.298, SNIP – 1.032 and CiteScore – 1.6

Nonlinear Dynamics and Systems Theory (ISSN 1562–8353 (Print), ISSN 1813–7385 (Online)) is an international journal published under the auspices of the S.P. Timoshenko Institute of Mechanics of National Academy of Sciences of Ukraine and Curtin University of Technology (Perth, Australia). It aims to publish high quality original scientific papers and surveys in areas of nonlinear dynamics and systems theory and their real world applications.

AIMS AND SCOPE

Nonlinear Dynamics and Systems Theory is a multidisciplinary journal. It publishes papers focusing on proofs of important theorems as well as papers presenting new ideas and new theory, conjectures, numerical algorithms and physical experiments in areas related to nonlinear dynamics and systems theory. Papers that deal with theoretical aspects of nonlinear dynamics and/or systems theory should contain significant mathematical results with an indication of their possible applications. Papers that emphasize applications should contain new mathematical models of real world phenomena and/or description of engineering problems. They should include rigorous analysis of data used and results obtained. Papers that integrate and interrelate ideas and methods of nonlinear dynamics and systems theory will be particularly welcomed. This journal and the individual contributions published therein are protected under the copyright by International InforMath Publishing Group.

PUBLICATION AND SUBSCRIPTION INFORMATION

Nonlinear Dynamics and Systems Theory will have 6 issues in 2025, printed in hard copy (ISSN 1562–8353) and available online (ISSN 1813–7385), by InforMath Publishing Group, Nesterov str., 3, Institute of Mechanics, Kiev, MSP 680, Ukraine, 03057. Subscription prices are available upon request from the Publisher, EBSCO Information Services (`mailto:journals@ebsco.com`), or website of the Journal: `http://e-ndst.kiev.ua`. Subscriptions are accepted on a calendar year basis. Issues are sent by airmail to all countries of the world. Claims for missing issues should be made within six months of the date of dispatch.

ABSTRACTING AND INDEXING SERVICES

Papers published in this journal are indexed or abstracted in: Mathematical Reviews / MathSciNet, Zentralblatt MATH / Mathematics Abstracts, PASCAL database (INIST–CNRS) and SCOPUS.

Nonlinear Dynamics and Systems Theory, **25** (1) (2025) 1–12

The Dynamics and Stability of Prey-Predator Model of Migration with Holling Type-III Response Function and Interspecific Competition for Prey

Syamsul Agus, Syamsuddin Toaha *, Kasbawati and Khaeruddin

Department of Mathematics, Hasanuddin University, Tamalanrea, 90245, Makassar, Indonesia

Received: April 30, 2024; Revised: January 11, 2025

Abstract: This paper discusses the prey-predator model with habitats in reserved and unreserved areas. The prey population can migrate from the reserved area to the unreserved area and vice versa. The prey lives in the reserved and unreserved areas. The predator freely hunts for the prey in the unreserved area. The Holling type III is considered on the basis of its predatory characteristics. Interspecific competition for prey occurs in the migration process. The dynamics of prey-predator is expressed as a system of nonlinear differential equations. The stability of the interior equilibrium point is analyzed locally. The eigenvalues of the Jacobian matrix together with the Routh-Hurwitz stability test are used to determine the stability of the equilibrium point. Using appropriate parameter values, simulations were conducted by varying the parameter values of migration and interspecific competition. It was found that there are up to three interior equilibrium points and there are conditions in which there is no interior equilibrium point. It was also found that there are three interior equilibrium points, one of which is unstable while the other two are bistable. The change in migration rates and competition levels allows the prey population in the reserved and unreserved areas and their predator to live together.

Keywords: *prey-predator; Holling type; reserved area; interspecific competition; bistable equilibrium points.*

Mathematics Subject Classification (2020): 70K42, 70K20, 93D05.

* Corresponding author: mailto::syamsuddint@gmail.com

© 2025 InforMath Publishing Group/1562-8353 (print)/1813-7385 (online)/http://e-ndst.kiev.ua

1 Introduction

A mangrove forest is an ecosystem developed between estuaries and coastal areas. Mangrove ecosystems are migration routes for many species of fish and other organisms. Mangrove forests are the habitat of many species, including mangrove crabs, for feeding, breeding, and protection from predators. In their life cycle, juvenile crabs migrate back to the estuary, gradually enter the mangrove area, and develop into adults [1]. Mangrove crabs are species that tend to attack and eat other mangrove crabs. Around mangrove forests and coastal areas, the crab is preyed on by many fish, including Red Snapper (*Lutjanidae*) and White Snapper (*Lates calcarifer*). In addition, various types of fish dominated by carnivorous fish approach mangrove forests at high tide to find food [2]. The dynamics of population changes of migrating mangrove crabs and their predators can be expressed in the form of a mathematical model.

The population dynamics dealing with the prey-predator model has been studied by many researchers from different angles and with different purposes. Some researchers focus on the effect of predation functions such as the Holling function and the Beddington-DeAngelis function, which consider the characteristics of predators in hunting to catch their prey, see for example, [3–5]. Population dynamics in ecology also includes many prey-predator interactions, harvesting and its consequences in the population dynamics mechanism [6]. For certain reasons and conditions, the habitat of a population is divided into a reserved area and an unreserved area for economic activities. Under such conditions, the population is divided based on where it is located and the population can still migrate from the reserved area to the unreserved area and vice versa [7, 8]. Migration and harvesting in a prey-predator model can also be used as a control in bio-economic models and an effort to prevent the population from extinction and to optimally utilize the population as a valuable stock [9, 10].

Based on the previous research, a prey-predator model with prey migration in the two areas and interspecific competition was developed. In this model, the influences of migration and interspecific competition on the stability of the equilibrium point and sustainability of the populations are analyzed. Mangrove crabs as the prey migrate from mangrove area to the coastal area and vice versa, with mangroves as a reserved area and the coastal zone as an unreserved area. Predator populations freely prey on mangrove crabs in the unreserved area and follow the Holling type III predation function according to the characteristics of populations. In the process of migration, interspecific competition between prey occurs naturally. The dynamics of prey and predator populations is expressed as a system of nonlinear differential equations. The population dynamics is analyzed by checking the conditions for the existence of interior equilibrium points and analyzing the local stability. The nonlinear model is complex enough to be solved analytically. The Routh-Hurwitz stability test is used to investigate the local stability of the interior equilibrium point of the model. The effects of migration rate and interspecific competition on prey are analyzed using numerical simulations. The plots of trajectory curves for prey and predator populations around the stable interior equilibrium point are given to visualize the dynamics of prey and predator populations.

2 Methodology of Prey-Predator Model with Migration

This paper considers the dynamics of mangrove crabs or mud crabs (*Scylla spp.*) living in the mangrove area and in marine waters. Mangrove crabs mate in the mangrove area

and migrate to marine waters to spawn. After spawning and growing into juvenile crabs, they migrate back to the upstream estuary or back to the mangrove area. When the mangrove crabs are in the mangrove area, they are relatively safe from predators, but in the marine waters, a certain fish as a predator will prey on the mangrove crabs. In this case, the mangrove crab habitat is divided into two parts, namely the mangrove area as the reserved area and the marine waters as the unreserved area. In the migration process of mangrove crabs, interspecific competition occurs and reduces the number of mangrove crabs [4, 11]. The mangrove crabs living in the mangrove area and marine waters are assumed to grow according to the logistic model. Predation on the mangrove crabs occurs only in the unreserved area and the predation function follows the Holling type III, which is consistent with the characteristics of predation on crabs [4]. In the predator populations, intraspecific competition occurs [12] and the prey and predator populations are reduced by natural mortality.

The population dynamics of mangrove crabs in the reserved and unreserved areas and of their predator are expressed in the following growth model:

$$\begin{aligned} \frac{dx}{dt} &= rx(1-\frac{x}{K}) - \sigma_1 x + \sigma_2 y - \frac{cx^2 z}{c_1 + x^2} - fx - uxy, \\ \frac{dy}{dt} &= sy(1-\frac{y}{L}) + \sigma_1 x - \sigma_2 y - hy - vxy, \\ \frac{dz}{dt} &= \frac{g_1 x^2 z}{c_1 + x^2} - ez - qz^2. \end{aligned} \tag{1}$$

In model (1), the variables $x = x(t)$, and $y = y(t)$ are the population densities of mangrove crab as prey in the unreserved and reserved areas at time t, respectively. The variable $z = z(t)$ is the population density of fish as the predator at time t. The initial conditions of all three populations are nonnegative, $x(0) \geq 0$, $y(0) \geq 0$, and $z(0) \geq 0$. Parameters $r, K, \sigma_1, \sigma_2, c, c_1, f, h, e, s, L, g_1, q, u$, and v successively express the intrinsic growth rate of the prey population in the unreserved area, the carrying capacity of the habitat for the prey population in the unreserved area, the weighting coefficient of prey migration from the unreserved area to the reserved area, the weighting coefficient of prey migration from the reserved area to the unreserved area, the maximum per capita consumption rate of the predator, the Michaelis-Menten constant rate, prey mortality rate in the unreserved area, prey mortality rate in the reserved area, predator mortality rate, intrinsic growth rate of the prey population in the reserved area, carrying capacity of the habitat for the prey population in the reserved area, conservation rate of predator, intraspecific competition coefficient, prey competition in the reserved area, and prey competition in the unreserved area. All parameters are assumed to be positive.

For simplicity, let $R = r - \sigma_1 - f$, $R_1 = \frac{r}{K}$, $S = s - \sigma_2 - h$, $S_1 = \frac{s}{L}$, $\gamma = \frac{g_1 - e}{q}$, $\gamma_1 = \frac{ec_1}{q}$. Furthermore, model (1) is expressed as

$$\frac{dx}{dt} = x[(R - R_1 x) - \frac{cx^2 z}{c_1 + x^2} - uy] + \sigma_2 y, \tag{2}$$

$$\frac{dy}{dt} = y[(S - S_1 y) - vx] + \sigma_1 x, \tag{3}$$

$$\frac{dz}{dt} = z(\frac{g_1 x^2}{c_1 + x^2} - e - q_3 z). \tag{4}$$

3 Positivity and Boundedness of Solution

The positivity and boundedness of the solution of model (1) with the initial conditions $x(0) > 0, y(0) > 0, z(0) > 0$ are stated in the form of theorems. The positivity and boundedness of the solution of the model are ecologically relevant.

Theorem 3.1 *The set* $\Psi = \left\{(x,\ y,\ z) \in \Re^3_{+0} : 0 < \omega = x + y + z \leq \frac{\rho}{\rho_1}\right\}$ *is the area for all solutions of the subsets in the positive octant, where* ρ_1 *is a constant which satisfies* $\rho_1 < e, \rho = \frac{K(r-f+\rho_1)^2}{4r} + \frac{L(s-h+\rho_1)^2}{4s}, g_1 \leq c$.

Proof. Let $\omega(t) = x(t) + y(t) + z(t)$ and $\rho_1 > 0$ be a constant. Then $\frac{d\omega}{dt} + \rho_1\omega = (r - f + \rho_1)x - \frac{rx^2}{K} - (u + v)xy + (s - h + \rho_1)y - \frac{sy^2}{L} - (c - g_1)\frac{x^2z}{c_1+x^2} - (e - \rho_1)z - qz^2$. It is natural to assume that $g_1 \leq c$, so the equation can be written as
$\frac{d\omega}{dt} + \rho_1\omega = -\frac{r}{K}(x - \frac{K}{2r}(r - f + \rho_1))^2 - \frac{s}{L}(y - \frac{L}{2s}(s - h + \rho_1))^2 + \frac{K}{4r}(r - f + \rho_1)^2 + \frac{L}{4s}(s - h + \rho_1)^2 - (u + v)xy - (c - g_1)\frac{x^2z}{c_1+x^2} - (e - \rho_1)z - qz^2$.
$\frac{d\omega}{dt} + \rho_1\omega \leq \frac{K}{4r}(r - f + \rho_1)^2 + \frac{L}{4s}(s - h + \rho_1)^2 = \rho$.
By the theory of differential inequalities, we have $0 < \omega(x(t), y(t), z(t)) \leq \frac{\rho}{\rho_1}(1 - \frac{1}{e^{\rho_1 t}}) + \omega(x(t), y(t), z(t))\frac{1}{e^{\rho_1 t}}$. Taking limit when $t \to \infty$, we get $0 < \omega \leq \frac{\rho}{\rho_1}$. This proves the theorem.

Theorem 3.2 *All solutions* $(x(t), y(t), z(t))$ *of the system of equations (2), (3), and (4) with the initial conditions* $x(0) > 0, y(0) > 0, z(0) > 0$ *are positive for all* $t \geq 0$.

Proof. From equation (2) together with the initial conditions $x(0) > 0, y(0) > 0, z(0) > 0$, we have $\frac{dx}{x} = \mu(x, y, z)dt + \mu_1(x, y)dt$, where $\mu(x, y, z) = (R - R_1x) - \frac{cxz}{c_1+x^2} - uy$, and $\mu_1(x, y) = \frac{\sigma_2 y}{x}$. Integrating the above equation on the interval $\lfloor 0, \tau \rfloor$, we have $x(t) = x(0)e^{\int_0^t \mu(x(\tau),y(\tau),z(\tau))d\tau + \int_0^t \mu_1(x(\tau),\ y(\tau))d\tau} > 0$ for all $\tau \in [0,\ t]$.
Next, from equation (3), we have $\frac{dy}{y} = \varphi_0(x, y)\,dt + \varphi_1(x,\ y)\,dt$, where
$\varphi_0(x, y) = (S - S_1y) - vx,\ \varphi_1(x,\ y) = \frac{\sigma_1 x}{y}$. Integrating the above equation on the interval $\lfloor 0, \tau \rfloor$, we have $y(t) = y(0)e^{\int_0^t \varphi_0(x(\tau),y(\tau))d\tau + \int_0^t \varphi_1(x(\tau),y(\tau))d\tau} > 0$ for all $\tau \in [0,\ t]$.
Next, from equation (4), we have $\frac{dz}{z} = \rho_0(x, z)\,dt$, where $\rho_0(x, z) = \frac{g_1x^2}{c_1+x^2} - e - qz$. Integrating the above equation on the interval $\lfloor 0, \tau \rfloor$, we have $z(t) = z(0)e^{\int_0^t \rho_0(x(\tau),z(\tau))d\tau} > 0$ for all $\tau \in [0,\ t]$. The solutions of the equations (2), (3), and (4) are all positive.

Theorem 3.3 *All solutions of the model (1) are bounded.*

Proof. We construct a function $\omega(t) = x(t) + y(t) + \frac{c}{g_1}z(t)$. If this equation is differentiated with respect to time (t), then we have $\frac{d\omega}{dt} = rx\left(1 - \frac{x}{K}\right) - fx - (u + v)xy + sy\left(1 - \frac{y}{L}\right) - hy - \frac{ec}{g_1}z - \frac{q_3c}{g_1}z^2$,
$\frac{d\omega}{dt} = rx + ex - \frac{rx^2}{K} - fx - (u + v)xy + sy + ey - \frac{sy^2}{L} - hy - \frac{ec}{g_1}z - \frac{q_3c}{g_1}z^2 - ex - ey$,
$\frac{d\omega}{dt} \leq rx + ex + sy + ey - \frac{ec}{g_1}z - ex - ey$.
The consumption rate of the predator population to prey is assumed to follow $0 < g_1 \leq c$. From the first two equations of model (1), we have $K + L$ is the total carrying capacity of the total prey population. We have $x(t) + y(t) \leq K + L + \epsilon$ as $t \to \infty$. Suppose we take $x(t) \leq K + \epsilon_1$ as $t \to \infty$ and $y(t) \leq L + \epsilon_2$ as $t \to \infty$, where $\epsilon,\ \epsilon_1,\ \epsilon_2$ are three positive numbers. Let $\omega(t) = x(t) + y(t) + \frac{c}{g_1}z$. The derivative of

$\omega(t)$ with respect to t takes the form

$$\begin{aligned}\frac{d\omega}{dt} &\leq (r+e)\,x+(s+e)\,y-\frac{ec}{g_1}z-ex-ey\\ &=-e\left(x+y+\frac{c}{g_1}z\right)+(e+r)\,x+(e+s)\,y\\ &=-e\omega+(e+r)\,x+(e+s)\,y,\\ \frac{d\omega}{dt}+e\omega &\leq\ (e+r)\,(K+\epsilon_1)+(e+s)\,(L+\epsilon_2).\end{aligned}$$

Let $K_1 = (e+r)\,(K+\epsilon_1)+(e+s)\,(L+\epsilon_2)$ and integrate both sides, we obtain the boundary $\omega(t)=\frac{K_1}{e}+C_1\,\frac{1}{e^{et}}$. The inequality $\frac{d\omega}{dt}\leq K_1-e\omega$ has the solution $\omega(t)\leq \frac{K_1}{e}+C_1\,\frac{1}{e^{et}}$ for $t\to\infty$. Then we obtain $\limsup_{t\to\infty}\omega(t)\leq\frac{K_1}{e}$. Therefore, (x,y,z) is bounded in $\mathfrak{R}^3$ and (x,y,z) belongs to $\Psi_1=\left\{(x,\ y,\ z)\in\mathfrak{R}^3_{+0}: x+y+\frac{ec}{g_1}z\leq\frac{K_1}{e}\right\}$.

4 Equilibrium Points and Local Stability Analysis

In order to investigate the behavior and changes of the populations x, y, and z, it is necessary to find the interior equilibrium point and determine its stability. The equilibrium points of model (1) are obtained by solving $\frac{dx}{dt}=\frac{dy}{dt}=\frac{dz}{dt}=0$. Further, the non-negative equilibrium points are obtained, namely $T_1=(0,0,0)$ and $T_2=(x_2,y_2,0)$. The values of components of the equilibrium point T_2 are $x_2=\frac{y_2(-y_2S_1+S)}{vy_2-\sigma_1}$ and y_2, where y_2 is the positive root of the polynomial $AX^3+BX^2+CX+D=0$, where $A=R_1{S_1}^2-uvS_1$, $B=RvS_1-2SS_1R_1+Suv+uS_1\sigma_1-\sigma_2v^2, C=S^2R_1-RSv-RS_1\sigma_1-Su\sigma_1+2\sigma_1\sigma_2v$, and $D=RS\sigma_1-\sigma_2{\sigma_1}^2$. The possible interior equilibrium point for model (1) is $T_3=(\bar{x},\ \bar{y},\ \bar{z})$. The values of components of the equilibrium point T_3 are $\bar{x}=\frac{\bar{y}(-\bar{y}S_1+S)}{v\bar{y}-\sigma_1}$, $\bar{z}=\frac{\gamma\bar{x}^2-\gamma_1}{\bar{x}^2+c_1}$, and $\bar{y}$, where $\bar{y}$ is the positive root of the polynomial $A_1Y^{11}+A_2Y^{10}+A_3Y^9+A_4Y^8+A_5Y^7+A_6Y^6+A_7Y^5+A_8Y^4+A_9Y^3+A_{10}Y^2+A_{11}Y+A_{12}=0$, where A_1, A_2, ..., A_{12} are real numbers that depend on the values of the model parameters.

The equilibrium point $T_3=(\bar{x},\ \bar{y},\ \bar{z})$ may not exist in the sense that not all of its components are positive. The equilibrium point $T_3=(\bar{x},\ \bar{y},\ \bar{z})$ may consist of only one, two, three or more components in the first octant. This condition depends on the parameter values of the model. The only equilibrium point to be analyzed is the interior equilibrium point, i.e., $T_3=(\bar{x},\ \bar{y},\ \bar{z})$. Due to the complexity of model (1), only the local stability of the interior equilibrium point is considered. For this purpose, the model is linearized around the equilibrium point and the Jacobian matrix evaluated at the equilibrium point $T_3=(\bar{x},\ \bar{y},\ \bar{z})$ is obtained as follows:

$$J(T_3)=\begin{pmatrix}d_1 & d_2 & d_3\\ d_4 & d_5 & 0\\ d_6 & 0 & d_7\end{pmatrix},$$

where $d_1 = R-2R_1\bar{x}-\frac{2c\bar{x}\bar{z}}{\bar{x}^2+c_1}-u\bar{y}+\frac{2c\bar{x}^3\bar{z}}{(\bar{x}^2+c_1)^2}$, $d_2=\sigma_2-u\bar{x}$, $d_3=-\frac{c\bar{x}^2}{\bar{x}^2+c_1}$, $d_4=\sigma_1-v\ \bar{y}, d_5=S-v\bar{x}-2\bar{y}S_1$, $d_6=\frac{2g_1c_1\bar{x}\bar{z}}{(\bar{x}^2+c_1)^2}$, and $d_7=\frac{g_1\bar{x}^2}{\bar{x}^2+c_1}-e-2q\bar{z}$.

The next step is obtaining the characteristic equation that corresponds to the equilibrium point $T_3=(\bar{x},\ \bar{y},\ \bar{z})$. Then we have $f(\lambda)=\lambda^3+a_1\lambda^2+a_2\lambda+a_3$, where $a_1=$

$-(d_1+d_5+d_7)$, $a_2 = d_1d_5+d_5d_7+d_1d_7-d_2d_4-d_3d_6$, and $a_3 = d_2d_4d_7-d_1d_5d_7+d_3d_5d_6$. In accordance with the Routh-Hurwitz stability test [13], the interior equilibrium point $T_3 = (\bar{x},\ \bar{y},\ \bar{z})$ is locally asymptotically stable if the conditions $a_1 > 0, a_3 > 0$, and $a_1a_2 - a_3 > 0$ are satisfied.

5 Numerical Simulation

The simulation is based on the analysis results obtained in the previous section. Simulations are performed to investigate the effect of migration and interspecific competition in the prey population on the existence of interior equilibrium points in the first octant and their stability. The parameter values used in the simulation of model (1) are based on the parameter values used by the previous researchers [6, 14, 15]. Some parameter values have been adjusted to get interesting results. The values of migration rates and interspecific competition are given in various combinations. The simulation is given in four cases, which are presented in the table and plot of prey and predator population curves in the reserved and unreserved areas.

Case 1. The value of σ_1 is fixed and the value of σ_2 varies.

For simulation, we use the parameter values $r = 0.9, K = 100, L = 100, c = 2.5, g_1 = 0.8, c_1 = 1, f = 0.02, h = 0.01, e = 0.3, q = 0.3, u = 0.02$, and $v = 0.02$ in the appropriate units. By using these parameter values, the equilibrium points, eigenvalues, and stability are obtained, as shown in Table 1.

$\sigma_2 = 0.1$	$\sigma_2 = 0.2$	$\sigma_2 = 0.4$	$\sigma_2 = 0.5$
$T_{3a}(7.66, 1.02, 1.62)$ (0.52,-0.87,-0.48) not stable	$T_{3a}(7.18, 0.95, 1.62)$ (0.51,-0.85,-0.47) not stable	$T_{3a}(6.39, 0.80, 1.60)$ (0.49,-0.84,-0.46) not stable	$T_{3a}(6.08, 0.73, 1.60)$ (0.49,-0.86,-0.45) not stable
	$T_{3b}(1.02, 54.01, 0.37)$ (-10.48,-0.13,-0.48) stable node	$T_{3b}(1.80, 15.63, 1.04)$ (-2.72,-0.45,-0.18) stable node	$T_{3b}(1.88, 5.40, 1.08)$ (-0.55±0.58i,-0.14) stable node
$T_{3c}(68.18, 0.53, 1.67)$ (-0.55,-12.86,-0.50) stable node	$T_{3c}(68.37, 0.53, 1.67)$ (-0.55,-12.99,-0.50) stable node	$T_{3c}(68.75, 0.52, 1.67)$ (-0.56,-13.27,-0.50) stable node	$T_{3c}(68.9, 0.51, 1.67)$ (-0.56,-13.41,-0.50) stable node

Table 1: The equilibrium point T_3, eigenvalues, and stability for the case $\sigma_1 = 0.1$.

Table 1 shows that there are initially two equilibrium points in the first octant, one equilibrium point is unstable and the other is locally asymptotically stable. By increasing the value of the migration coefficient (σ_2) from the reserved to the unreserved area, three equilibrium points are obtained in the first octant, where one equilibrium point remains unstable while the other two are locally asymptotically stable. In this case, there is a bistable equilibrium point, i.e., the coexistence of two equilibrium points that are jointly stable, and the type of stability is the same, i.e., they are locally asymptotically stable with node type. By increasing the value of the migration coefficient (σ_2), three equilibrium points are still obtained in the first octant and their stability does not change.

Increasing the value of σ_2 only changes the value of the equilibrium point T_{3a}, i.e., the values of the equilibrium points of the populations x, y, and z are all decreasing. The equilibrium point T_{3b} does not appear at first. By increasing the value of σ_2, the equilibrium point T_{3b} appears, and the increase in the value of σ_2 changes the values of the equilibrium points T_{3b} and T_{3c}; that is, the values of the equilibrium points of the populations x and z increase while the value of the equilibrium point of the population y decreases.

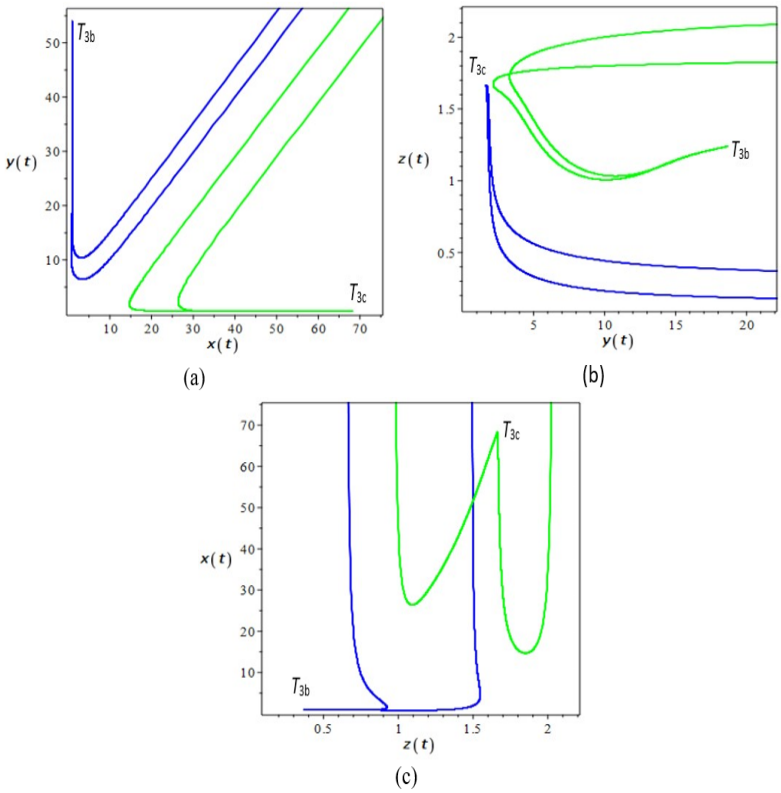

Figure 1: Populations behaviour around the bistable equilibrium points for $\sigma_1 = 0.1, \sigma_2 = 0.2$.

Figure 1 shows the behaviour of the populations x, y and z around the two stable equilibrium points. Both equilibrium points T_{3b} and T_{3c} are asymptotically stable, i.e., they are bistable equilibrium points. This means that none of the three populations will become extinct. The initial value of the population plays an important role in determining where the population converges. In Figure 1(a), there is a line dividing the stability domain for the equilibrium points T_{3b} and T_{3c}, but in Figures 1(b) and 1(c), the line which divides the stability domain for the equilibrium points T_{3b} and T_{3c} is not clearly visible.

Case 2. The value of σ_2 is fixed and the value of σ_1 varies.

For simulation, we use the parameter values $r = 0.9, K = 100, L = 100, c = 2.5, g_1 =$

$0.8, c_1 = 1, f = 0.02, h = 0.01, e = 0.3, q = 0.3, u = 0.02$, and $v = 0.02$ in the appropriate units. By using these parameter values, the equilibrium points, eigenvalues, and stability are obtained, as shown in Table 2.

$\sigma_1 = 0.05$	$\sigma_1 = 0.1$	$\sigma_1 = 0.2$	$\sigma_1 = 0.25$
$T_{3a}(6.02, 0.72, 1.60)$ (-0.45±0.03i,0.62) not stable, spiral	$T_{3a}(7.66, 1.02, 1.62)$ (0.52,-0.87,-0.48) not stable	$T_{3a}(14.39, 1.37, 1.66)$ (0.23,-2.20,-0.49) not stable	T_{3a} does not appear
$T_{3b}(80.68, 0.26, 1.67)$ (-0.67,-15.35,-0.50) stable node	$T_{3b}(68.18, 0.53, 1.67)$ (-0.55,-12.86,-0.50) stable node	$T_{3b}(39.52, 1.11, 1.67)$ (-0.23,-7.16,-0.50) stable node	T_{3b} does not appear

Table 2: The equilibrium point T_3, eigenvalues, and stability for the case $\sigma_2 = 0.1$.

There are two equilibrium points in the first octant, as Table 2 demonstrates. At first, one equilibrium point exhibits spiral stability, while the other displays local asymptotic stability. By increasing the value of the migration coefficient (σ_1) from the unreserved to the reserved area, two equilibrium points are still obtained in the first octant, but the spiral unstable equilibrium point becomes an unstable node and the other equilibrium point remains locally asymptotically stable. When increasing the value of σ_1 again, there are still two equilibrium points with the type of stability unchanged. However, when $\sigma_1 = 0.25$, the equilibrium point in the first octant is no longer obtained. The increase of the migration value from the unreserved to the reserved area can lead to the non-existence of the equilibrium point in the first octant.

Case 3. The value of u is fixed and the value of v varies.

For simulation, we use the parameter values $r = 0.9, K = 100, L = 100, c = 2.5, g_1 = 0.8, c_1 = 1, f = 0.02, h = 0.01, e = 0.3, q = 0.3, \sigma_1 = 0.3$, and $\sigma_2 = 0.3$ in the appropriate units. By using these parameter values, the equilibrium points, eigenvalues, and stability are obtained, as shown in Table 3.

$v = 0.1$	$v = 0.2$	$v = 0.4$	$v = 0.5$
	$T_{3a}(13.04, 1.92, 1.65)$ (0.18,-2.09,-0.49) not stable	$T_{3a}(9.26, 0.89, 1.63)$ (0.31,-3.14,-0.48) not stable	$T_{3a}(8.87, 0.69, 1.63)$ (0.33,-3.86,-0.48) not stable
$T_{3b}(2.63, 38.6, 1.33)$ (-3.51,-0.49,-0.38) stable node	$T_{3b}(2.29, 18.79, 1.24)$ (-1.00±0.02i,-0.27) stable spiral	$T_{3b}(1.58, 5.17, 0.91)$ (-0.38±0.74i,-0.38) stable spiral	$T_{3b}(1.41, 3.02, 0.77)$ (-0.28±0.71i,-0.19) stable spiral
	$T_{3c}(34.42, 1.64, 1.66)$ (-0.19,-6.34,-0.49) stable node	$T_{3c}(46.44, 0.77, 1.66)$ (-0.33,-18.00,-0.49) stable node	$T_{3c}(48.5, 0.61, 1.66)$ (-0.35,-23.67,-0.50) stable node

Table 3: The equilibrium point T_3, eigenvalues, and stability for the case $u = 0.1$.

Table 3 shows that initially there is only one equilibrium point in the first octant, which is locally asymptotically stable. When increasing the value of the competition coefficient in the population y, three equilibrium points appear in the first octant, one equilibrium point is unstable, while the other two are spiral stable and nodal stable. If we increase the value of the competition coefficient in the population y again, we find that there are still three equilibrium points in the first octant, and their stability does not change. Increasing the competition coefficient only affects the value of the equilibrium points. For the equilibrium points T_{3a} and T_{3b}, increasing the competition coefficient decreases the values of the equilibrium points for the populations x, y, and z. While for the equilibrium point T_{3c}, the values of the equilibrium point for the population y decreases, but the values of the equilibrium points for the populations x and z increase.

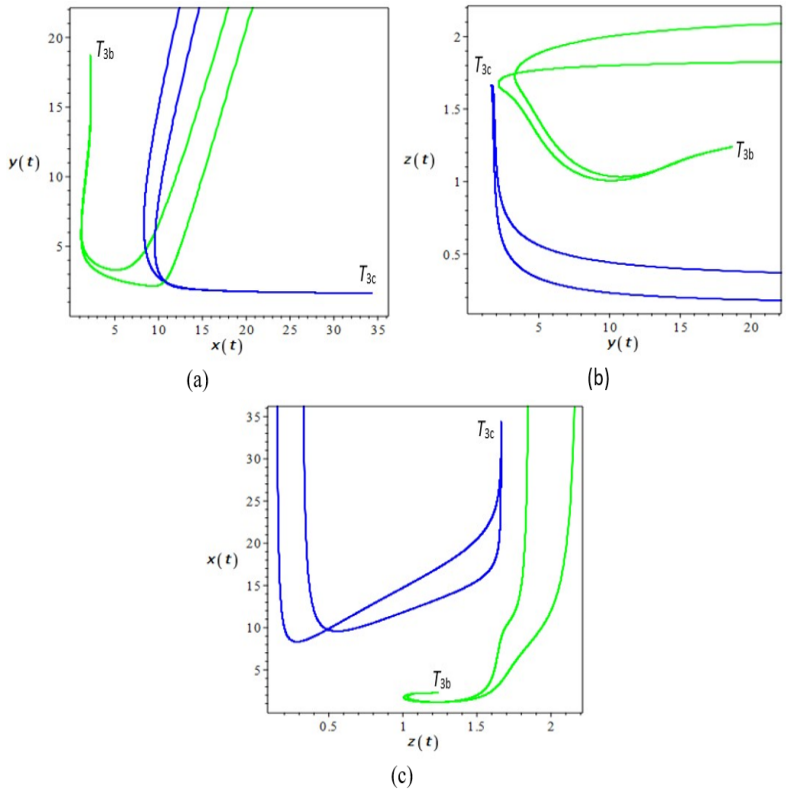

Figure 2: Populations behaviour around the bistable equilibrium points for $u = 0.1, v = 0.2$.

Figure 2 shows the behaviour of the populations x, y, and z around two stable equilibrium points. Both equilibrium points T_{3b} and T_{3c} are asymptotically stable, bistable equilibrium points. This means that none of the three populations will become extinct. The initial value of the population determines to what interior equilibrium point the population converges. In Figure 2(a), there is no clear curve that divides the domain of stability for the equilibrium points T_{3b} and T_{3c}, but in Figures 2(b) and 2(c), there is a clear curve that divides the domain of stability for the equilibrium points T_{3b} and T_{3c}.

Case 4. The value of v is fixed and the value of u varies.

For simulation, we use the parameter values $r = 0.9, K = 100, L = 100, c = 2.5, g_1 = 0.8, c_1 = 1, f = 0.02, h = 0.01, e = 0.3, q = 0.3, \sigma_1 = 0.3$, and $\sigma_2 = 0.3$ in the appropriate units. By using these parameter values, the equilibrium points, eigenvalues, and stability are obtained as shown in Table 4.

$u = 0.1$	$u = 0.2$	$u = 0.3$	$u = 0.4$
$T_{3a}(13.04, 1.92, 1.65)$ (0.18,-2.09,-0.49) not stable			
$T_{3b}(2.29, 18.79, 1.24)$ (-1.00±0.02i,-0.27) stable spiral	$T_{3b}(1.43, 35.19, 0.79)$ (-7.03,-0.35,-0.27) stable node	$T_{3b}(1.01, 43.87, 0.35)$ (-13.02,-0.12,-0.40) stable node	T_{3b} does not appear, z becomes negative
$T_{3c}(34.42, 1.64, 1.66)$ (-0.19,-6.34,-0.49) stable node			

Table 4: The equilibrium point T_3, eigenvalues, and stability for the case $v = 0.2$.

Table 4 shows that there are initially three equilibrium points in the first octant, i.e., the equilibrium point T_{3a} is unstable, while the equilibrium points T_{3b} and T_{3c} are spiral stable and node stable, respectively. By increasing the value of the competition coefficient (u), only one unstable node equilibrium point is obtained. However, for the competition coefficient $u = 0.4$, there is no equilibrium point in the first octant. Increasing the value of the competition coefficient can lead from three equilibrium points to only one node-stable equilibrium point, and then no more equilibrium points exist in the first octant.

6 Conclusion

The population dynamics of prey living in the reserved and unreserved areas and of their predators living in the unreserved areas are expressed by a system of nonlinear differential equations. This model can describe the population dynamics of mangrove crabs living in mangrove forests and the coastal area. Mangrove crabs in the coastal area are preyed upon by predatory fish that follow the Holling type III predation function. The solution of the model is positive and bounded in the first octant. Simulations with the relevant values of the model parameters have found one, two, three, and even no interior equilibrium points. Some of these interior equilibrium points are stable, and some are unstable.

Simulations were carried out by changing the value of the migration rates in the prey population living in the reserved and unreserved areas. In case 1, initially, only two interior equilibrium points were found, one stable and the other unstable. Once the value of the migration rate σ_2 is increased and three equilibrium points are obtained, one equilibrium point is unstable and the other two equilibrium points are stable; bistable equilibrium points occur. In case 2, two interior equilibrium points are initially obtained,

one equilibrium point is stable and the other is unstable. By increasing the migration rate (σ_1), two interior equilibrium points are still obtained, but there is a change in the type of stability, from unstable spiral to unstable saddle. By increasing the migration rate (σ_1) again, the interior equilibrium point is no longer found.

Simulations were also conducted by changing the level of competition in the prey population. In case 3, initially, there is only one stable interior equilibrium point. Once the competition level (v) is increased, three equilibrium points are obtained: one equilibrium point is unstable, and the other two equilibrium points are stable, stable node and stable spiral. In this case, there are bistable equilibrium points. In case 4, initially, three interior equilibrium points are obtained, two equilibrium points are stable, stable node and stable spiral, and the other one is unstable. By increasing the competition level (u), only one stable node interior equilibrium point is obtained. By increasing the competition level (u) again, the interior equilibrium point is no longer found.

References

[1] L. Le Vay. Ecology and management of mud crab Scylla spp. *Asian Fisheries Science* **14** (2) (2001) 101–112.

[2] I. Nagelkerken, S. J. M. Blaber, S. Bouillon, P. Green, M. Haywood, L. G. Kirton and J. O. Meynecke *et al.* The habitat function of mangroves for terrestrial and marine fauna: A Review. *Aquatic Botany* **89** (2) (2008) 155–185.

[3] Noor S. Sh. Barhoom, and S. Al-Nassir. Dynamical behaviors of a fractional-order three-dimensional prey-predator model. *Abstract and Applied Analysis* **2021** (1366797) (2021) 1–10.

[4] R. Banerjee, P. Das and D. Mukherjee. Global dynamics of a Holling Type-III two prey–one predator discrete model with optimal harvest strategy. *Nonlinear Dynamics* **99** (4) (2020) 3285-3300.

[5] B. Roy, and S. K. Roy. Prey-predator model in drainage system with migration and harvesting *Nonautonomous Dynamical Systems* **8** (1) (2021) 152–167.

[6] S. Toaha, Firman and A. Ribal. Global Stability and Optimal Harvesting of Predator-Prey Model with Holling Response Function of Type II and Harvesting in Free Area of Capture *Nonlinear Dyn. Syst. Theory* **22** (1) (2022) 105–116.

[7] K. Agnihotri and S. Nayyer. Stability Analysis of a Predator (Bird) – Prey (Fish) Harvesting Model In The Reserved and Unreserved Area *Malaya Journal of Matematik* **6** (3) (2018) 678–684.

[8] M. R. Lemnaouar, H. Benazza, M. Khalfaoui and Y. Louartassi. Dynamical behaviours of prey-predator fishery model with two reserved area for prey in the presence of toxicity and response function Holling type IV. *J. Math. Comput* **11** (3) (2021) 2893-2913.

[9] A. Pradhan, A. Johri and S. Jain. A Model for Fishery Resource with Reserve Area and Facing Prey-Predator Interaction. *International Journal of Contemporary Mathematical Sciences* **12** (6) (2017) 255–264.

[10] H. Huo, H. Jiang and X. Meng. A dynamic model for fishery resource with reserve area and taxation. *Journal of Applied Mathematics* **2012** (3) (2012) 1–15.

[11] C. Raymond, A. Hugo and M. Kung'aro. Modeling dynamics of prey-predator fishery model with harvesting: A bioeconomic model. *Journal of Applied Mathematics* **2019** (1) (2019) 1–13.

[12] N. A. Maziun and Subchan. Stability and Bifurcation Analysis of Time Delayed Prey-Predator System with Holling Type-III Response Function. *International Journal of Computing Science and Applied Mathematics* **6** (2) (2020) 59–65.

[13] F. Brauer, and C. Castillo-Chavez. *Mathematical Models in Population Biology and Epidemiology*. Second Editions. Springer, New York, 2012.

[14] B. Dubey, S. Agarwal and A. Kumar. Optimal harvesting policy of a prey–predator model with Crowley–Martin-type functional response and stage structure in the predator. *Nonlinear Analysis: Modelling and Control* **23** (4) (2018) 493–514.

[15] Didiharyono, S. Toaha, J. Kusuma and Kasbawati. Harvesting Strategies in the Migratory Prey-Predator Model with a Crowley-Martin Type Response Function and Constant Efforts *Nonlinear Dyn. Syst. Theory* **23** (1) (2023) 14–23.

Nonlinear Dynamics and Systems Theory, **25** (1) (2025) 13–26

Φ-Hilfer Proportional Fractional Differential System: Uniqueness and Stability Result

Ahmad Alhababheh [1], Ma'mon Abu Hammad [2], Oualid Zentar [3], Mohamed Ziane [3], Shameseddin Alshorm [4*] and Ali Ateiwi [5]

[1] *Department of Basic and Applied Sciences, Shoubak University College, Al-Balqa Applied University, P.O. Box 71911, Shoubak, Jordan.*
[2] *Department of Mathematics, Al-Zaytoonah University of Jordan, Amman 11733, Jordan.*
[3] *Department of Computer Science, University of Tiaret, Tiaret, Algeria and Laboratory of Research in Artificial Intelligence and Systems (LRAIS), University of Tiaret, Algeria.*
[4] *Department of Mathematics, Al al-Bayt University, Mafraq 25113, Jordan.*
[5] *Department of Mathematics, Faculty of Science, Al-Hussein Bin Talal University, P.O. Box 20, Ma'an, Jordan.*

Received: May 16, 2024; Revised: January 30, 2025

Abstract: This work derives uniqueness and Ulam-Hyers (UH) stability results for a coupled system with the Φ-Hilfer proportional fractional derivative. We first construct a new Bielecki-type vector-valued norm in weighted space and then use the fixed-point argument to achieve a new uniqueness criterion. Secondly, the UH and the generalized Ulam-Hyers (GUH) stability is established. To verify the obtained result, an example is provided.

Keywords: *Φ-Hilfer proportional fractional derivative; uniqueness; Ulam-Hyers stability; fixed point theorem.*

Mathematics Subject Classification (2020): 26A33, 34A07, 34A08, 70K20.

* Corresponding author: mailto:alshormanshams@gmail.com

© 2025 InforMath Publishing Group/1562-8353 (print)/1813-7385 (online)/http://e-ndst.kiev.ua

1 Introduction

Fractional calculus stands as a cornerstone in applied mathematics owing to its profound implications across various scientific and technological domains. The prevalence of fractional differential equations (FDEs) in modeling diverse natural and engineered phenomena underscores its significance [1, 9, 13, 16, 18, 22, 28]. Notably, the exploration of coupled systems featuring fractional derivatives, in their assorted manifestations, has been the subject of extensive inquiry by numerous researchers [7, 15, 29, 30].

This pervasive utility instigates a scholarly endeavor towards the exploration of novel fractional operators, to enrich our understanding and refine the accuracy in modeling real-world phenomena [3, 12, 23–25].

A recent milestone in this realm is the introduction by Jarad et al. [10]. of a new definition of generalized fractional derivatives, as elucidated within the frameworks of Caputo and Riemann-Liouville calculus. This innovation, utilizing a specialized instantiation of proportional derivatives, offers a nuanced perspective [10]. Furthermore, by leveraging the notion of proportional derivatives within the context of functional analysis, the research presented in [11] extends and generalizes prior investigations [10]. Notably, Ahmed et al. [2] present the Hilfer proportional fractional derivative (PFD) by amalgamating operators delineated in prior works [2]. Subsequently, in [17], the authors offer a further refinement, denoted as the Φ-Hilfer PFD, accompanied by a comprehensive examination of its properties.

Concurrently, the exploration of the Ulam-Hyers (UH) stability for fractional differential systems has emerged as a focal point of research interest [14]. This pursuit, characterized by its aim to approximate solutions with minimal error vis-à-vis exact counterparts, has engendered a manifold of investigations [1].

This work, in alignment with this scholarly discourse, embarks on a rigorous examination of a coupled system involving the Φ-Hilfer PFD, seeking to illuminate its dynamics and ramifications.

$$\begin{cases} \mathcal{D}_{\mathtt{a}^+}^{\alpha,\beta,\sigma,\Phi}\mathtt{u}_1(z) = \xi_1\mathtt{u}_1(z) + \mathtt{g}_1(z,\mathtt{u}_1(z),\mathtt{u}_2(z)), \quad z \in \mathfrak{J}' := (\mathtt{a},\mathtt{b}], \\ \mathcal{D}_{\mathtt{a}^+}^{\alpha,\beta,\sigma,\Phi}\mathtt{u}_2(z) = \xi_2\mathtt{u}_2(z) + \mathtt{g}_2(z,\mathtt{u}_1(z),\mathtt{u}_2(z)), \quad z \in \mathfrak{J}' := (\mathtt{a},\mathtt{b}], \\ \left(\left(\mathcal{I}_{\mathtt{a}^+}^{1-\delta,\sigma,\Phi}\mathtt{u}_1\right)(\mathtt{a}^+), \left(\mathcal{I}_{\mathtt{a}^+}^{1-\delta,\sigma,\Phi}\mathtt{u}_2\right)(\mathtt{a}^+)\right) = (\zeta_1,\zeta_2), \end{cases} \tag{1}$$

where $\mathcal{D}_{\mathtt{a}^+}^{\alpha,\beta,\sigma,\Phi}$ are the Φ-Hilfer PFDs of order $0 < \alpha < 1$, type $\beta \in [0,1]$ and index $\sigma \in (0,1]$, $\mathcal{I}_{\mathtt{a}^+}^{1-\delta,\sigma,\Phi}$ is the fractional proportional integral (FPI) of order $1-\delta$, where $0 < \delta = \alpha + \beta(1-\alpha) < 1$ and index σ, $\mathtt{g}_i : \mathfrak{J} \times \mathbb{R}^n \times \mathbb{R}^n \longrightarrow \mathbb{R}^n$ are given appropriate functions specified later, $\zeta_i \in \mathbb{R}^n$ and $\xi_i \in \mathbb{R}^{n\times n}$.

System (1) applies to a vast range of models, necessitating further investigation. For instance, the authors in [6] employed it to study the dynamics of a measles epidemic model. Zaitri et al. [31] use it to understand the relationship between pharmacological effects and drugs in anesthesia modeling. Therefore, exploring coupled systems within the Φ-Hilfer PFD with specific configurations becomes essential. We base our study on the fixed-point argument with the vector-valued norm theory in the weighted space of continuous functions. Finally, it is important to highlight that the findings obtained in this study build upon and directly extend the results presented in the related literature, see [2, 4, 5, 17].

The work is divided into three sections. Some necessary background materials are provided in Section 2. The main result of the work is given in Section 3 by using Perov's fixed point principle associated with the Bielecki vector-valued norm. The UH stability of solutions to problem (1) is established in Section 4. An example is given in the last section to illustrate the applicability of our result.

2 Preliminaries

This section presents some background material that will be used throughout this work.

$C(\mathfrak{J}, \mathbb{R}^n)$ is the space of $\mathbb{R}^n$–valued continuous functions on $\mathfrak{J}$ equipped with

$$\|\mathtt{u}\|_{\mathfrak{J}} = \sup_{z\in\mathfrak{J}} \|\mathtt{u}(z)\|.$$

$C^n(\mathfrak{J}, \mathbb{R}^n)$ denotes the space of n-times continuously differentiable functions from $\mathfrak{J}$ into $\mathbb{R}^n$.

$L^\infty(\mathfrak{J}, \mathbb{R}^n)$ is the set of all equivalence classes of measurable functions which are essentially bounded on $\mathfrak{J}$ equipped with

$$\|\mathtt{u}\|_\infty = \sup_{z\in\mathfrak{J}} \|\mathtt{u}(z)\| = \inf\{M > 0;\ \|\mathtt{u}(z)\| \le M \text{ for almost every } \mathtt{u} \in \mathfrak{J}$$

For our convenience, define the set

$$\mathbb{S}^1_+(\mathfrak{J}, \mathbb{R}) = \{\Phi \ :\ \Phi \in C(\mathfrak{J}, \mathbb{R}) \ \text{ and } \ \Phi'(z) > 0 \ \text{ for all } \ z \in \mathfrak{J}.\}$$

For $\Phi \in \mathbb{S}^1_+(\mathfrak{J}, \mathbb{R})$ and $z, s \in \mathfrak{J}$, $(z > s)$, we set

$$\Psi(z, s) = \Phi(z) - \Phi(s) \ \text{ and } \ \Psi(z, s)^\alpha = (\Phi(z) - \Phi(s))^\alpha .$$

We endow the weighted space $\mathfrak{C}_{\delta,\Phi}(\mathfrak{J}, \mathbb{R}^n)$ defined by

$$\mathfrak{C}_{\delta,\Phi}(\mathfrak{J}, \mathbb{R}^n) = \left\{\mathtt{u} : \mathfrak{J} \to \mathbb{R}^n \ :\ \Psi(\cdot, \mathtt{a})^{1-\delta}\mathtt{u}(\cdot) \in C(\mathfrak{J}, \mathbb{R}^n)\right\},$$

with the norm

$$\|\mathtt{u}\|_\delta = \sup_{z\in\mathfrak{J}} \Psi(z, \mathtt{a})^{1-\delta}\|\mathtt{u}(z)\|. \tag{2}$$

Definition 2.1 [8] The Mittag-Leffler function $\mathbb{E}_{\mu,\delta}(\cdot)$ is given by

$$\mathbb{E}_{\mu,\kappa}(\mathtt{u}) = \sum_{j=0}^{\infty} \frac{\mathtt{u}^j}{\Gamma(j\mu + \kappa)}, \quad \mathtt{u} \in \mathbb{R}, \ \text{ and } \ \mu, \kappa > 0,$$

where $\Gamma(\cdot)$ is the Gamma function.

Definition 2.2 [11, 12] Let $\sigma \in (0, 1]$, $\alpha > 0$ and $\Phi \in \mathbb{S}^1_+(\mathfrak{J}, \mathbb{R})$. The left-sided FPI of order α and index σ of the function $\mathtt{u}$ w.r.t Φ is given by

$$\mathcal{I}^{\alpha,\sigma,\Phi}_{\mathtt{a}^+}\mathtt{u}(z) = \frac{1}{\sigma^\alpha\Gamma(\alpha)} \int_{\mathtt{a}}^{z} \mathfrak{L}^{\alpha-1}_{\sigma,\Psi}(z, s)\Phi'(s)\mathtt{u}(s)ds,$$

where $\mathfrak{L}^{\alpha-1}_{\sigma,\Psi}(z, s) = e^{\frac{\sigma-1}{\sigma}\Psi(z,s)}\Psi(z, s)^{\alpha-1}$.

Definition 2.3 [11, 12] Let $\sigma \in (0,1]$, $0 < \alpha < 1$ and $\Phi \in \mathbb{S}^1_+(\mathfrak{J},\mathbb{R})$, the FPD of order α and index σ of the function $\mathtt{u}$ w.r.t Φ is given by

$$\mathcal{D}^{\alpha,\sigma,\Phi}_{\mathtt{a}^+}\mathtt{u}(z) = \mathcal{D}^{1,\sigma,\Phi}_{z}\left(\mathcal{I}^{1-\alpha,\sigma,\Phi}_{\mathtt{a}^+}\mathtt{u}(z)\right),$$

where $\mathcal{D}^{1,\sigma,\Phi}_{z}\mathtt{u}(z) = \mathcal{D}^{\sigma,\Phi}_{z}\mathtt{u}(z) = \sigma\frac{\mathtt{u}'(z)}{\Phi'(z)} + (1-\sigma)\mathtt{u}(z)$.

Definition 2.4 [17] Let $\mathtt{u} \in C^1(\mathfrak{J},\mathbb{R}^n)$ and $\Phi \in \mathbb{S}^1_+(\mathfrak{J},\mathbb{R})$. The Φ-Hilfer FPD (right-sided/left-sided) of order $0 < \alpha < 1$, type $0 \le \beta \le 1$ and index $\sigma \in (0,1]$ of $\mathtt{u}$ w.r.t Φ is given by

$$\mathcal{D}^{\alpha,\beta,\sigma,\Phi}_{\mathtt{a}^\pm}\mathtt{u}(z) = \left(\mathcal{I}^{\beta(1-\alpha),\sigma,\Phi}_{\mathtt{a}^\pm}(\mathcal{D}^{1,\sigma,\Phi}_{z})\mathcal{I}^{(1-\beta)(1-\alpha),\sigma,\Phi}_{\mathtt{a}^\pm}\mathtt{u}\right)(z).$$

Lemma 2.1 [12, 17] *If $\alpha \ge 0$ and $\beta > 0$, then for any $\sigma > 0$, we have*

$$\mathcal{I}^{\alpha,\sigma,\Phi}_{\mathtt{a}^+}\mathfrak{L}^{\beta-1}_{\sigma,\Psi}(z,\mathtt{a}) = \frac{\Gamma(\beta)}{\sigma^\alpha\Gamma(\alpha+\beta)}\mathfrak{L}^{\alpha+\beta-1}_{\sigma,\Psi}(z,\mathtt{a}). \tag{3}$$

Remark 2.1 If $\alpha \ge 0$, $\beta > 0$ and $\sigma \in (0,1]$, then by the fact that $e^{\frac{\sigma-1}{\sigma}\Psi(z,s)} \le 1$, for all $a \le s < z \le b$, we get

$$\mathcal{I}^{\alpha,\sigma,\Phi}_{\mathtt{a}^+}\Psi(z,a)^{\beta-1} \le \sigma^{-\alpha}\mathcal{J}^{\alpha;\Phi}_{\mathtt{a}^+}\Psi(z,\mathtt{a})^{\beta-1},$$

where $\mathcal{J}^{\alpha;\Phi}_{\mathtt{a}^+}(\cdot)$ is the integral defined in [25]. On the order hand, by Lemma 2 from [25], we conclude that

$$\mathcal{I}^{\alpha,\sigma,\Phi}_{\mathtt{a}^+}\Psi(z,\mathtt{a})^{\beta-1} \le \frac{\Gamma(\beta)}{\sigma^\alpha\Gamma(\alpha+\beta)}\Psi(z,\mathtt{a})^{\alpha+\beta-1}. \tag{4}$$

Remark 2.2 Let $\alpha \ge 0$ and $\sigma > 0$, then, by Definition 2.4 and Lemma 2.1, we get

$$\mathcal{D}^{\alpha,\sigma,\Phi}_{\mathtt{a}^+}\mathfrak{L}^{\alpha-1}_{\sigma,\Psi}(z,\mathtt{a}) = 0.$$

Suppose the parameters α, β, δ fulfill the relations

$$\delta = \alpha + \beta(1-\alpha), \quad 0 < \alpha \le \delta \le 1, \quad 1 \geqslant \beta \geqslant 0, \quad \beta < \delta, \quad 1-\delta < 1-\beta(1-\alpha).$$

Therefore, we consider the following spaces:

$$\mathfrak{C}^{\delta}_{\delta,\Phi}(\mathfrak{J},\mathbb{R}^n) = \left\{\mathtt{u} \in \mathfrak{C}_{\delta,\Phi}(\mathfrak{J},\mathbb{R}^n) : \mathcal{D}^{\delta,\sigma,\Phi}_{\mathtt{a}^+}\mathtt{u} \in \mathfrak{C}_{\delta,\Phi}(\mathfrak{J},\mathbb{R}^n)\right\},$$

$$\mathfrak{C}^{\alpha,\beta}_{\delta,\Phi}(\mathfrak{J},\mathbb{R}^n) = \left\{\mathtt{u} \in \mathfrak{C}_{\delta,\Phi}(\mathfrak{J},\mathbb{R}^n) : \mathcal{D}^{\alpha,\beta,\sigma,\Phi}_{\mathtt{a}^+}\mathtt{u} \in \mathfrak{C}_{\delta,\Phi}(\mathfrak{J},\mathbb{R}^n)\right\}.$$

Since $\mathcal{D}^{\alpha,\beta,\sigma,\Phi}_{\mathtt{a}^+}\mathtt{u} = \mathcal{I}^{\beta(1-\alpha),\sigma,\Phi}_{\mathtt{a}^+}\mathcal{D}^{\delta,\sigma,\Phi}_{\mathtt{a}^+}\mathtt{u}$, it follows that

$$\mathfrak{C}^{\delta}_{\delta,\Phi}(\mathfrak{J},\mathbb{R}^n) \subset \mathfrak{C}^{\alpha,\beta}_{\delta,\Phi}(\mathfrak{J},\mathbb{R}^n).$$

Lemma 2.2 [17] *Let $\delta = \beta(1-\alpha)+\alpha$ with $0 < \alpha < 1$, $0 < \sigma \leqslant 1$ and $0 \leqslant \beta \leqslant 1$. If $f \in \mathfrak{C}^{\delta}_{\delta,\Phi}(\mathfrak{J},\mathbb{R}^n)$, then*

1. $\mathcal{D}^{\delta,\sigma,\Phi}_{\mathtt{a}^+}\mathcal{I}^{\alpha,\sigma,\Phi}_{\mathtt{a}^+}\mathtt{u} = \mathcal{D}^{\beta(1-\alpha),\sigma,\Phi}_{\mathtt{a}^+}\mathtt{u}$,

2. $\mathcal{I}_{\mathtt{a}^+}^{\delta,\sigma,\Phi}\mathcal{D}_{\mathtt{a}^+}^{\delta,\sigma,\Phi}\mathtt{u} = \mathcal{I}_{\mathtt{a}^+}^{\alpha,\sigma,\Phi}\mathcal{D}_{\mathtt{a}^+}^{\alpha,\beta,\sigma,\Phi}\mathtt{u}$.

Let $u, v \in \mathbb{R}^n$, $u = (\mathtt{u}_1, \ldots, \mathtt{u}_n)$, $v = (\mathtt{v}_1, \ldots, \mathtt{v}_n)$, by $u \leq v$ we mean $\mathtt{u}_l \leq \mathtt{v}_l$ for all $l = 1, \ldots, n$. Also $|u| = (|\mathtt{u}_1|, \ldots, |\mathtt{u}_n|)$, $\max(u, v) = (\max(\mathtt{u}_1, \mathtt{v}_1), \ldots,$ $\max(\mathtt{u}_n, \mathtt{v}_n))$ and $\mathbb{R}_+^n = \{u \in \mathbb{R}^n : \ \mathtt{u}_l > 0\}$. If $c \in \mathbb{R}$, then $u \leq c$ means $\mathtt{u}_l \leq c$ for each $l = 1, \ldots, n$.

Definition 2.5 [20] Let for a nonempty set $\mathbb{X}$, a map $d : \mathbb{X} \times \mathbb{X} \to \mathbb{R}_+^n$ be called the vector-valued metric on $\mathbb{X}$ if for all $x, y, z \in \mathbb{X}$, the following properties hold:

(a) $d(x, y) = 0$, then $x = y$,

(b) $d(x, y) = d(y, x)$,

(c) $d(x, y) \leq d(x, z) + d(z, y)$.

$(\mathbb{X}, d)$ is called a generalized metric space with
$d(x, y) := (d_1(x, y), \cdots, d_n(x, y))$.

Definition 2.6 [27] We said that a matrix $\mathsf{M} \in \mathsf{M}_{n\times n}(\mathbb{R})$ converges to zero if the spectral radius $\rho(\mathsf{M}) < 1$.

Theorem 2.1 [27] *For any positive matrix* $\mathsf{M} \in \mathsf{M}_{n\times n}(\mathbb{R})$*, the following assertions are equivalent:*

1. $\rho(\mathsf{M}) < 1$*;*

2. M *is convergent to zero;*

3. $I - \mathsf{M}$ *is nonsingular and* $(I - \mathsf{M})^{-1}$ *is a nonnegative matrix.*

Lemma 2.3 *Let* $\alpha, \delta, \varpi > 0$ *and* $\sigma \in (0, 1]$*, then*

$$\mathcal{I}_{\mathtt{a}^+}^{\alpha,\sigma,\Phi}\mathfrak{L}_{\sigma,\Psi}^{\delta-1}(z, \mathtt{a})\mathbb{E}_{\alpha,\delta}(\varpi\Psi(z, \mathtt{a})^\alpha) \quad = \tfrac{\mathfrak{L}_{\sigma,\Psi}^{\delta-1}(z,\mathtt{a})}{\varpi\sigma^\alpha}\left(\mathbb{E}_{\alpha,\delta}(\varpi\Psi(z, \mathtt{a}))^\alpha) - \tfrac{1}{\Gamma(\delta)}\right).$$

Proof. First, we can write

$$\begin{aligned}\mathcal{O} = \mathcal{I}_{\mathtt{a}^+}^{\alpha,\sigma,\Phi}\mathfrak{L}_{\sigma,\Psi}^{\delta-1}(z, \mathtt{a})\mathbb{E}_{\alpha,\delta}(\varpi\Psi(z, \mathtt{a})^\alpha) \quad &= \mathcal{I}_{\mathtt{a}^+}^{\alpha,\sigma,\Phi}\left(\mathfrak{L}_{\sigma,\Psi}^{\delta-1}(z, \mathtt{a})\sum_{j=0}^{\infty}\frac{(\varpi\Psi(z, \mathtt{a})^\alpha)^j}{\Gamma(j\alpha + \delta)}\right)\\ &= \sum_{j=0}^{\infty}\frac{\varpi^j}{\Gamma(j\alpha + \delta)}\ \mathcal{I}_{\mathtt{a}^+}^{\alpha,\sigma,\Phi}\ \mathfrak{L}_{\sigma,\Psi}^{j\alpha+\delta-1}(z, \mathtt{a}).\end{aligned}$$

From Lemma 2.1, one gets

$$\mathcal{O} \quad = \textstyle\sum_{j=0}^{\infty}\frac{\varpi^{j+1}\mathfrak{L}_{\sigma,\Psi}^{\alpha(j+1)+\delta-1}(z,\mathtt{a})}{\sigma^\alpha\varpi\Gamma(\alpha(j+1)+\delta)} = \frac{\mathfrak{L}_{\sigma,\Psi}^{\delta-1}(z,\mathtt{a})}{\sigma^\alpha\varpi}\ \sum_{j=0}^{\infty}\frac{(\varpi\Psi(z,\mathtt{a})^\alpha)^{j+1}}{\Gamma(\alpha(j+1)+\delta)}.$$

Replace $j + 1$ by j', we obtain

$$\mathcal{O} \quad = \quad \frac{\mathfrak{L}_{\sigma,\Psi}^{\delta-1}(z,\mathtt{a})}{\sigma^\alpha\varpi}\ \sum_{j=1}^{\infty}\frac{(\varpi\Psi(z,\mathtt{a})^\alpha)^{j'}}{\Gamma(\alpha j'+\delta)} = \frac{\mathfrak{L}_{\sigma,\Psi}^{\delta-1}(z,\mathtt{a})}{\sigma^\alpha\varpi}\ \left[\sum_{j'=0}^{\infty}\frac{(\varpi\Psi(z,\mathtt{a})^\alpha)^{j'}}{\Gamma(\alpha j'+\delta)} - \frac{1}{\Gamma(\delta)}\right],$$

and this completes the proof.

Lemma 2.4 *We define a Bielecki-type norm, denoted by $\|\cdot\|_{\sigma,B}$, on the Banach space $\mathfrak{C}_{\delta,\Phi}(\mathfrak{J},\mathbb{R}^n)$ as follows:*

$$\|\mathtt{u}\|_{\sigma,B} = \sup_{z\in\mathfrak{J}} \frac{\|\mathtt{u}(z)\|}{\mathfrak{L}^{\delta-1}_{\sigma,\Psi}(z,\mathtt{a})\mathbb{E}_{\alpha,\delta}(\varpi\Psi(z,\mathtt{a})^{\alpha})}. \tag{5}$$

Then the norms $\|\cdot\|_{\sigma,B}$ and $\|\cdot\|_{\delta}$ defined by (2) are equivalent.

Proof. Since $\mathbb{E}_{\alpha,\delta}(\varpi\Psi(z,\mathtt{a})^{\alpha}) > 0$ and $e^{\frac{\sigma-1}{\sigma}\Psi(\mathtt{b},\mathtt{a})} \leq e^{\frac{\sigma-1}{\sigma}\Psi(z,\mathtt{a})} \leq 1$, for $z \in \mathfrak{J}$, one obtains

$$\frac{1}{\mathbb{E}_{\alpha,\delta}(\varpi\Psi(z,\mathtt{a})^{\alpha})} \leq \frac{e^{\frac{1-\sigma}{\sigma}\Psi(z,\mathtt{a})}}{\mathbb{E}_{\alpha,\delta}(\varpi\Psi(z,\mathtt{a})^{\alpha})} \leq \frac{e^{\frac{1-\sigma}{\sigma}\Psi(\mathtt{b},\mathtt{a})}}{\mathbb{E}_{\alpha,\delta}(\varpi\Psi(z,\mathtt{a})^{\alpha})}.$$

Moreover, the function $\mathbb{E}_{\alpha,\delta}(\varpi\Psi(z,\mathtt{a})^{\alpha})$ is continuous on $\mathfrak{J}$, then there exists $c^*, c_* > 0$ so that $c^* = \sup_{z\in\mathfrak{J}} \mathbb{E}_{\alpha,\delta}(\varpi\Psi(z,\mathtt{a})^{\alpha})$ and $c_* = \inf_{z\in\mathfrak{J}} \mathbb{E}_{\alpha,\delta}(\varpi\Psi(z,\mathtt{a})^{\alpha})$. Accordingly,

$$\frac{1}{c^*}\|u\|_{\mathfrak{C}_{\delta,\Phi}} \leq \|u\|_{\sigma,B} \leq \frac{\|u\|_{\mathfrak{C}_{\delta,\Phi}}}{c_* e^{\frac{\sigma-1}{\sigma}\Psi(\mathtt{b},\mathtt{a})}},$$

which means that $\|\cdot\|_{\sigma,B}$ and $\|\cdot\|_{\delta}$ are equivalent.

3 Uniqueness of the Solution

This section introduces sufficient conditions to prove the uniqueness of solutions of the system (1). Firstly, consider the Banach space $\mathbf{E} := \mathfrak{C}_{\delta,\Phi}(\mathfrak{J},\mathbb{R}^n) \times \mathfrak{C}_{\delta,\Phi}(\mathfrak{J},\mathbb{R}^n)$ equipped with the Bielecki vector-valued norm

$$\|(\mathtt{u}_1,\mathtt{u}_2)\|_{\mathbf{E},B} = \begin{pmatrix} \|\mathtt{u}_1\|_{\sigma,B} \\ \|\mathtt{u}_2\|_{\sigma,B} \end{pmatrix}.$$

Next, we need the following hypotheses:

$(\mathcal{H}_1)$ $\mathtt{g}_i : \mathfrak{J}\times\mathbb{R}^n\times\mathbb{R}^n \longrightarrow \mathbb{R}^n$ $(i = 1, 2)$ are functions and

$$\mathtt{g}_i(z,\mathtt{u}_1(\cdot),\mathtt{u}_2(\cdot)) \in \mathfrak{C}^{\beta(1-\alpha)}_{\delta,\Phi}(\mathfrak{J},\mathbb{R}^n) \quad \text{for any} \quad \mathtt{u}_1,\mathtt{u}_2 \in \mathfrak{C}^{\beta(1-\alpha)}_{\delta,\Phi}(\mathfrak{J},\mathbb{R}^n),$$

$(\mathcal{H}_2)$ There exist functions $\chi_i, \widehat{\chi}_i \in L^{\infty}(\mathfrak{J},\mathbb{R}^+)$ such that

$$\|\mathtt{g}_i(z,\mathtt{u}_1,\mathtt{u}_2) - \mathtt{g}_i(z,\mathtt{v}_1,\mathtt{v}_2)\| \leq \chi_i(z)\|\mathtt{u}_1-\mathtt{v}_1\| + \widehat{\chi}_i(z)\|\mathtt{u}_2-\mathtt{v}_2\|$$

for all $z \in \mathfrak{J}$ and each $\mathtt{u}_1,\mathtt{u}_2,\mathtt{v}_1,\mathtt{v}_2 \in \mathbb{R}^n$.

For the sake of brevity, we will use the notation

$$N_{\sigma,\Phi}(\alpha,z) = \frac{\Psi(\mathtt{z},\mathtt{a})^{\alpha}}{\sigma^{\alpha}\Gamma(\alpha+1)} \quad \text{and} \quad N_{\sigma,\Phi}(\alpha,\mathtt{b},c_*) = \frac{\Psi(\mathtt{b},\mathtt{a})^{1-\beta(1-\alpha)}}{\sigma^{\alpha}\Gamma(\alpha+1)e^{\frac{\sigma-1}{\sigma}\Psi(\mathtt{b},\mathtt{a})}c_*}.$$

Theorem 3.1 *Assume that the conditions $(\mathcal{H}_1)-(\mathcal{H}_2)$ hold. Then system (1) has a unique global solution in $\mathbf{F} := \mathfrak{C}^{\delta}_{\delta,\Phi}(\mathfrak{J},\mathbb{R}^n) \times \mathfrak{C}^{\delta}_{\delta,\Phi}(\mathfrak{J},\mathbb{R}^n)$.*

Proof. By Lemma 3.9 from [17], the solutions of the system (1) are the solutions of the following coupled integral equations:

$$\begin{cases} \mathtt{u}_1(z) &= \frac{\zeta_1}{\sigma^{\delta-1}\Gamma(\delta)}\mathfrak{L}^{\delta-1}_{\sigma,\Psi}(z,\mathtt{a}) + \mathcal{I}^{\alpha,\sigma,\Phi}_{\mathtt{a}^+}\left(\xi_1\mathtt{u}_1(z) + \mathtt{g}_1(z,\mathtt{u}_1(z),\mathtt{u}_2(z))\right), \\ \mathtt{u}_2(z) &= \frac{\zeta_2}{\sigma^{\delta-1}\Gamma(\delta)}\mathfrak{L}^{\delta-1}_{\sigma,\Psi}(z,\mathtt{a}) + \mathcal{I}^{\alpha,\sigma,\Phi}_{\mathtt{a}^+}\left(\xi_2\mathtt{u}_2(z) + \mathtt{g}_2(z,\mathtt{u}_1(z),\mathtt{u}_2(z))\right). \end{cases} \tag{6}$$

We define the operator $\mathcal{L} = (\mathcal{L}_1, \mathcal{L}_2) : \mathbf{E} \longrightarrow \mathbf{E}$ by

$$\mathcal{L}(\mathtt{u}_1,\mathtt{u}_2) = (\mathcal{L}_1(\mathtt{u}_1,\mathtt{u}_2), \mathcal{L}_2(\mathtt{u}_1,\mathtt{u}_2)), \tag{7}$$

where for $i = 1, 2$,

$$\mathcal{L}_i(\mathtt{u}_1,\mathtt{u}_2)(z) = \frac{\zeta_i}{\sigma^{\delta-1}\Gamma(\delta)}\mathfrak{L}^{\delta-1}_{\sigma,\Psi}(z,\mathtt{a}) + \mathcal{I}^{\alpha,\sigma,\Phi}_{\mathtt{a}^+}\left(\xi_i\mathtt{u}_i(z) + \mathtt{g}_i(z,\mathtt{u}_1(z),\mathtt{u}_2(z))\right). \tag{8}$$

Now, let $(\mathtt{u}_1,\mathtt{u}_2), (\mathtt{v}_1,\mathtt{v}_2) \in \mathbf{E}$ and $z \in \mathfrak{J}$, using $(\mathcal{H}_2)$, one gets

$$\begin{aligned}
&\|\mathcal{L}_1(\mathtt{u}_1,\mathtt{u}_2)(z) - \mathcal{L}_1(\mathtt{v}_1,\mathtt{v}_2)(z)\| \\
&\leq \|\xi_1\|\mathcal{I}^{\alpha,\sigma,\Phi}_{\mathtt{a}^+}\left(\|\mathtt{u}_1(z) - \mathtt{v}_1(z)\|\right) + \mathcal{I}^{\alpha,\sigma,\Phi}_{\mathtt{a}^+}\left(\|\mathtt{g}_1(z,\mathtt{u}_1(z),\mathtt{u}_2(z)) - \mathtt{g}_1(z,\mathtt{v}_1(z),\mathtt{v}_2(z))\|\right), \\
&\leq \|\xi_1\|\mathcal{I}^{\alpha,\sigma,\Phi}_{\mathtt{a}^+}\left(\|\mathtt{u}_1(z) - \mathtt{v}_1(z)\|\right) + \mathcal{I}^{\alpha,\sigma,\Phi}_{\mathtt{a}^+}\left(\chi_1(z)\|\mathtt{u}_1(z) - \mathtt{v}_1(z)\| + \widehat{\chi}_1(z)\|\mathtt{u}_2(z) - \mathtt{v}_2(z)\|\right), \\
&\leq \|\xi_1\|\|\mathtt{u}_1 - \mathtt{v}_1\|_{\sigma,B}\mathcal{I}^{\alpha,\sigma,\Phi}_{\mathtt{a}^+}\left(\mathfrak{L}^{\delta-1}_{\sigma,\Psi}(z,\mathtt{a})\mathbb{E}_{\alpha,\delta}(\varpi\Psi(z,\mathtt{a})^\alpha)\right), \\
&\quad + \left(\|\chi_1\|_\infty\|\mathtt{u}_1 - \mathtt{v}_1\|_{\sigma,B} + \|\widehat{\chi}_1\|_\infty\|\mathtt{u}_2 - \mathtt{v}_2\|_{\sigma,B}\right)\mathcal{I}^{\alpha,\sigma,\Phi}_{\mathtt{a}^+}\left(\mathfrak{L}^{\delta-1}_{\sigma,\Psi}(z,\mathtt{a})\mathbb{E}_{\alpha,\delta}(\varpi\Psi(z,\mathtt{a})^\alpha)\right).
\end{aligned}$$

By Lemma 2.3, we have

$$\begin{aligned}
&\|\mathcal{L}_1(\mathtt{u}_1,\mathtt{u}_2)(z) - \mathcal{L}_1(\mathtt{v}_1,\mathtt{v}_2)(z)\| \\
&\leq \Big(\left(\|\xi_1\| + \|\chi_1\|_\infty\right)\|\mathtt{u}_1 - \mathtt{v}_1\|_{\sigma,B} + \|\widehat{\chi}_1\|_\infty\|\mathtt{u}_2 - \mathtt{v}_2\|_{\sigma,B}\Big)\times \\
&\quad \frac{\mathfrak{L}^{\delta-1}_{\sigma,\Psi}(z,\mathtt{a})}{\varpi\sigma^\alpha}\left(\mathbb{E}_{\alpha,\delta}(\varpi\Psi(z,\mathtt{a})^\alpha) - \frac{1}{\Gamma(\delta)}\right).
\end{aligned}$$

Hence

$$\begin{aligned}
\|\mathcal{L}_1(\mathtt{u}_1,\mathtt{u}_2) - \mathcal{L}_1(\mathtt{v}_1,\mathtt{v}_2)\|_{\sigma,B} &\leq \Big(\left(\|\xi_1\| + \|\chi_1\|_\infty\right)\|\mathtt{u}_1 - \mathtt{v}_1\|_{\sigma,B} + \|\widehat{\chi}_1\|_\infty\|\mathtt{u}_2 - \mathtt{v}_2\|_{\sigma,B}\Big)\times \\
&\quad \frac{1}{\varpi\sigma^\alpha}\left(1 - \frac{1}{\Gamma(\delta)\mathbb{E}_{\alpha,\delta}(\varpi\Psi(z,\mathtt{a})^\alpha)}\right) \\
&\leq \frac{\|\xi_1\| + \|\chi_1\|_\infty}{\varpi\sigma^\alpha}\|\mathtt{u}_1 - \mathtt{v}_1\|_{\sigma,B} + \frac{\|\widehat{\chi}_1\|_\infty}{\varpi\sigma^\alpha}\|\mathtt{u}_2 - \mathtt{v}_2\|_{\sigma,B}.
\end{aligned}$$

By the same technique, one obtains

$$\|\mathcal{L}_2(\mathtt{u}_1,\mathtt{u}_2) - \mathcal{L}_2(\mathtt{v}_1,\mathtt{v}_2)\|_{\sigma,B} \leq \frac{\|\chi_2\|_\infty}{\varpi\sigma^\alpha}\|\mathtt{u}_1 - \mathtt{v}_1\|_{\sigma,B} + \frac{\|\xi_2\| + \|\widehat{\chi}_2\|_\infty}{\varpi\sigma^\alpha}\|\mathtt{u}_2 - \mathtt{v}_2\|_{\sigma,B}.$$

This implies that

$$\|\mathcal{L}(\mathtt{u}_1,\mathtt{u}_2) - \mathcal{L}(\mathtt{v}_1,\mathtt{v}_2)\|_{\mathbf{E},B} \leq \mathsf{A}_\varpi\|(\mathtt{u}_1,\mathtt{u}_2) - (\mathtt{v}_1,\mathtt{v}_2)\|_{\mathbf{E},B},$$

where

$$\mathsf{A}_{\varpi} = \frac{1}{\varpi\sigma^{\alpha}} \begin{pmatrix} \|\xi_1\| + \|\chi_1\|_{\infty} & \|\widehat{\chi}_1\|_{\infty} \\ \|\chi_2\|_{\infty} & \|\xi_2\| + \|\widehat{\chi}_2\|_{\infty} \end{pmatrix}. \tag{9}$$

When taking ϖ large enough, the matrix A_{ϖ} converges to zero. Therefore, by applying Perov's theorem [19], we show that $\mathcal{L}$ has a unique fixed point $(\mathtt{u}_1, \mathtt{u}_2) \in \mathbf{E}$. Therefore, the system (1) has a unique global solution.

Next, we show that such a fixed point $(\mathtt{u}_1, \mathtt{u}_2) \in \mathbf{E}$ is actually in $\mathbf{F}$. Since $\mathtt{y}_1$ and $\mathtt{y}_2$ are the unique fixed points of $\mathcal{L}_1$ and $\mathcal{L}_2$ in $\mathbf{E}$, respectively, for $z \in (a, b]$, we have

$$\begin{cases} \mathtt{y}_1(z) &= \frac{\zeta_1}{\sigma^{\delta-1}\Gamma(\delta)} \mathfrak{L}^{\delta-1}_{\sigma,\Psi}(z, \mathtt{a}) + \mathcal{I}^{\alpha,\sigma,\Phi}_{\mathtt{a}^+} \left(\xi_1 \mathtt{y}_1(z) + \mathtt{g}_1(z, \mathtt{y}_1(z), \mathtt{y}_2(z))\right), \\ \mathtt{y}_2(z) &= \frac{\zeta_2}{\sigma^{\delta-1}\Gamma(\delta)} \mathfrak{L}^{\delta-1}_{\sigma,\Psi}(z, \mathtt{a}) + \mathcal{I}^{\alpha,\sigma,\Phi}_{\mathtt{a}^+} \left(\xi_2 \mathtt{y}_2(z) + \mathtt{g}_2(z, \mathtt{y}_1(z), \mathtt{y}_2(z))\right). \end{cases}$$

After multiplying both sides of the last system by $\mathcal{D}^{\delta,\sigma,\Phi}_{\mathtt{a}^+}$, it follows from Remark 2.2 and Lemma 2.2 that

$$\begin{cases} \mathcal{D}^{\delta,\sigma,\Phi}_{\mathtt{a}^+} \mathtt{y}_1(z) &= \mathcal{D}^{\beta(1-\alpha),\sigma,\Phi}_{\mathtt{a}^+} \left(\xi_1 \mathtt{y}_1(z) + \mathtt{g}_1(z, \mathtt{y}_1(z), \mathtt{y}_2(z))\right), \\ \mathcal{D}^{\delta,\sigma,\Phi}_{\mathtt{a}^+} \mathtt{y}_2(z) &= \mathcal{D}^{\beta(1-\alpha),\sigma,\Phi}_{\mathtt{a}^+} \left(\xi_2 \mathtt{y}_2(z) + \mathtt{g}_2(z, \mathtt{y}_1(z), \mathtt{y}_2(z))\right). \end{cases}$$

Since $\delta \geq \alpha$ and by $(\mathcal{H}_1)$, we get

$$\begin{cases} \mathcal{D}^{\beta(1-\alpha),\sigma,\Phi}_{\mathtt{a}^+} \left(\xi_1 \mathtt{y}_1(z) + \mathtt{g}_1(z, \mathtt{y}_1(z), \mathtt{y}_2(z))\right) \in \mathfrak{C}_{\delta,\Phi}(\mathfrak{J}, \mathbb{R}^n), \\ \mathcal{D}^{\beta(1-\alpha),\sigma,\Phi}_{\mathtt{a}^+} \left(\xi_2 \mathtt{y}_2(z) + \mathtt{g}_2(z, \mathtt{y}_1(z), \mathtt{y}_2(z))\right) \in \mathfrak{C}_{\delta,\Phi}(\mathfrak{J}, \mathbb{R}^n). \end{cases}$$

Hence $\mathcal{D}^{\delta,\sigma,\Phi}_{\mathtt{a}^+} \mathtt{y}_i \in \mathfrak{C}_{\delta,\Phi}(\mathfrak{J}, \mathbb{R}^n)$, $i = 1, 2$, it follows from the definition of the space $\mathfrak{C}^{\beta(1-\alpha)}_{\delta,\Phi}(\mathfrak{J}, \mathbb{R}^n)$ that $\mathtt{y}_i \in \mathfrak{C}^{\delta}_{\delta,\Phi}(\mathfrak{J}, \mathbb{R}^n)$, $i = 1, 2$. As a sequel to the steps outlined above, we infer that the coupled system (1) has a unique solution in $\mathbf{F}$.

4 Stability Results

This section discusses the stability in the UH and GUH sense of the coupled system (1).

Let $\eta_1, \eta_2 > 0$. We consider the inequalities

$$\begin{cases} \|\mathcal{D}^{\alpha,\beta,\sigma,\Phi}_{\mathtt{a}^+} \mathtt{u}_1(z) - \xi_1 \mathtt{u}_1(z) - \mathtt{g}_1(z, \mathtt{u}_1(z), \mathtt{u}_2(z))\| \leq \eta_1, \\ \|\mathcal{D}^{\alpha,\beta,\sigma,\Phi}_{\mathtt{a}^+} \mathtt{u}_2(z) - \xi_2 \mathtt{u}_2(z) - \mathtt{g}_2(z, \mathtt{u}_1(z), \mathtt{u}_2(z))\| \leq \eta_2, \end{cases} \quad z \in \mathfrak{J}. \tag{10}$$

Definition 4.1 [14, 26] The system (1) is stable in the UH sense if we can find $\Omega_i \geqslant 0$, $i = \overline{1,4}$, such that for any $\eta_1, \eta_1 > 0$ and any solution $(\mathtt{v}_1, \mathtt{v}_2) \in \mathbf{E}$ of inequalities (10), there exists a solution $(\mathtt{u}_1, \mathtt{u}_2) \in \mathbf{E}$ of the problem (1) with $\zeta_i = \left(\mathcal{I}^{1-\delta,\sigma,\Phi}_{\mathtt{a}^+} \mathtt{v}_i\right)(\mathtt{a}^+)$, $i = 1, 2$, such that

$$\begin{cases} \|\mathtt{v}_1 - \mathtt{u}_1\|_{\sigma,B} \leq \Omega_1 \eta_1 + \Omega_2 \eta_2, \\ \|\mathtt{v}_2 - \mathtt{u}_2\|_{\sigma,B} \leq \Omega_3 \eta_1 + \Omega_4 \eta_2. \end{cases} \tag{11}$$

Definition 4.2 The system (1) is stable in the GUH sence if we can find $\mathcal{N} = (\mathcal{N}_1, \mathcal{N}_2) \in C(\mathbb{R}_+, \mathbb{R}_+) \times C(\mathbb{R}_+, \mathbb{R}_+)$ with $\mathcal{N}(0) = (\mathcal{N}_1(0), \mathcal{N}_2(0)) = (0, 0)$ such that for any $\eta = (\eta_1, \eta_2) > 0$ and any solution $(\mathtt{v}_1, \mathtt{v}_2) \in \mathbf{E}$ of inequalities (10), there exists a solution $(\mathtt{u}_1, \mathtt{u}_2) \in \mathbf{E}$ of the problem (1) with $\zeta_i = \left(\mathcal{I}_{\mathtt{a}^+}^{1-\delta,\sigma,\Phi}\mathtt{v}_i\right)(\mathtt{a}^+)$, $i = 1, 2$, complying with

$$\|(\mathtt{v}_1, \mathtt{v}_2) - (\mathtt{u}_1, \mathtt{u}_2)\|_{\mathbf{E},B} \leq \mathcal{N}(\eta).$$

Theorem 4.1 (Stability results) *Suppose that*

1. *All hypotheses of Theorem 3.1 are verified,*
2. *For any $\eta_1, \eta_2 > 0$, the inequalities (10) have at least one solution.*

Then the problem (1) is UH and GUH stable w.r.t to the Bielecki vector-valued norm.

Proof. Let $\eta_1, \eta_2 > 0$ be arbitrary numbers and let $(\mathtt{v}_1, \mathtt{v}_2) \in \mathbf{E}$ be a solution of the inequalities (10). According to Theorem 3.1, there exists a solution $(\mathtt{u}_1, \mathtt{u}_2)$ of the system (1) on $\mathfrak{J}$ with

$$\zeta_i = \left(\mathcal{I}_{\mathtt{a}^+}^{1-\delta,\sigma,\Phi}\mathtt{v}_i\right)(\mathtt{a}^+), \quad i = 1, 2,$$

and it is a fixed point of the operator $\mathcal{L}$ defined by (7).

On the other hand, applying operator $\mathcal{I}_{\mathtt{a}^+}^{\alpha,\sigma,\Phi}$ on both sides of (10), we get

$$\|\mathcal{I}_{\mathtt{a}^+}^{\alpha,\sigma,\Phi}\mathcal{D}_{\mathtt{a}^+}^{\alpha,\beta,\sigma,\Phi}\mathtt{v}_i(z) - \mathcal{I}_{\mathtt{a}^+}^{\alpha,\sigma,\Phi}\left(\xi_i\mathtt{v}_i(z) + \mathtt{g}_i(z, \mathtt{v}_1(z), \mathtt{v}_2(z))\right)\| \leq \mathcal{I}_{\mathtt{a}^+}^{\alpha,\sigma,\Phi}\eta_i, \quad i = 1, 2.$$

Using Lemma 3.8 from [17] yields

$$\|\mathtt{v}_i(z) - \mathcal{L}_i(\mathtt{v}_1, \mathtt{v}_2)(z)\| \leq \eta_i \left(\mathcal{I}_{\mathtt{a}^+}^{\alpha,\sigma,\Phi}1\right)(z), \quad i = 1, 2.$$

Hence, we have by Remark 2.1,

$$\|\mathtt{v}_i(z) - \mathcal{L}_i(\mathtt{v}_1, \mathtt{v}_2)(z)\| \quad \leq \quad \tfrac{\eta_i\Psi(z,\mathtt{a})^\alpha}{\sigma^\alpha\Gamma(\alpha+1)} := \eta_i N_{\sigma,\Phi}(\alpha, z), \quad i = 1, 2. \tag{12}$$

Now, by $(\mathcal{H}_2)$ and using (12) and Lemma 2.3, we have

$$\begin{aligned}
&\|\mathtt{v}_1(z) - \mathtt{u}_1(z)\| \\
&\quad = \|\mathtt{v}_1(z) - \mathcal{L}_1(\mathtt{v}_1, \mathtt{v}_2)(z) + \mathcal{L}_1(\mathtt{v}_1, \mathtt{v}_2)(z) - \mathtt{u}_1(z)\|, \\
&\quad \leq \|\mathtt{v}_1(z) - \mathcal{L}_1(\mathtt{v}_1, \mathtt{v}_2)(z)\| + \|\mathcal{L}_1(\mathtt{v}_1, \mathtt{v}_2)(z) - \mathcal{L}_1(\mathtt{u}_1, \mathtt{u}_2)(z)\|, \\
&\quad \leq \eta_1 N_{\sigma,\Phi}(\alpha, z) + \left(\left(\|\xi_1\| + \|\chi_1\|_\infty\right)\|\mathtt{v}_1 - \mathtt{u}_1\|_{\sigma,B} + \|\widehat{\chi}_1\|_\infty\|\mathtt{v}_2 - \mathtt{u}_2\|_{\sigma,B}\right) \\
&\qquad \times \tfrac{\mathfrak{L}_{\sigma,\Psi}^{\delta-1}(z,\mathtt{a})}{\varpi\sigma^\alpha}\left(\mathbb{E}_{\alpha,\delta}(\varpi\Psi(z, \mathtt{a})^\alpha) - \tfrac{1}{\Gamma(\delta)}\right).
\end{aligned}$$

Hence, we get

$$\|\mathtt{v}_1 - \mathtt{u}_1\|_{\sigma,B} \leq N_{\sigma,\Phi}(\alpha, \mathtt{b}, c_*)\eta_1 + \frac{\|\xi_1\| + \|\chi_1\|_\infty}{\varpi\sigma^\alpha}\|\mathtt{v}_1 - \mathtt{u}_1\|_{\sigma,B} + \frac{\|\widehat{\chi}_1\|_\infty}{\varpi\sigma^\alpha}\|\mathtt{v}_2 - \mathtt{u}_2\|_{\sigma,B}. \tag{13}$$

Similarly, we have

$$\|\mathtt{v}_2-\mathtt{u}_2\|_{\sigma,B} \leq N_{\sigma,\Phi}(\alpha,\mathtt{b},c_*)\eta_2+\frac{\|\chi_2\|_\infty}{\varpi\sigma^\alpha}\|\mathtt{v}_1-\mathtt{u}_1\|_{\sigma,B}+\frac{\|\xi_2\|+\|\widehat{\chi}_2\|_\infty}{\varpi\sigma^\alpha}\|\mathtt{v}_2-\mathtt{u}_2\|_{\sigma,B}. \quad (14)$$

Inequalities (13) and (14) yield

$$(\mathsf{I}-\mathsf{A}_\varpi)\begin{pmatrix}\|\mathtt{v}_1-\mathtt{u}_1\|_{\sigma,B}\\ \|\mathtt{v}_2-\mathtt{u}_2\|_{\sigma,B}\end{pmatrix} \leq \begin{pmatrix}N_{\sigma,\Phi}(\alpha,\mathtt{b},c_*)\eta_1\\ N_{\sigma,\Phi}(\alpha,\mathtt{b},c_*)\eta_2\end{pmatrix}, \quad (15)$$

where A_ϖ is defined in (9). Hence, A_ϖ converges to zero when taking ϖ large enough, by Theorem 2.1, $(\mathsf{I}-\mathsf{A}_\varpi)^{-1}$ has nonnegative elements since the matrix $(\mathsf{I}-\mathsf{A}_\varpi)$ is non-singular. Accordingly, (15) is equivalent to

$$\begin{pmatrix}\|\mathtt{v}_1-\mathtt{u}_1\|_{\sigma,B}\\ \|\mathtt{v}_2-\mathtt{u}_2\|_{\sigma,B}\end{pmatrix} \leq (\mathsf{I}-\mathsf{A}_\varpi)^{-1}\begin{pmatrix}N_{\sigma,\Phi}(\alpha,\mathtt{b},c_*)\eta_1\\ N_{\sigma,\Phi}(\alpha,\mathtt{b},c_*)\eta_2\end{pmatrix}, \quad (16)$$

which means that

$$\begin{cases}\|\mathtt{v}_1-\mathtt{u}_1\|_{\sigma,B} & \leq & \Omega_1\eta_1+\Omega_2\eta_2,\\ \|\mathtt{v}_2-\mathtt{u}_2\|_{\sigma,B} & \leq & \Omega_3\eta_1+\Omega_4\eta_2,\end{cases} \quad (17)$$

where $\Omega_i=\theta_i N_{\sigma,\Phi}(\alpha,\mathtt{b},c_*)$ and $(\theta_i)_{i=\overline{1,4}}$ are the elements of $(\mathsf{I}-\mathsf{A}_\varpi)^{-1}$. This proves that system (1) is UH stable.

Moreover, let

$$\theta=(\theta_1,\theta_2)=(\Omega_1+\Omega_3,\Omega_2+\Omega_4),$$

we can write inequalities (17) as

$$\|(\mathtt{v}_1,\mathtt{v}_2)-(\mathtt{u}_1,\mathtt{u}_2)\|_{\mathbf{E},B} \leq \mathcal{N}(\eta),$$

where $\mathcal{N}(\eta)=\theta\eta$ with $\mathcal{N}(0)=(0)$. This shows that the coupled system (1) is GUH stable.

5 Examples

Here, we provide some illustrative examples to validate the obtained results.

Example 1. We consider a particular case of our systems (1) with $\mathfrak{J}=[0,\mathtt{b}]$ and

$$\xi_1=\begin{pmatrix}1/2 & 1\\ 3/2 & 2\end{pmatrix}, \quad \xi_2=\begin{pmatrix}5 & 6\\ 7 & 8\end{pmatrix},$$

and $\mathtt{g}_1,\mathtt{g}_2:\mathfrak{J}\times\mathbb{R}^2\times\mathbb{R}^2\to\mathbb{R}^2$ such that $\mathtt{u}_1=(\mathtt{t}_1,\mathtt{t}_2),\mathtt{u}_2=(\mathtt{r}_1,\mathtt{r}_2)$ with

$$\mathtt{g}_1(z,\mathtt{u}_1(z),\mathtt{u}_2(z))=\begin{pmatrix}\frac{|\mathtt{t}_1(z)|+|\mathtt{t}_2(z)|}{z+5}\\ e^{-2z-1}\log_e\left(1+|\mathtt{r}_1(z)|+|\mathtt{r}_2(z)|\right)\end{pmatrix},$$

$$\mathtt{g}_2(z,\mathtt{u}_1(z),\mathtt{u}_2(z))=\frac{1}{e^z+5}\begin{pmatrix}\sin(|\mathtt{r}_1(z)|+|\mathtt{r}_2(z)|)\\ \tan^{-1}\left(\mathtt{t}_1(z)+\mathtt{t}_2(z)\right)\end{pmatrix}.$$

Clearly, the functions $\mathtt{u}_i$, $i = 1, 2$, are continuous. Furthermore, for all $\mathtt{x}_1, \mathtt{x}_2, \bar{\mathtt{x}}_1, \bar{\mathtt{x}}_2 \in \mathbb{R}^2$ and $z \in \mathfrak{J}$, one has

$$\|\mathtt{g}_1(z, \mathtt{x}_1, \mathtt{x}_2) - \mathtt{g}_1(z, \bar{\mathtt{x}}_1, \bar{\mathtt{x}}_2)\|_1 \leq \frac{1}{z+5}\|\mathtt{x}_1 - \bar{\mathtt{x}}_1\|_1 + \frac{1}{e^{2z+1}}\|\mathtt{x}_2 - \bar{\mathtt{x}}_2\|_1$$

and

$$\|\mathtt{g}_2(z, \mathtt{x}_1, \mathtt{x}_2) - \mathtt{g}_2(z, \bar{\mathtt{x}}_1, \bar{\mathtt{x}}_2)\|_1 \leq \frac{1}{e^z+5}\|\mathtt{x}_1 - \bar{\mathtt{x}}_1\|_1 + \frac{1}{e^z+5}\|\mathtt{x}_2 - \bar{\mathtt{x}}_2\|_1,$$

where $\|\cdot\|_1$ is a norm in $\mathbb{R}^2$ defined as follows:

$$\|(\mathtt{x}_1, \mathtt{x}_2)\|_1 = |\mathtt{x}_1| + |\mathtt{x}_2|.$$

Hence the hypothesis $(\mathcal{H}_2)$ is satisfied with

$$\chi_1(z) = \frac{1}{z+5}, \quad \widehat{\chi}_1(z) = \frac{1}{e^{2z+1}}, \quad \chi_2(z) = \widehat{\chi}_2(z) = \frac{1}{e^z+5}.$$

Obviously,

$$\|\chi_1\|_{L^\infty} = \frac{1}{5}, \quad \|\widehat{\chi}_1\|_{L^\infty} = \frac{1}{e}, \quad \|\chi_2\|_{L^\infty} = \|\widehat{\chi}_2\|_{L^\infty} = \frac{1}{6},$$

and

$$\|\xi_1\|_{\max} = 2, \quad \|\xi_2\|_{\max} = 8,$$

where $\|\cdot\|_{\max}$ is a norm of the matrix $\mathsf{A} = (a_{k,j})$ defined as follows:

$$\|\mathsf{A}\|_{\max} = \max_{k,j} |a_{k,j}|.$$

Moreover, the matrix A_ϖ defined by (9) has the following form:

$$\mathsf{A}_\varpi = \begin{pmatrix} \frac{11}{5\varpi\sigma^\alpha} & \frac{1}{e\varpi\sigma^\alpha} \\ \frac{1}{6\varpi\sigma^\alpha} & \frac{49}{6\varpi\sigma^\alpha} \end{pmatrix}.$$

It converges to zero for ϖ large enough. By Theorem 3.1, system (1) with the above conditions, has a unique solution. System (1) is not only UH stable but also GUH stable, according to Theorem 4.1.

Example 2. Consider the following systems:

$$\begin{cases} \mathcal{D}_{0^+}^{\frac{1}{2},\frac{1}{2},\frac{1}{4},\Phi}\mathtt{u}_1(z) = \frac{2}{3}\mathtt{u}_1(z) + \mathtt{g}_1(z, \mathtt{u}_1(z), \mathtt{u}_2(z)), \\ \mathcal{D}_{0^+}^{\frac{1}{2},\frac{1}{2},\frac{1}{4},\Phi}\mathtt{u}_2(z) = \frac{1}{5}\mathtt{u}_2(z) + \mathtt{g}_2(z, \mathtt{u}_1(z), \mathtt{u}_2(z)), \end{cases} \quad z \in (0, 1] \tag{18}$$

with the initial conditions

$$\begin{cases} \left(\mathcal{I}_{0^+}^{1-\frac{3}{4},\frac{1}{4},\Phi}\mathtt{u}_1\right)(0^+) &= \sqrt{2}, \\ \left(\mathcal{I}_{0^+}^{1-\frac{3}{4},\frac{1}{4},\Phi}\mathtt{u}_2\right)(0^+) &= \sqrt{3}. \end{cases} \tag{19}$$

In this case, we take

$$\alpha = \beta = \frac{1}{2}, \delta = \frac{3}{4}, \sigma = \frac{1}{4}, \xi_1 = \frac{2}{3}, \xi_2 = \frac{1}{5}, \zeta_1 = \sqrt{2}, \zeta_2 = \sqrt{3}, \mathtt{a} = 0, \mathtt{b} = 1, n = 1,$$

and

$$\begin{aligned}\mathtt{g}_1(z,\mathtt{u}_1(z),\mathtt{u}_2(z)) &= \tfrac{\sin(\mathtt{u}_1(z))}{e^{-z}+8} + (z+\sqrt{2})\ln(|\mathtt{u}_2(z)|+1),\\ \mathtt{g}_2(z,\mathtt{u}_1(z),\mathtt{u}_2(z)) &= \tfrac{1}{e^{z}+8}\left(1+\tfrac{|\mathtt{u}_1(z)|}{1+|\mathtt{u}_1(z)|}\right) + (e^z+1)(\arctan(\mathtt{u}_2(z))+1).\end{aligned}$$

Then

$$\mathfrak{C}_{\delta,\Phi}(\mathfrak{J},\mathbb{R}^n) = \mathfrak{C}_{3/4,\Phi}([0,1],\mathbb{R}) = \left\{\mathtt{u}:[0,1]\to\mathbb{R}:\ \Psi(z,0)^{1/4}\mathtt{u}\in\mathfrak{C}([0,1],\mathbb{R})\right\},$$

$$\mathfrak{C}^{\beta(1-\alpha)}_{\delta,\Phi}(\mathfrak{J},\mathbb{R}^n) = \mathfrak{C}^{1/4}_{3/4,\Phi}([0,1],\mathbb{R}) = \left\{\mathtt{u}\in\mathfrak{C}_{3/4,\Phi}([0,1],\mathbb{R}):\ \mathcal{D}^{1/4,1/4,\Phi}_{0^+}\mathtt{u}\in\mathfrak{C}_{3/4,\Phi}([0,1],\mathbb{R})\right\}.$$

It is clear that the continuous functions $\mathtt{g}_i \in \mathfrak{C}^{1/4}_{3/4,\Phi}([0,1],\mathbb{R})$, $i=1,2$. So, hypothesis $(\mathcal{H}_1)$ is satisfied. And, for any $\mathtt{u}_1,\mathtt{v}_1,\mathtt{u}_2,\mathtt{v}_2\in\mathbb{R}$ and $z\in\mathfrak{J}$, we have

$$|\mathtt{g}_1(z,\mathtt{u}_1(z),\mathtt{u}_2(z)) - \mathtt{g}_1(z,\mathtt{v}_1(z),\mathtt{v}_2(z))| \le \chi_1(z)|\mathtt{u}_1(z)-\mathtt{v}_1(z)| + \widehat{\chi}_1(z)|\mathtt{u}_2(z)-\mathtt{v}_2(z)|,$$
$$|\mathtt{g}_2(z,\mathtt{u}_1(z),\mathtt{u}_2(z)) - \mathtt{g}_2(z,\mathtt{v}_1(z),\mathtt{v}_2(z))| \le \chi_2(z)|\mathtt{u}_1(z)-\mathtt{v}_1(z)| + \widehat{\chi}_2(z)|\mathtt{u}_2(z)-\mathtt{v}_2(z)|,$$

where

$$\chi_1(z) = \frac{1}{e^{-z}+8},\quad \widehat{\chi}_1(z) = z+\sqrt{2},\quad \chi_2(z) = \frac{1}{e^{z}+8},\quad \widehat{\chi}_2(z) = e^z+1.$$

Obviously,

$$\|\chi_1\|_\infty = \frac{1}{e^{-1}+8},\quad \|\widehat{\chi}_1\|_\infty = 1+\sqrt{2},\quad \|\chi_2\|_\infty = \frac{1}{9},\quad \|\widehat{\chi}_2\|_\infty = e+1.$$

Then the matrix A_ϖ has the following representation:

$$\mathsf{A}_\varpi = \frac{2}{\varpi}\begin{pmatrix} \frac{2+19e}{3+24e} & 1+\sqrt{2} \\ \frac{1}{9} & e+\frac{6}{5}\end{pmatrix}.$$

For $\varpi>0$ suitably chosen, by virtue of Theorem 3.1, the system (18)-(19) has a unique solution in $\mathfrak{C}_{3/4,\Phi}([0,1],\mathbb{R})\times\mathfrak{C}_{3/4,\Phi}([0,1],\mathbb{R})$. Therefore, from Theorem 4.1, coupled system (18)-(19) is UH and GUH stable.

Example 3. In a particular case, for $\alpha=\frac{1}{2}$, $\beta=1$, $\Phi(z)=z$, the coupled system for Φ-Hilfer proportional FDE (1) reduces to the coupled system for the Caputo proportional FDE given by

$$\begin{cases} \mathcal{D}^{\frac{1}{2},\frac{1}{4}}_{0^+}\mathtt{u}_1(z) &= \frac{2\mathtt{u}_1(z)}{3} + \frac{\sin(\mathtt{u}_1(z))}{e^{-z}+8} + (z+\sqrt{2})\ln(|\mathtt{u}_2(z)|+1),\ z\in(0,1],\\ \mathcal{D}^{\frac{1}{2},\frac{1}{4}}_{0^+}\mathtt{u}_2(z) &= \frac{\mathtt{u}_2(z)}{5} + \frac{1}{e^{z}+8}\left(1+\frac{|\mathtt{u}_1(z)|}{1+|\mathtt{u}_1(z)|}\right) + \frac{\arctan(\mathtt{u}_2(z))+1}{(e^z+1)^{-1}},\ z\in(0,1],\end{cases} \tag{20}$$

and

$$(\mathcal{I}^{0,\frac{1}{2},z}_{0^+}\mathtt{u}_1(0^+), \mathcal{I}^{0,\frac{1}{2},z}_{0^+}\mathtt{u}_2(0^+)) = (0,0). \tag{21}$$

We have

$$\mathfrak{C}_{\delta,\Phi}(\mathfrak{J},\mathbb{R}^n) = \mathfrak{C}_{1,z}([0,1],\mathbb{R})$$

and

$$\mathfrak{C}^{\beta(1-\alpha)}_{\delta,\Phi}(\mathfrak{J},\mathbb{R}^n) = \mathfrak{C}^{1/2}_{1,z}([0,1],\mathbb{R}).$$

As all the hypotheses of Theorem 3.1 and Theorem 4.1 are satisfied, then system (18)-(19) has a unique solution in $\mathfrak{C}_{1,z}([0,1],\mathbb{R})\times\mathfrak{C}_{1,z}([0,1],\mathbb{R})$ and is UH and GUH stable.

6 Conclusion

In this paper, we successfully employed the fixed-point approach in a vector-valued Banach space to establish qualitative results for a coupled system driven by the Φ-Hilfer PFD. Our analysis relies on the convergence to zero of the matrices and introduces a new Bielecki-type vector-valued norm, allowing us to avoid any extra assumptions. We also investigate Ulam's types stability. Consequently, numerous findings in the literature can be recovered through our results. By varying the functions Φ, β, and σ, one can explore several cases of our system (1). More precisely:

1. Proportional Φ-Riemann–Liouville FD : By taking $\beta = 0$.
2. Proportional Φ-Caputo FD : By taking $\beta = 1$.
3. Φ-Hilfer FD : By taking $\sigma = 1$.
4. Hilfer-Hadmard FD : By taking $\Phi(z) = \ln(z)$.
5. Hilfer-Katugampola FD : By taking $\Phi(z) = z^{\mu}$, where $\mu > 0$.

References

[1] S. Abbas, A. Bashir, M. Benchohra and A. Salim. *Fractional Difference, Differential Equations, and Inclusions. Analysis and stability.* Elsevier, Amsterdam, 2024.

[2] I. Ahmed, P. Kumam, F. Jarad, P. Borisut and W. Jirakitpuwapat. On Hilfer generalized proportional fractional derivative. *Advances in Difference Equations* **1** (2020) 1–18.

[3] B. Ahmad, A. Alsaedi, S. K. Ntouyas and J. Tariboon. *Hadamard-Type Fractional Differential Equations, Inclusions and Inequalities.* Springer, Berlin, New York, 2017.

[4] C. Derbazi and Z. Baitiche. Coupled systems of ψ-Caputo differential equations with initial conditions in Banach spaces. *Mediterranean Journal of Mathematics* **17** (2020) 169.

[5] C. Derbazi, Z. Baitiche and M. Benchohra. Coupled system of ψ-Caputo fractional differential equations without and with delay in generalized Banach spaces. *Results in Nonlinear Analysis* **5** (1) (2022) 42–61.

[6] M. Farman, A. Shehzad, A. Akgül, D. Baleanu and M. D. Sen. Modelling and analysis of a measles epidemic model with the constant proportional Caputo operator. *Symmetry* **15** (2) (2023) 468.

[7] V. Gafiychuk, B. Datsko and V. Meleshko. Mathematical modeling of time fractional reaction-diffusion systems. *Journal of Computational and Applied Mathematic*s **220** (2008) 215–225.

[8] R. Gorenflo, A. A. Kilbas, F. Mainardi and S. V. Rogosin. *Mittag-Leffler Functions, Related Topics and Applications.* Springer, Berlin, New York, 2020.

[9] R. Hilfer. *Applications of Fractional Calculus in Physics.* World Scientific, Singapore, 2000.

[10] F. Jarad, T. Abdeljawad and J. Alzabut. Generalized fractional derivatives generated by a class of local proportional derivatives. *European Physical Journal Special Topics* **226** (2017) 3457–3471.

[11] F. Jarad, M. Alqudah and T. Abdeljawad. On more general forms of proportional fractional operators. *Open Mathematics* **18** (2020) 167–176.

[12] F. Jarad, T. Abdeljawad, S. Rashid and Z. Hammouch. More properties of the proportional fractional integrals and derivatives of a function with respect to another function. *Advances in Difference Equations* **303** (2020) 1–16.

[13] A. Kilbas, H. M. Srivastava and J. J. Trujillo. *Theory and Application of Fractional Differential Equations*. North-Holland, Amsterdam, 2006.

[14] P. Kumam, A. Ali, K. Shah and R. Khan. Existence results and Hyers-Ulam stability to a class of nonlinear arbitrary order differential equations. *Journal of Nonlinear Sciences and Applications* **10** (2017) 2986–2997.

[15] J. Liang, Z. Liu and X. Wang. Solvability for a coupled system of nonlinear fractional differential equations in a Banach space. *Fractional Calculus and Applied Analysis* **16** (1) (2013) 51–63.

[16] R. L. Magin. *Fractional Calculus in Bioengineering*. Begell House Publishers, Danbury, CT, 2006.

[17] I. Mallah, I. Ahmed, A. Akgül, F. Jarad and S. Alha. On Φ-Hilfer generalized proportional fractional operators. *AIMS Mathematics* **7** (2022) 82–103.

[18] F. Mainardi. *Fractional Calculus and Waves in Linear Viscoelasticity: An Introduction to Mathematical Models*. Imperial College Press, London, 2010.

[19] A. I. Perov. On the Cauchy problem for a system of ordinary differential equations. *Pviblizhen. Met. Reshen. Differ. Uvavn.* **2** (1964) 115–134. [Russian]

[20] I. Petre and A. Petruşel. Krasnoselskii's theorem in generalized Banach spaces and application. *Electronic Journal of Qualitative Theory of Differential Equations* **85** (2012) 1–20.

[21] R. Precup. The role of matrices that are convergent to zero in the study of semilinear operator systems. *Mathematical and Computer Modelling* **49** (2009) 703–708.

[22] I. Podlubny. *Fractional Differential Equations*. Academic Press, San Diego, 1999.

[23] S. Rashid, F. Jarad, M. Noor, H. Kalsoom and Y. Chu. Inequalities by means of generalized proportional fractional integral operators with respect to another function. *Mathematics* **7** (2019) 1225.

[24] S. G. Samko, A. A. Kilbas and O. I. Marichev. *Fractional Integrals and Derivatives*. Gordon and Breach Science, New York, 1993.

[25] J. Sousa and E. De Oliveira. On the Φ-Hilfer fractional derivative. *Communications in Nonlinear Science and Numerical Simulation* **60** (2018) 72–91.

[26] C. Urs. Coupled fixed point theorems and applications to periodic boundary value problems. *Miskolc Mathematical Notes* **14** (2013) 323–333.

[27] R. S. Varga. *Matrix Iterative Analysis*. Springer-Verlag, Berlin, 2000.

[28] Y. Zhou. *Basic Theory of Fractional Differential Equations*. World Scientific, Singapore, 2014.

[29] A. Dababneh, B. Sami, M. A. Hammad and A. Zraiqat. A new impulsive sequential multi-orders fractional differential equation with boundary conditions. *Journal of Mathematics and Computer Science* **10** (6) (2020) 2871–2890.

[30] H. Al-Zoubi, T. Hamadneh, M. A. Hammad and M. Al-Sabbagh. Tubular surfaces of finite type Gauss map. *Journal of Geometry and Graphics* **25** (2021) 45–52.

[31] M. A. Zaitri, H. Zitane and D. F. Torres. Pharmacokinetic/Pharmacodynamic anesthesia model incorporating ψ-Caputo fractional derivatives. *Computers in Biology and Medicine* **167** (2023) Article 107679.

Nonlinear Dynamics and Systems Theory, **25** (1) (2025) 27–36

Simulation of Tsunami Wave Propagation Using the Finite Difference Method for Disaster Early Warning System

Ahmad Zaenal Arifin [1*], Sriwulan [2], Marita Ika Joesidawati [3], Teguh Herlambang [4], Saeful Mizan [5] and Andik Adi Suryanto [6]

[1] *Department of Mathematics, Universitas PGRI Ronggolawe, Tuban, Indonesia.*
[2] *Department of Biology, Universitas PGRI Ronggolawe, Tuban, Indonesia.*
[3] *Departmen of Marine Science, Universitas PGRI Ronggolawe, Tuban, Indonesia.*
[4] *Department of Information Systems, Universitas Nahdlatul Ulama Surabaya, Surabaya, Indonesia.*
[5] *Department of Teacher Profession Education, Universitas PGRI Ronggolawe, Tuban, Indonesia.*
[6] *Department of Informatics Enginering, Universitas PGRI Ronggolawe, Tuban, Indonesia.*

Received: March 27, 2024; Revised: January 30, 2025

Abstract: Indonesia is a country that is the meeting point of three active tectonic plates in the world and it is located in the Pacific Ring of Fire, which makes it prone to disasters. One of the disasters that may occur is a tsunami that appears due to an earthquake or an active volcano that erupts in the sea. Tsunami waves are one of the fluid problems, tsunami waves modelling can be solved using the Finite Difference Method. This research aims to model the propagation of tsunami waves. This modelling is important for early detection of a tsunami formed and can calculate its impact. This research uses the finite difference as a method for constructing discretization equations to find a numerical solution for tsunami propagation modelling. From the modelling results, the highest tsunami wave was 0.005 km at the 0th km, then the wave height decreased at the 30th and 60th seconds by 0.0034552 km and 0.0031604 km at the 3rd and 9th km, and at the 90th second, the waves rose to 0.0036794 km at the 14th km.

Keywords: *finite difference method; modeling; tsunami wave propagation; tsunami.*

Mathematics Subject Classification (2020): 86A15, 65M06.

* Corresponding author: mailto:az_arifin@unirow.ac.id

© 2025 InforMath Publishing Group/1562-8353 (print)/1813-7385 (online)/http://e-ndst.kiev.ua

1 Introduction

As a maritime country, Indonesia has an ocean area larger than the land area, it is located in Southeast Asia and is flanked by two Asian countries and the Australian continent. Indonesia holds the title of a country that has the second longest coastline in the world, consisting mostly of islands, with a length of 99,093 km [1]. Indonesia is a country that is the meeting place of three active tectonic plates of the world, these three active tectonic plates make Indonesia a country that has many active mountains and is the epicenter of earthquakes. The factors above make Indonesia an earthquake-prone area [2–4]. The Indo-Australian Ocean Plate in the south, the Pacific Ocean Plate in the east, the Eurasian Plate in the north, the Philippine Sea Plate added, are the world's active tectonic plates with dynamic movements and mutual urges between the plates that make the territory of Indonesia prone to tsunami disasters [5].

A very long water wave commonly called a tsunami is a large displacement of sea water from the sea to the mainland. The cause of a tsunami is due to an external force such as an underwater earthquake, volcanic eruption, or a meteor so that the waves radiate outward in all directions [6]. More than 10% of tsunamis are caused by underwater and aerial landslides with the resulting water waves reaching a maximum run-up of possibly 10-15 km from the tsunami source along the coastline and 5% are caused by volcanic eruptions [7]. One of the biggest tsunamis in Indonesia was in Aceh in 2004, which was caused by an earthquake measuring 9.1 on the Richter Scale. As a result of the tsunami, approximately 130,013 people lost their lives and 37,066 were reported missing [8]. In addition, the aftermath of the Aceh tsunami had an impact on people's livelihoods. A lot of damage was experienced, in particular in the construction sector, the fishing sector, the agricultural sector because the people living around the coast depend on livelihood strategies such as fishing, gardening, which utilize the surrounding nature [9].

A tsunami is a collection of tidal water waves that move quickly towards the mainland, it usually occurs on the coast, especially in Indonesia. Tsunamis are caused by active volcanic eruptions at sea or by earthquakes [10]. Indonesia often experiences tsunamis, the largest tsunamis that have ever occurred in Indonesia were in Aceh, 2004 [11, 12], in Pangandaran, 2006, and in Mentawai, 2010. A tsunami in Indonesia in the last five years occurres in Palu and the Sunda Strait in 2018. Many sectors of life are affected if a tsunami occurres, including the Construction Sector, Fisheries Sector, Agriculture Sector, it has impacts on the coastline and non-structural impacts.

Research on computational fluid dynamics has been carried our intensively, including the Airway Pressure Valve [13], Solitary Wave [14]. To reduce the impact of losses due to the tsunami disaster, a prediction can be made by simulating the propagation of tsunami waves using the finite difference method equation. The finite difference method is a method that is often used to solve partial differential equations [15, 16]. This method has the advantage that it is easy to understand and simple [17]. The finite difference method is also easy to use to solve physical problems that have regular geometric shapes, for example square domains in two dimensions, cubic in three dimensions and intervals in one dimension [18].

The finite difference method is widely used for research, including the analysis of the convergence of the finite difference method in approaching the diffusion equation, it is found that the numerical solution in the finite difference method converges to the analytical solution of the diffusion equation. Research on simulations of tsunami waves includes the application of the implicit Crank-Nicolson finite difference method to deter-

mine the case of 2D advection-diffusion in the distribution of pollutants in the water by simulating the concentration distribution pattern in the Kapuas River, showing a more distant distribution and a very small RMSE value from several time variations so that the results obtained are close to the expected ones [19]. Then, in the simulation study of the impact of the barrier on the tsunami wave using the finite difference method, it was found that the shallow water equation used can identify tsunami waves with the construction of the barrier [20].

Extensive research has been conducted on simulating tsunami wave propagation. A study by Nisa [2] highlighted the significance of modeling tsunami wave propagation, particularly in light of the substantial losses incurred following a tsunami. Another study by Chasanah [10] aimed to model the propagation of tsunami waves caused by the eruption of Mount Anak Krakatau and explored multiple scenarios to mitigate tsunami wave height in Jakarta Bay.

Based on the explanations and previous studies that have been described, research will be conducted on the simulation of tsunami wave propagation using the finite difference method. From the simulation, one can determine the wave height and the distance of the wave propagation from the initial point of the wave formation and the effect of seabed material on the wave propagation. The purpose of this study is to create a model for tsunami wave propagation so that it can be used to predict the impacts that occur due to the tsunami disaster. In addition, the height and propagation distance of the tsunami waves obtained in this study can be used as information for disaster mitigation, so that people, especially those living in coastal areas, can evacuate earlier to higher ground.

2 Literature Review

2.1 Tsunami

A tsunami is a movement of sea water caused by a seaquake, an underwater volcanic eruption, or a meteor strike. The speed of tsunami waves can reach 500-1000 km/hour [1]. Tsunamis often occur after an earthquake, but not always. A tsunami occurs when an earthquake has a strength of more than 6.5 on the Richter Scale and occurs out at sea at a depth of 30 km. The height of the tsunami waves will increase as they get closer to the shore due to the reduction in sea depth [21].

Tsunami waves can have a dangerous impact on humans, from material losses to loss of life. This disaster can occur at any time so it is almost unavoidable [22]. The tsunami disaster in the Sunda Strait in 2018, provides a clear picture because it occurred suddenly, caused by an underwater landslide due to the eruption of Mount Anak Krakatau. The resulting impact was very large, 437 fatalities were recorded [23]. Therefore, it is very necessary to understand the implementation of disaster mitigation so that it does not cause a very large impact.

2.2 Tsunami wave propagation modeling

A tsunami results from the movement of tectonic plates with the strength of an earthquake, causing vibrations. Even though they occur in very deep waters, tsunamis have a wavelength between 2 peaks of more than 100 km on the high seas and the time difference between peaks is estimated to be 10 minutes to 1 hour [24]. It is necessary to model the propagation of tsunami waves to be able to predict disasters that occur. Modeling can be done using shallow water theory or the so-called shallow water equation (SWE) which

is a simple differential equation for water waves and is close to the actual behavior of ocean waves [2].

The shallow water equations used are based on the derivation of the law of conservation of mass and conservation of momentum in the fluid. The following are the equations for shallow water waves expressed through the three-dimensional equations [2]:

1. Mass Conservation Equation

$$\frac{\partial u}{\partial x} + \frac{\partial v}{\partial y} + \frac{\partial w}{\partial z} = 0. \tag{1}$$

2. Momentum Equations

$$\frac{\partial u}{\partial t} + u\frac{\partial u}{\partial x} + v\frac{\partial u}{\partial y} + w\frac{\partial u}{\partial z} + \frac{1}{\rho}\frac{\partial \rho}{\partial y} + \frac{1}{\partial \rho}\left(\frac{\partial \tau_{xy}}{\partial x} + \frac{\partial \tau_{yy}}{\partial y} + \frac{\partial \tau_{yz}}{\partial z}\right) = 0, \tag{2}$$

$$\frac{\partial v}{\partial t} + u\frac{\partial v}{\partial x} + v\frac{\partial v}{\partial y} + w\frac{\partial v}{\partial z} + \frac{1}{\rho}\frac{\partial \rho}{\partial y} + \frac{1}{\partial \rho}\left(\frac{\partial \tau_{xy}}{\partial x} + \frac{\partial \tau_{yy}}{\partial y} + \frac{\partial \tau_{yz}}{\partial z}\right) = 0, \tag{3}$$

$$\frac{\partial w}{\partial t} + u\frac{\partial w}{\partial x} + v\frac{\partial w}{\partial y} + w\frac{\partial w}{\partial z} + \frac{1}{\rho}\frac{\partial \rho}{\partial y} + \frac{1}{\partial \rho}\left(\frac{\partial \tau_{xy}}{\partial x} + \frac{\partial \tau_{yy}}{\partial y} + \frac{\partial \tau_{yz}}{\partial z}\right) = 0. \tag{4}$$

x and y are the horizontal axes, while z is the vertical axes. It shows the height of the water surface from a balanced state at a position (x, y), τ_{ij} is a shear or tangential stress. In the direction of the axis, the momentum equation has a surface $\rho = 0$ under dynamic conditions, which results in hydrostatic pressure. In tsunami wave propagation, the mass and momentum conservation equations are used with dynamic and kinematic boundary conditions. The kinematic boundary conditions are divided into two kinds, namely the kinematics on the free surface and at the bottom of the channel. The kinematic boundary conditions of the free surface are stated as follows:

$$\frac{\partial \eta}{\partial t} = -u\frac{\partial \eta}{\partial x} - v\frac{\partial \eta}{\partial y} + w. \tag{5}$$

The kinematic boundary conditions at the bottom of the channel are stated as follows.

$$u\frac{\partial h}{\partial x} + v\frac{\partial h}{\partial y} + w = 0. \tag{6}$$

In uniform flow, in general, the friction on the seabed can be expressed as follows [2]:

$$\frac{\tau_x}{\rho} = \frac{1}{2g}\frac{f}{D^2}M\sqrt{M^2 + N^2}, \tag{7}$$

$$\frac{\tau_y}{\rho} = \frac{1}{2g}\frac{f}{D^2}N\sqrt{M^2 + N^2}. \tag{8}$$

The equations (7) and (8) represent the coefficient of friction. The relationship between the Manning roughness value and the coefficient can be expressed in the following equations:

$$n = \sqrt{\frac{fD^{\frac{1}{3}}}{2g}}, \tag{9}$$

$$f = \frac{2gn^2}{D^{\frac{1}{3}}}. \tag{10}$$

Material type	n value
Pure cement, fine metal	0.010
Rubble	0.017
Fine soil	0.018
Natural channel in good condition	0.025
Natural channel with seabed rocks and plants	0.035
Natural channel with bad condition	0.060

Table 1: Sea Level Condition.

By substituting equation (9) and equation (10) into equation (7) and equation (8), we get equation (11) and (12) as follows:

$$\frac{\tau_x}{\rho} = \frac{n^2}{D^{\frac{7}{3}}} M\sqrt{M^2+N^2}, \tag{11}$$

$$\frac{\tau_y}{\rho} = \frac{n^2}{D^{\frac{7}{3}}} N\sqrt{M^2+N^2}. \tag{12}$$

3 Research Methods

This study aims to determine the height and distance of the tsunami wave propagation from the center of the vibration by using the finite difference method with an explicit scheme.

The finite difference method is a numerical method for solving problems of physical phenomena or technical problems. This method can be used in converting partial differential equations into linear equations [23]. The equation for the finite difference method is obtained using the Taylor series from equations (13) and (14) of one variable function around x as follows [24]:

$$f(x+\Delta x) = f(x) + f'(x)\Delta x + \frac{f''(x)}{2!}\Delta x^2 + \cdots, \tag{13}$$

$$f(x-\Delta x) = f(x) - f'(x)\Delta x + \frac{f''(x)}{2!}\Delta x^2 + \cdots. \tag{14}$$

The finite difference method is divided into two types, namely explicit and implicit. The explicit finite difference method uses an approximation of the forward difference $u(x, t+\Delta t)$ around the point t and the center difference $u(x+\Delta x, t)$ and around the point x. Meanwhile, the implicit finite difference method uses backward difference an approximation $u(x, t)$ of the approx $t+\Delta t$ and the center $u(x+\Delta x, t+\Delta t)$ and $u(x-\Delta x, t+\Delta t)$ approx x [25].

In modeling the propagation of tsunami waves using an explicit finite difference method with a forward difference approach of more than one independent variable, the equation [26]

$$\frac{\partial f}{\partial x} \approx \frac{f(x_{i+1}, t_j) - f(x_i, t_j)}{\Delta x} \tag{15}$$

can be simplified to

$$\frac{\partial f}{\partial x} \approx \frac{f_{i+1,j} - f_{i,j}}{\Delta x}.$$

4 Result and Discussion

By deriving the shallow water formula from the mass and momentum conservation equations, and by spatial discretization using the finite difference method using equations (1) to (6), we obtain

$$\eta_{i,j}^{n+1} = rM_{i,j}^{n} - rM_{i+1,j}^{n} + rN_{i,j}^{n} - rN_{i,j+1}^{n} + \eta_{i,j}^{n}, \tag{16}$$

$$M_{i,j}^{n+1} = r\rho\eta_{i,j}^{n} - r\rho\eta_{i+1,j}^{n} + M_{i,j}^{n}, \tag{17}$$

$$N_{i,j}^{n+1} = r\rho\eta_{i,j}^{n} - r\rho\eta_{i+1,j}^{n} + N_{i,j}^{n}. \tag{18}$$

Equations (16)-(18) are the result of discretization using the finite difference method and the equations (16)-(18) are a numerical solution that will be used in the tsunami wave propagation simulation. The simulation was carried out by several trials using the approximate values of $\Delta x, \Delta y$ and Δt which varied.

4.1 Trial 1

The value of Δx and Δy is 1 and Δt is equal to 0.009. The amplitude value used is 0.004 km, the wavelength is 4 km, and the distance from the center of the wave formation is 25 km with the seabed material used being fine cement or fine metal. The following is the result of the simulation in Trial 1 of the propagation of tsunami waves with the Manning roughness value.

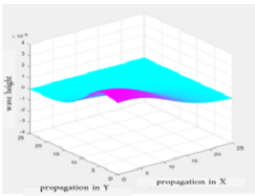

(a) Tsunami Propagation in 0 second

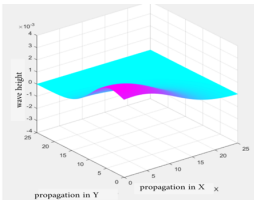

(b) Tsunami Propagation in 30 seconds

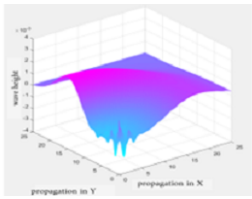

(c) Tsunami Propagation in 60 seconds

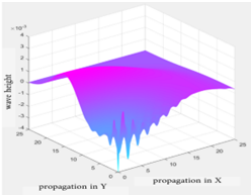

(d) Tsunami Propagation in 90 seconds

Figure 1: Simulation in the first trial of 3D Tsunami Propagation.

The tsunami wave is formed as high as 4 m at 0 second and is located at 0 km and moves in the positive x-axis direction on the coast which is as high as 1.3175×10^{-8} m. At the 30th second, the initial wave height decreased to 2.6214 m with the highest wave crest located at 4 km from the initial point of the wave formation and the wave condition on the shore as high as 2.696×10^{-7} m. Then, at the 60th second, the highest wave crest is located at 9 km from the initial point of wave formation with a wave height of 30008

m and a wave condition on the shore as high as 1.0302×10^{-5} m. At the 90th second, the highest wave crest is located at 13 km from the initial point of wave formation with a wave height of 4.2654 m and a wave condition on the shore as high as $3,6287 \times 10^{-4} m$.

4.2 Trial 2

The value of Δ_x and Δ_y is 1 and Δ_t is 0.01. The amplitude value used is 0.005 km, the wavelength is 5 km, and the distance from the center of the wave formation is 25 km with the seabed material used being fine cement or fine metal. The following is the result of the simulation in Trial 2 of the propagation of tsunami waves with the Manning roughness value.

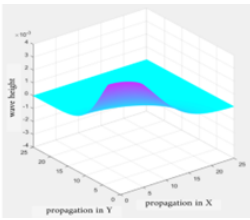

(a) Tsunami Propagation in 0 second

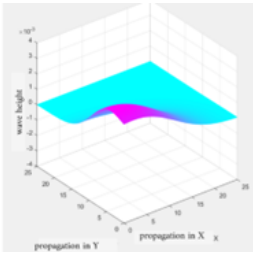

(b) Tsunami Propagation in 30 seconds

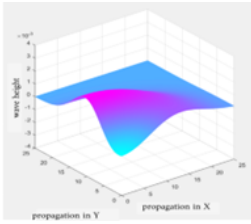

(c) Tsunami Propagation in 60 seconds

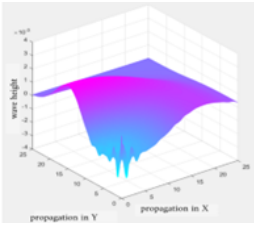

(d) Tsunami Propagation in 90 seconds

Figure 2: Simulation in the second trial of 3D Tsunami Propagation.

The wave is formed as high as 5 m at the 0th second and is located at 0 km from the starting point of the wave formation and the state of the wave on the beach is as high as $1.8633 \times 10^{-5} m$. Then the wave decreased to 3.4552 m at the 30th second with the highest wave crest located at 3 km from the initial point of the wave formation and the wave condition on the shore only as high as 1.7682×10^{-4} m. At the 60th second, the wave height decreased to 3.1604 m with the highest wave crest located at 9 km from the starting point of the wave formation and the condition of the waves on the shore as high as $2.9034 \times 10^{-3} m$. At the 90th second, the highest wave crest is located at 14 km from the starting point of the wave formation with a wave height of 3.6794 m and the condition of the waves on the shore only as high as 3.9867×10^{-2} km.

According to the simulation results obtained through several trials, the height of the tsunami waves moving to the coast has increased from the center of the wave formation. The highest wave that moves to the shore, according to the tests carried out in the third trial, in 90 seconds is 0.28291 meter, with the initial wave height of 6 meters. However, from the simulations carried out, the material that makes up the seabed does not affect

the formation of tsunami waves because the waves produced have the same shape and height.

From the simulation results, three values are obtained, namely the highest wave height, the distance the wave travels, and the wave height when it reaches the beach. The results of this study are different from those of the research that also uses the theory of shallow water equations in shallow seas but with a case study in Manado Bay [25]. The results obtained in this study were the height of the tsunami waves that occurred after the earthquake on the coast of Manado Bay , it was about 1.5-3 m with a period of 20-24 minutes. The wave height can reach 3 m due to the conditions of the Manado beach which is in the form of a bay so that tsunami wave amplification can occur [26].

Then the results of the tsunami simulation in another study using the continuity and momentum equations with a case study in the city of Palu obtained the initial height of the tsunami wave reaching 1.5 m and spreading to the mouth of the Palu bay with a height of 1.6 m. The maximum wave height obtained is close to the actual height of 3.65 m. The time taken by the tsunami waves to reach the mouth of the bay, which is 62 km away, is 10 minutes. While the tsunami waves from the mouth of the bay to the city of Palu, which is 32 km away, run for 12 minutes [27].

In contrast, the research on tsunamis used for disaster mitigation at Manakarra Beach, stated that the waves started hitting the beach 39 minutes after the earthquake. The maximum wave height occurred at the 50th minute was a height of 8,306 m. At the highest tide, the height of the Manakarra Beach pier is 2 m. So, the waves that came at the 50th minute were 6,306 m high. Therefore, there are about 30 minutes to evacuate to higher ground [28]. Therefore, for further research, it is expected to use data in areas that have been affected by the tsunami so that the accuracy of the simulation in this study can be known. The modeling of tsunami wave propagation uses the shallow water equation where the equation is based on the derivation of the law of conservation of mass and conservation of momentum [29]. The shallow water equation can be used in the presence of dynamic and kinematic boundary conditions. The equation used is derived from the formula with known initial conditions. The method used in the modelling propagation of tsunami waves is an explicit finite difference method, where the equations used will be discretized without any friction on the seabed. The discretization results using the finite difference method provide a numerical solution or simulating the propagation of tsunami waves.

5 Conclusion

The shallow water equation can be used in the presence of dynamic and kinematic boundary conditions. The method used for modelling the propagation of tsunami waves is an explicit finite difference method, where the equations used are discretized without any friction on the seabed. The discretization results using the finite difference method provide a numerical solution for simulating the propagation of tsunami waves. According to the simulation results obtained through several trials, the height of the tsunami waves moving to the coast increases from the center of the wave formation. The highest wave that moves to the shore, according to the tests carried out in the third trial, in 90 seconds, is 0.28291 meters with the initial wave being 6 meters. However, from the simulations carried out, the material that makes up the seabed does not affect the formation of tsunami waves because the waves produced have the same shape and height. Three values are obtained, namely the highest wave height, the distance the wave travels, and the

wave height when it reaches the beach.

Acknowledgment

We are grateful to the Mathematic Department, Universitas PGRI Ronggolawe.

References

[1] D. P. Utomo and B. Purba. Penerapan Data mining pada Data Gempa Bumi terhadap Potensi Tsunami di Indonesia. In: *Prosiding Seminar Nasional Riset Information Science(SENARIS)*. Mataram, Indonesia, 2019, 846–853.

[2] K. Nisa, L. Ambarwati and T. Murdiyanto. Simulasi Penjalaran Gelombang Tsunami Menggunakan Metode Optimal Time Stepping. *JMT J. Mat. dan Terap.* **3** (1) (2021) 10–19.

[3] R. Jena, B. Pradhan, G. Beydoun, A. M. Alamri and H. Sofyan. Earthquake hazard and risk assessment using machine learning approaches at Palu, Indonesia. *Science of the total Environment* **749** (2020) 141582.

[4] A. I. Hadi, K. S. Brotopuspito, S. Pramumijoyo and H. C. Hardiyatmo. Regional landslide potential mapping in earthquake-prone areas of Kepahiang Regency, Bengkulu Province, Indonesia. *Geosciences* **8** (6) (2018) 219.

[5] B. Hartanto and N. Astriawati. Identifikasi Pendekatan Shallow Water Equation Dalam Simulasi 2D Gelombang Tsunami di Pantai Keburuhan Purworejo. *Majalah Ilmiah Bahari Jogja* **18** (1) (2020) 127–152.

[6] T. R. Varsoliwala and A. C. Singh. Mathematical Modeling of Tsunami Wave Propagation at Mid Ocean and Its Amplification and Run-Up on Shore. *Journal of Ocean Engineering and Science* **6** (4) (2021) 367–375.

[7] A. Kozelkov. Landslide-Type Tsunami Modelling Based on the Navier-Stokes Equations. *Journal of Tsunami Society International.* **35** (3) (2016) 106–144.

[8] W. Swesti. Dampak Pariwisata Terhadap Kondisi Sosial Budaya Masyarakat di Banda Aceh. *Jurnal Kepariwisataan Indonesia: Jurnal Penelitian dan Pengembangan Kepariwisataan Indonesia.* **13** (2) (2019) 49–65.

[9] P. Daly, A. Halim, D. Hundlani, E. Ho and S. Mahdi. Rehabilitating Coastal Agriculture and Aquaculture After Inundation Events: Spatial Analysis of Livelihood Recovery in Post-Tsunami Aceh, Indonesia. *Ocean Coast and Management* **142** (2017).

[10] N. Chasanah, H. D. Armono and W. Radianta. Pemodelan Penjalaran Tsunami Akibat Erupsi Gunung Anak Krakatau Beserta Skenario Dike. Studi Kasus Teluk Jakarta. *Jurnal Teknik ITS* **9** (1) (2020) G23–G30.

[11] Syamsidik, A. Nugroho, R. S. Oktari and M. Fahmi. Aceh Pasca 15 Tahun Tsunami: Kilas Balik dan Proses Pemulihan. In: *Tsunami and Disaster Mitigation Research Center (TDMRC)*, Universitas Syiah Kuala, Aceh, 2019.

[12] R. S. Oktari, A. Nugroho, M. Fahmi, A. Suppasri, K. Munadi and R. Amra. Fifteen years of the 2004 Indian Ocean Tsunami in Aceh-Indonesia: Mitigation, preparedness and challenges for a long-term disaster recovery process. *International Journal of Disaster Risk Reduction* **54** (2021) 102052.

[13] S. Bentouati, M. I. Soualhi, A. A. E. Hadj and H. Yeklef. Design and Analysis of Continuous Positive Airway Pressure Valve Using a 3D Printing and Computational Fluid Dynamic. *Nonlinear Dynamics and Systems Theory* **21** (3) (2021) 229–237.

[14] M. Alquran, A. Jarrah and E. V. Krishnan. Solitary Wave Solutions of the Phi-Four Equation and the Breaking Soliton System by Means of Jacobi Elliptic Sine-Cosine Expansion Method. *Nonlinear Dynamics and Systems Theory* **18** (3) (2021) 233–240.

[15] S. Mazumder. *Numerical methods for partial differential equations: finite difference and finite volume methods.* Academic Press, 2015.

[16] J. W. Thomas. *Numerical partial differential equations: finite difference methods*, vol. 22. Springer Science and Business Media, 2013.

[17] S. P. D. Sriyanto, N. Nurfitriani, M. Zulkifli and S. N. E. Wibowo. Pemodelan Inundasi dan Waktu Tiba Tsunami Di Kota Bitung, Sulawesi Utara Berdasarkan Skenario Gempabumi Laut Maluku. *Geomatika* **25** (1) (2019) 47–54.

[18] Nurhayati, R. Tiryono, A. Dorrah and N. Aang. Pemodelan Matematika Laju Aliran Panas pada Wajan Pembuatan Arang Aktif-13 dengan Menggunakan Metode Beda Hingga (Finite Difference Method. In: *Seminar Nasional Sains, Matematika, Informatika, dan Aplikasinya*, Universitas Lampung, Lampung, Indonesia, 2019, 125–130.

[19] Sampera, Holand and Apriansyah. Aplikasi Metode Beda Hingga Crank-Nicolson Implisit untuk Menentukan Kasus Adveksi Difusi 2D pada Sebaran Polutan di Suatu Perairan. *Prisma Fisika* **4** (2) (2016) 56–62.

[20] S. W. Suciyati, Warsito and F. Almafakir. Visualisasi Distribusi Suhu pada Bahan Homogen dan Multilayer Menggunakan Metode Beda Hingga. In: *Prosiding Semirata*, Jambi, Indonesia, 2017, 974–986.

[21] Aeda, S. Alma, S. Saputro and P. Subardjo. Simulasi Penjalaran dan Penentuan Run-Up Gelombang Tsunami di Teluk Pangandaran, Jawa Barat. *Jurnal Oseanografi* **6** (1) (2017) 254–262.

[22] A. Z. Arifin. Simulasi Dampak Penghalang pada Gelombang Tsunami Menggunakan Persamaan Air Dangkal dengan Metode Beda Hingga. *Jambura Journal of Mathematics* **3** (2) (2021) 93–102.

[23] Maryanti. Studi Lapangan Rehabilitasi dan Rekonstruksi Oleh BPBD Provinsi Lampung Pasca Bencana Tsunami Selat Sunda Tahun 2018. *Jurnal Manajemen Bencana (JMB).* **6** (2) (2020) 25–40.

[24] C. Wuwungan, G. Pasau and S. H. J. Tongkukut. Pemodelan Perambatan Gelombang Tsunami di Laut Berdasarkan Skenario Gempa 8.0 dan 9.0 Mw. *Jurnal MIPA.* **10** (2) (2021) 55–58.

[25] J. C. Kumaat, S. T. B. Kandoli and F. Laeloma. Spatial Modeling of Tsunami Impact in Manado City using Geographic Information System. In: *IOP Conference Series: Materials Science and Engineering.* IOP Publishing, 2018, 12069.

[26] G. Pasau, G. H. Tamuntuan and A. Tanauma. Numerical modelling for tsunami wave propagation (case study: Manado bays). In: *IOP Conference Series: Materials Science and Engineering.* IOP Publishing, 2019, 012005.

[27] R. R. R. Alam, M. B. Adityawan, M. Farid, A. Chrysanti, Widyaningtias and M. A. Kusuma. Tsunami-induced inundation on the coast of Palu City. In: *IOP Conference Series: Earth and Environmental Science.* IOP Publishing, 2021, 012003.

[28] A. Y. Baeda, D. A. Suriamihardja, H. Umar and T. Rachman. Tsunami mitigation plan for Manakarra Beach of West Sulawesi province, Indonesia. *Procedia Enginering.* **116** (1) (2015) 134–140.

[29] K. Oktafianto, A. Z. Arifin, E. F. Kurniawati, T. Tafrikan, T. Herlambang and F. Yudianto. Tsunami Wave Simulation in the Presense of a Barrier. *Nonlinear Dynamics and Systems Theory* **23** (1) (2023) 69–78.

Nonlinear Dynamics and Systems Theory, **25** (1) (2025) 37–52

On Neumann Systems with Singularity Applied in Quenching Phenomena in Museilack Spaces

A. Elouardani [1], A. Aberqi [2] and M. Elmassoudi [1*]

[1] *Faculty of Sciences Dhar El Mahraz, Sidi Mohamed Ben Abdellah University, Fez, Morocco.*
[2] *National School of Applied Sciences, Sidi Mohamed Ben Abdellah University, Fez, Morocco.*

Received: March 7, 2024; Revised: January 17, 2025

Abstract: In this study, by the uniform control of the singularity and energy estimates, we establish the existence of solutions for the reaction-diffusion model with singularity due to Quenching phenomena in the boundary.

$$\begin{cases} \dfrac{\partial u_1}{\partial t} - \operatorname{div}\Big(a(x,t,\nabla u_1)\Big) = f_1(t,x)h_\gamma(u_1,u_2) & \text{in} \quad Q_T, \\ \dfrac{\partial u_2}{\partial t} - \operatorname{div}\Big(a(x,t,\nabla u_2)\Big) = f_2(t,x)h_\gamma(u_1,u_2) & \text{in} \quad Q_T, \end{cases} \tag{1}$$

where the operator $A(u) = \operatorname{div}\Big(a(x,t,\nabla u_i)\Big)$ is a generalized Leray-Lions operator defined on the inhomogeneous Musielak-Orlicz spaces (the vector field $a(x,t,\nabla u_i)$ has a growth prescribed by a generalized N-function).

Keywords: *quenching phenomena, Museilack-Orlciz spaces, local singularity, nonlinear dynamical systems.*

Mathematics Subject Classification (2020): 35K57, 35K67, 70K30, 93-01, 46E35.

* Corresponding author: mailto:elmassoudi09@gmail.com

© 2025 InforMath Publishing Group/1562-8353 (print)/1813-7385 (online)/http://e-ndst.kiev.ua

1 Introduction

Let Ω be an open subset of $\mathbb{R}^N$ $(N \geq 2)$, and let $T > 0$, $Q_T = \Omega \times (0,T)$, $\Gamma_1$and Γ_2 are such that $\Gamma_1 \cup \Gamma_2 = \partial\Omega$ and $\Gamma_1 \cap \Gamma_2 = \emptyset$. The Haussdorff measure of Γ_1 and Γ_2 does not vanish. Here ν denotes the outer normal to $\partial\Omega$.

This paper is concerned with the existence of solutions for a nonlinear parabolic singular reaction-diffusion system of the form (i=1,2)

$$(\mathcal{S}) \begin{cases} \dfrac{\partial u_i}{\partial t} - \operatorname{div}\big(a(x,t,\nabla u_1)\big) = F_i(t,x,u_1,u_2) & \text{in} \quad Q_T, \\ u_i(0,x) = u_{i,0}(x) & \text{in} \quad \Omega. \end{cases} \tag{2}$$

The following boundary conditions:

$$\begin{cases} u_i(t,x) = 0 & \text{on} \quad \Gamma_i \times (0,T), \\ \dfrac{\partial u_1}{\partial \nu} = 0 & \text{on} \quad \Gamma_2 \times (0,T), \\ \dfrac{\partial u_2}{\partial \nu} = 0 & \text{on} \quad \Gamma_1 \times (0,T) \end{cases} \tag{3}$$

hold with

$$F_i(t,x,r,s) = f_i(t,x)h_\gamma(s,r). \tag{4}$$

The functions f_1, f_2 :$Q_T \mapsto R$ satisfy the following conditions:

$$f_1, f_2 \in L^1(Q_T), \quad f_1 \geq 0, \quad \text{and} \quad f_1 + f_2 \leq 0. \tag{5}$$

The singular sourcing $h_\gamma : \mathbb{R}^* \times \mathbb{R} \mapsto \mathbb{R}$ is continuous and must verify $0 \leq h_\gamma(s,r) \leq \frac{s}{r^\gamma}$ with γ being a real parameter such as $0 < \gamma \leq 1$.

We assume that the functions

$$u_{1,0} \text{ and } u_{2,0} \text{ are such that } u_{1,0}, u_{2,0} \geq 0 \text{ and } \quad u_{1,0}, u_{2,0} \in L^\infty(\Omega). \tag{6}$$

Define the following spaces:

$$V_1 = \left\{\varphi \in W^1L_M(\Omega) : \varphi = 0 \text{ on } \Gamma_1\right\} \text{ and } V_2 = \left\{\psi \in W^1L_M(\Omega) : \psi = 0 \text{ on } \Gamma_2\right\},$$

where $W^1L_M(\Omega)$ is the Musielak-Orlicz-Sobolev space defined below.

The operator $A(u_i) = -div\Big(a(x,t,\nabla u_i)\Big)$ is a generalized Leray-Lions operator defined on the inhomogeneous Musielak-Orlicz spaces (see assumptions (7)–(9)).

The investigation of quenching phenomena traces back to 1975, when Kawarada published a paper [10] delving into a dynamical model. This pivotal work catalyzed an extensive exploration of the quenching systems by numerous researchers dedicating their efforts to the aspects such as the existence and characterization of quenching points, and the asymptotic behaviour of solutions, among other topics.

The solution maintains its boundedness in quenching systems, but the first-order time derivative undergoes unbounded growth within a finite time frame. This concept is also elaborated upon in Salin's research [15] and Selçuk's work [16]. For the numerical approach, Beauregard M.A. et al. [3] proposed a fully adaptive approximation for quenching systems over circular domains. Recently, Marion P.T. [13] studied quenching phenomena due to a concentrated nonlinear source in an infinitely long cylinder.

Hence, the aim here is to explore a concept referred to as "quenching", which extends the notion of explosion. Our goal is to investigate systems exhibiting nonstandard growth and inhomogeneous nonlinearities, which have notable relevance in the realm of physics. Furthermore, we consider the inclusion of non-homogeneous Neumann boundary conditions, where we introduce a generalization of systems previously studied in [5] for the $(p,q)-$Laplacian with the Dirichlet boundaries ($M(x,t)=|t|^p$ in Lebesgue spaces).

$$\begin{cases} -\mathrm{div}\big(h_1(x)|\nabla u|^{p-2}\nabla u)\big) = \lambda F_{u_1}(x,u_1,u_2) & \text{in} \quad \Omega, \\ -\mathrm{div}\big(h_2(x)|\nabla u|^{q-2}\nabla u)\big) = \lambda F_{u_2}(x,u_1,u_2) & \text{in} \quad \Omega, \\ u_1(x) = u_2(x) & \text{in} \quad \partial\Omega, \end{cases}$$

where F is a $\mathcal{C}^1-$function with $\nabla F = (F_{u_1}, F_{u_2})$. And $(p(x),q(x))-$Laplacian systems were considered in [9], where the authors explore the system with cross-diffusion in Lebesgue spaces with variable exponents.

$$\begin{cases} \partial_t u - \mathrm{div}\big(a(x,t,\nabla u)\big) = \mathrm{div}(|F|^{p(x,t)-2}F) & \text{in} \quad \Omega, \\ \partial_t v - \mathrm{div}\big(a(x,t,\nabla u)\big) = \delta\Delta u & \text{in} \quad \Omega, \end{cases}$$

where $\delta \geq 0$, and $a(x,t,.)$ is a Leray-Lions vector field, see also [1, 2] and references therein.

To our knowledge, the results obtained in this paper have not been covered in the existing literature. The organization of this contribution is given as follows. We start in Section 2 by presenting some definitions and properties in the framework of Museilack spaces. After that, in Section 3, we give our essential assumptions and set up the definition of the weak solution of the system (**S**). Then we establish the main existence Theorem 4.1.

2 Mathematical Preliminaries

2.1 Musielak-Orlicz function

In addressing the issue presented in system (2)-(3), we employ the framework of Orlicz-Sobolev spaces. This choice arises from the presence of a nonhomogeneous function $M(x,t)$ within the differential operator of system (2)-(3). Consequently, our approach commences by introducing fundamental concepts on Museilack-Orlicz-Sobolev spaces (see [14]). Let $M : \Omega \times \mathbb{R}_+ \to \mathbb{R}$ satisfy

(M_1): $M(x,.)$ is an N-function for all $x \in \Omega$ (i.e., it is convex, non-decreasing, continuous, $M(x,0)=0$, $M(x,t)>0$ for $t>0$, $\lim\limits_{t\to 0}\sup\limits_{x\in\Omega}\dfrac{M(x,t)}{t}=0$ and $\lim\limits_{t\to\infty}\inf\limits_{x\in\Omega}\dfrac{M(x,t)}{t}=\infty$).

(M_2): $M(.,t)$ is a measurable function for all $t \geq 0$. A function M which satisfies the conditions (M_1) and (M_2) is called a Musielak-Orlicz function.

We say that γ grows essentially less rapidly than M at 0 (resp. near infinity), and we write $\gamma \ll M$. For every positive constant c, we have
$\lim\limits_{t\to 0}\big(\sup\limits_{x\in\Omega}\dfrac{\gamma(x,ct)}{M(x,t)}\big)=0$ (resp. $\lim\limits_{t\to\infty}\big(\sup\limits_{x\in\Omega}\dfrac{\gamma(x,ct)}{M(x,t)}\big)=0$).

2.2 Musielak-Orlicz space

For a Musielak-Orlicz function M and a measurable function $u : \Omega \to \mathbb{R}$, we define the functional, $\varrho_{M,\Omega}(u) = \displaystyle\int_\Omega M(x, |u(x)|)dx$.

$$L_M(\Omega) = \{u : \Omega \to \mathbb{R} \quad \text{mesurable} : \quad \varrho_{M,\Omega}(\frac{u}{\lambda}) < \infty, \quad \text{for some} \quad \lambda > 0\}.$$

For any Musielak-Orlicz function M, we put $\bar{M}(x, s) = \sup_{t\geq 0}(st - M(x, s))$, the conjugate of M. We say that a sequence of function $u_n \in L_M(\Omega)$ is modularly convergent to $u \in L_M(\Omega)$ if there exists a constant $\lambda > 0$ such that $\lim_{n\to\infty} \varrho_{M,\Omega}(\frac{u_n-u}{\lambda}) = 0$.

This implies convergence for $\sigma(\Pi L_M, \Pi L_{\bar{M}})$ (see [4]).

In the space $L_M(\Omega)$, we define the following norm:

$$\|u\|_M = \inf\big\{\lambda > 0 : \int_\Omega M(x, \frac{|u(x)|}{\lambda})dx \leq 1\big\},$$

which is called the Luxemburg norm. The closure in $L_M(\Omega)$ of the set of bounded measurable functions with compact support in $\overline{\Omega}$ is denoted $E_M(\Omega)$. It is a separable space and $(E_M(\Omega))^* = L_M(\Omega)$. We define

$$W^1L_M(\Omega) = \{u \in L_M(\Omega) : D^\alpha u \in L_M(\Omega), \quad \forall\alpha \leq 1\}$$
$$W^1E_M(\Omega) = \{u \in E_M(\Omega) : D^\alpha u \in E_M(\Omega), \quad \forall\alpha \leq 1\},$$

where $D^\alpha u$ denotes the distributional derivatives. The space $W^1L_M(\Omega)$ is called the Musielak-Orlicz-Sobolev space. Let $\overline{\varrho}_{M,\Omega}(u) = \sum_{|\alpha|\leq 1} \varrho_{M,\Omega}(D^\alpha u)$ and $\|u\|^1_{M,\Omega} = \inf\{\lambda > 0 : \overline{\varrho}_{M,\Omega}(\frac{u}{\lambda}) \leq 1\}$ for $u \in W^1L_M(\Omega)$. The pair $(W^1L_M(\Omega), \|u\|^1_{M,\Omega})$ is a Banach space if M satisfies the following condition (see [14]). There exists a constant $c > 0$ such that $\inf_{x\in\Omega} M(x, 1) > c$.

2.3 Inhomogeneous Musielak-Orlicz-Sobolev spaces

For each $\alpha \in \mathbb{N}^N$, denote by D^α_x the distributional derivative on Q of order α with respect to the variable $x \in \mathbb{R}^N$. The inhomogeneous Musielak-Orlicz-Sobolev spaces of order 1 are defined as follows:

$$W^{1,x}L_M(Q) = \big\{u \in L_M(Q) : \forall|\alpha| \leq 1, \quad D^\alpha_x u \in L_M(Q)\big\}$$
$$W^{1,x}E_M(Q) = \big\{u \in E_M(Q) : \forall|\alpha| \leq 1, \quad D^\alpha_x u \in E_M(Q)\big\}.$$

The last is a subspace of the first one, and both are Banach spaces under the norm

$$\|u\| = \sum_{|\alpha|\leq m} \|D^\alpha_x u\|_{M,Q}.$$

$\mathcal{D}(\Omega)$ is dense in $L_M(\Omega)$ with respect to the modular topology, $\mathcal{D}(\Omega)$ is dense in $W^1_0L_M(\Omega)$ for the modular convergence and $\mathcal{D}(\overline{\Omega})$ is dense in $W^1_0L_M(\Omega)$ for the modular convergence.

Lemma 2.1 *(see [8]) Suppose that Ω satisfies the segment property and let $u \in W^1_0L_M(\Omega)$. Then there exists a sequence $u_n \in \mathcal{D}(\Omega)$ such that $u_n \to u$ for modular convergence in $W^1_0L_M(\Omega)$. Furthermore, if $u \in W^1_0L_M(\Omega) \cap L^\infty(\Omega)$, then $\|u_n\|_\infty \leq (N + 1)\|u\|_\infty$.*

Lemma 2.2 *(see [8]) If a sequence $u_n \in L_M(\Omega)$ converges a.e. to u and if u_n remains bounded in $L_M(\Omega)$, then $u \in L_M(\Omega)$ and $u_n \rightharpoonup u$ for $\sigma(L_M(\Omega), E_{\bar{M}}(\Omega))$.*

Lemma 2.3 *(see [8]) Let $u_n, u \in L_M(\Omega)$. If $u_n \to u$ with respect to the modular convergence, then $u_n \rightharpoonup u$ for $\sigma(L_M(\Omega), L_{\bar{M}}(\Omega))$.*

3 Essential Assumptions

Suppose Ω satisfies the segment property, and let M and γ be two Musielak-Orlicz functions such that M and its complementary $\bar{M}$ satisfy conditions of Lemma 2.2 from [1], $\gamma \ll M$ and $t^2 \leq M(x,t)$.

$A : D(A) \subset W^{1,x}L_M(\Omega) \to W^{-1,x}L_{\bar{M}}(\Omega)$ defined by $A(u_i) = -\mathrm{div}(a(x,t,\nabla u_i))$, where $a : Q_T \times \mathbb{R} \times \mathbb{R}^N \to \mathbb{R}^N$ is a Carathéodory function such that for a.e. $x \in \Omega$ and for all $s \in \mathbb{R}$, $\xi, \xi^* \in \mathbb{R}^N$ with $\xi \neq \xi^*$.

$$|a(x,t,\xi)| \leq \beta(c(x) + \bar{M}_x^{-1}(M(x,\nu_2|\xi|))),\ \beta > 0,\ c(x) \in E_{\bar{M}}(\Omega), \tag{7}$$

$$(a(x,t,\xi) - a(x,t,\xi^*)(\xi - \xi^*) > 0, \tag{8}$$

$$a(x,t,\xi)\xi \geq \alpha M(x,|\xi|). \tag{9}$$

$f_i : \Omega \times \mathbb{R} \times \mathbb{R} \to \mathbb{R}$ is a Carathéodory function.

Lemma 3.1 *The following continuous inclusions are valid: $L_M(\Omega) \hookrightarrow L^2(\Omega) \hookrightarrow L_{\bar{M}}(\Omega)$. In particular, $W_0^1 L_M(\Omega) \hookrightarrow H_0^1(\Omega)$, $H^{-1}(\Omega) \hookrightarrow W^{-1}L_{\bar{M}}(\Omega)$, $L^2(0,T,H^{-1}(\Omega)) \hookrightarrow W^{-1,x}L_{\bar{P}}(\Omega)$ and $\hookrightarrow W^{-1,x}L_{\bar{M}}(\Omega)$.*

Example 3.1 The N-function $M(t) = m(x)t^2 log(e+t)$, where $m \in (L^\infty(\Omega))^+$, verifies the assumptions above.

In all the rest of this paper and for all measurable subset E of Q_T, we designate by $meas(E)$ the Lebesgue measure of E. First, we will define the weak solution of the problem (2)-(4) used here.

Definition 3.1 A weak solution to problem (3)-(4) is a nonnegative couple

$$(u_1, u_2) \in \Big[L^2(0,T;V_1) \cap L^\infty(0,T;L^2(\Omega))\Big] \times \Big[L^2(0,T;V_2) \cap L^\infty(0,T;L^2(\Omega))\Big]$$

with

$$(u_{1,t}, u_{2,t}) \in \Big[L^2(0,T;V_1^*) + L^1\big(0,T;L^1_{loc}(\Omega)\big)\Big] \times \Big[L^2(0,T;V_2^*) + L^\infty\big(0,T;L^1_{loc}(\Omega)\big)\Big],$$

$$u_1(0,x) = u_{1,0}(x), u_2(0,x) = u_{2,0}(x), \quad a.e. \quad x \in \Omega.$$

$$\int_\Omega f_1 \frac{u_2}{(u_1)^\gamma}\phi < \infty \quad , \quad \int_\Omega f_2 \frac{u_2}{(u_1)^\gamma}\eta < \infty,$$

and

$$-\int_\Omega u_{1,0}(x)\varphi(0,x) - \int_{Q_T} u_1 \frac{\partial \varphi}{\partial t} + \int_{Q_T} a(t,x,\nabla u_1)\nabla\varphi = \int_{Q_T} F_1\varphi,$$

$$-\int_\Omega u_{2,0}(x)\psi(0,x) - \int_{Q_T} u_2 \frac{\partial \psi}{\partial t} + \int_{Q_T} a(t,x,\nabla u_2)\nabla\psi = \int_{Q_T} F_2\psi$$

for all $\varphi, \psi, \eta, \phi \in C_0^\infty([0,T) \times \Omega)$.

4 Existence Result

We shall establish the following existence theorem.

Theorem 4.1 *Suppose that* (5)–(6) *hold, then system (3)-(4) admits at least a couple of weak solutions in the sense of Definition 3.1.*

The proof is divided into 5 steps.

4.1 Step 1: Regularized system.

For $n > 0$ and $i = 1, 2$,

$$f_{1,n}(t,x) = \min\big\{n, f_1(t,x)\big\}, \tag{10}$$

$$f_{2,n}(t,x) = \text{-min}\big\{n, -f_2(t,x)\big\}. \tag{11}$$

The functions $f_{1,n}$ and $f_{2,n}$ verify the same properties as f_1 and f_2, moreover, $0 \le f_{1,n} \le f_1$, $\lim\limits_{n\to+\infty} f_{1,n} = f_1$, and $f_2 \le f_{2,n} \le 0$, $\lim_{n\to+\infty} f_{2,n} = f_2$. Let us now consider the regularized problem

$$(\mathcal{S}_n)\begin{cases} \dfrac{\partial u_{i,n}}{\partial t} - div\big(a(x,t,\nabla u_{i,n})\big) = F_{i,n}(t,x,u_{1,n},u_{2,n}) & \text{in} \quad Q_T, \\ u_{i,n}(0,x) = u_{i,n}^{(0)}(x) & \text{in} \quad \Omega, \\ u_{i,n}(t,x) = 0 & \text{on} \quad \Gamma_i \times (0,T), \\ \dfrac{\partial u_{1,n}}{\partial \nu} = 0 & \text{on} \quad \Gamma_2 \times (0,T), \\ \dfrac{\partial u_{2,n}}{\partial \nu} = 0 & \text{on} \quad \Gamma_1 \times (0,T). \end{cases} \tag{12}$$

$$F_{i,n}(t,x,u_{1,n},u_{2,n}) = \begin{cases} f_{i,n}(t,x)h_\gamma(u_{1,n} + \dfrac{1}{n}, u_{2,n}) & \text{if } u_{1,n} \ge 0 \text{ and } u_{2,n} \ge 0, \\ 0 & \text{otherwise.} \end{cases}$$

Without obviating that $u_{1,n}^{(0)}, u_{2,n}^{(0)} \in L_\infty(\Omega) \cap W_0^1 L_M(\Omega)$ is a couple of regularized sequences of the initial data obtained since $W_0^1 L_M(\Omega) \hookrightarrow H_0^1(\Omega)$), by a standard technique (see [6]), we have

$$\lim_{n\to+\infty} \frac{1}{n} ||u_{1,n}^{(0)}||_{W_0^1 L_M(\Omega)} = 0 \qquad \text{and} \qquad \lim_{n\to+\infty} \frac{1}{n} ||u_{2,n}^{(0)}||_{W_0^1 L_M(\Omega)} = 0. \tag{13}$$

Lemma 4.1 *The problem (12) admits a nonnegative couple of solutions*

$$(u_{1,n}, u_{2,n}) \in [L^2(0,T;V_1) \cap L^\infty(Q_T)] \times [L^2(0,T;V_2) \cap L^\infty(Q_T)]$$

such that

$$-\int_\Omega u_{1,n}^{(0)}(x)\varphi(0,x) - \int_{Q_T} u_{1,n}\frac{\partial \varphi}{\partial t} + \int_{Q_T} a(t,x,\nabla u_{1,n})\nabla\varphi = \int_{Q_T} F_{1,n}(t,x,u_{1,n},u_{2,n})\varphi, \tag{14}$$

$$-\int_\Omega u_{2,n}^{(0)}(x)\psi(0,x) - \int_{Q_T} u_{2,n}\frac{\partial \psi}{\partial t} + \int_{Q_T} a(t,x,\nabla u_{2,n})\nabla\psi = \int_{Q_T} F_{2,n}(t,x,u_{1,n},u_{2,n})\psi \tag{15}$$

for every $\varphi, \psi, \in C_0^\infty([0,T) \times \Omega)$.

Proof. Without losing generality, we assume $u_{1,n}^{(0)} = 0$ and $u_{2,n}^{(0)} = 0$. Then, by using the Stampacchia method [18], we show the positivity of the solution. Take $\varphi = -u_{1,n}^-$ as a test function in the first equation of the problem (12), where $u_{1,n} = u_{1,n}^+ - u_{1,n}^-$, $u_{1,n}^+ = \max\{u_{1,n}, 0\}, u_{1,n}^- = \max\{-u_{1,n}, 0\}$.

Since $u_{1,n}^+ = 0$ on supp$u_{1,n}^-$, the right-hand side of (14) is zero because

$$F_n(t,x,u_{1,n},u_{2,n}) = \begin{cases} f_{1,n}(t,x)h_\gamma(u_{1,n} + \dfrac{1}{n}, u_{2,n}) & \text{if } u_{1,n} \geq 0 \text{ and } u_{2,n} \geq 0, \\ 0 & \text{otherwise.} \end{cases}$$

So we have

$$\int_{Q_T} (u_{1,n})_t(-u_{1,n}^-) + \int_{Q_T} a(t,x,\nabla u_{1,n})\nabla(-u_{1,n}^-) = 0,$$

which gives

$$\int_{Q_T} (u_{1,n}^+ - u_{1,n}^-)_t(-u_{1,n}^-) + \int_{Q_T} a(t,x,\nabla u_{1,n})\nabla(-u_{1,n}^-) = 0.$$

We observe that on the support of $u_{1,n}$, we have $u_{1,n}^+ u_{1,n}^- = 0$ on supp$u_{1,n}$, it comes

$$\int_{Q_T} (u_{1,n}^+ - u_{1,n}^-)_t(-u_{1,n}^-) + \int_{Q_T \cap \{u_{1,n} \geq 0\}} a(t,x,\nabla u_{1,n})\nabla(-u_{1,n}^-)$$

$$+ \int_{Q_T \cap \{u_{1,n} \leq 0\}} a(t,x,\nabla u_{1,n})\nabla(-u_{1,n}^-) = 0$$

$$\int_\Omega \frac{1}{2}(u_{1,n})^2 + \int_{Q_T} a(t,x,\nabla(-u_{1,n}^-))\nabla(-u_{1,n}^-) = 0$$

$$\int_\Omega \frac{1}{2}(u_{1,n})^2 + \int_{Q_T} a\big(t,x,,\nabla(-u_{1,n}^-)\big)\nabla(-u_{1,n}^-) \geq \int_\Omega \frac{1}{2}(u_{1,n}^-)^2 + \alpha \int_{Q_T} M\big(|\nabla(u_{1,n}^-)|\big),$$

$$u_{1,n}^- = 0 \quad \text{a.e in } Q_T, \tag{16}$$

i.e., $u_{1,n} \geq 0$ a.e. in Ω and for all $t \in [0,T)$. Analogously, we prove that $u_{2,n} \geq 0$ by the testing function $\psi = -u_{2,n}^-$. Let us denote by T_k the truncation function $T_k(s) = \max\{-k, \min\{k,s\}\}$, $k \geq 0, s \in \mathbb{R}$, where $\langle .,. \rangle$ denotes the duality product between V_i^* and V_i for $i = 1, 2$.

4.2 Step 2: L^∞ and energy estimates for $(u_{1,n}, u_{2,n})$

Proposition 4.1 *There exist positive constants C_1 and C_2, independent of n, such that*

$$||u_{1,n}||_{L^\infty(Q_T)} \leq C_1, \text{ and } ||u_{2,n}||_{L^\infty(Q_T)} \leq C_2. \tag{17}$$

Proof. The estimate (17) for $\{u_{1,n}\}$ follows directly by Proposition 2.13 [7] with some abbreviations that go along with our problem, it remains to prove the uniform boundedness of $u_{2,n}$.

For simplicity, we suppose $u_{2,n}^{(0)}(x) = 0$, to handle the equation solved by $u_{2,n}$, we choose as a test function $\psi = (u_{2,n} - C_2)^+$, with $C_2 > 1$ fixed, we obtain with $Q_t = \Omega \times [0, t)$,

$$\int_\Omega (u_{2,n})_t (u_{2,n} - C_2)^+ + \int_{Q_T} a(t, x, \nabla u_{2,n}) \nabla (u_{2,n} - C_2)^+$$

$$= \int_\Omega f_{2,n}(t, x) h_\gamma(u_{1,n} + \frac{1}{n}, u_{2,n})(u_{2,n} - C_2)^+ \leq 0. \tag{18}$$

$$\begin{aligned}\int_{Q_T} a(t, x, \nabla u_{2,n}) \nabla (u_{2,n} - C_2)^+ &= \int_{\{(t,x) \in Q_T / u_{2,n}(t,x) \leq C_2\}} a(t, x, \nabla u_{2,n}) \nabla (v_n - C_2)^+ \\ &+ \int_{\{(t,x) \in Q_T / u_{2,n}(t,x) \geq C_2\}} a(t, x, \nabla u_{2,n}) \nabla (u_{2,n} - C_2)^+ \\ &= \int_{\{(t,x) \in Q_T / u_{2,n}(t,x) \geq C_2\}} a(t, x, , \nabla u_{2,n}) \nabla u_{2,n}.\end{aligned} \tag{19}$$

When neglecting the nonnegative term on the left-hand side of (18), it comes

$$(u_{2,n} - C_2)^+ = 0, \quad \text{a.e.} \quad \text{in } Q_T,$$

which completes the proof. Choosing as a test function $\varphi = u_{1,n} \in L^2(0, T; V)$ in the first equation of problem (12), by integrating over $\Omega \times [0, t)$, we obtain

$$\frac{1}{2} \frac{d}{dt} \int_{Q_T} (u_{1,n})^2 + \int_{Q_T} a(t, x, \nabla u_{1,n}) \nabla u_{1,n} = \int_{Q_T} f_{1,n}(t, x) h_\gamma(u_{1,n} + \frac{1}{n}, u_{2,n}) u_{1,n},$$

in other words,

$$\frac{1}{2} \int_\Omega u_{1,n}^2(t) + \int_{Q_T} a(t, x, \nabla u_{1,n}) \nabla u_{1,n} = \frac{1}{2} ||u_{0,n}||^2_{L^2(\Omega)} + \int_{Q_T} f_{1,n}(t, x) h_\gamma(u_{1,n} + \frac{1}{n}, u_{2,n}) u_{1,n}.$$

Due to the fact that $h_\gamma(u_{1,n} + \frac{1}{n}, u_{2,n}) \leq \frac{u_{1,n}}{(u_{1,n} + \frac{1}{n})^\gamma} \leq u_{1,n}^{1-\gamma}$ and $0 < 1 - \gamma < 1$, we deduce

$$\int_{Q_T} f_{1,n}(t, x) h_\gamma(u_{1,n} + \frac{1}{n}, u_{2,n}) u_{2,n} \leq \int_{Q_T} f_{1,n}(t, x) u_{1,n}^{1-\gamma} u_{2,n} \leq \sup u_{1,n}^{1-\gamma} u_{2,n} \int_{Q_T} f_{1,n} \leq C,$$

again, we have

$$||u_{1,n}||_{L^\infty(0,T;L^2(\Omega))} \leq C.$$

For the second equation of problem (12), we choose as a test function $\psi = u_{2,n} \in L^2(0, T; V_2)$. We obtain

$$\begin{aligned}\frac{1}{2} \int_\Omega u_{2,n}^2(t) + \int_{Q_T} a(t, x, \nabla u_{2,n}) \nabla u_{2,n} &= \frac{1}{2} ||u_{2,n}^{(0)}||^2_{L^2(\Omega)} + \int_\Omega f_{2,n}(t, x) h_\gamma(u_{1,n} + \frac{1}{n}, u_{2,n}) u_{2,n} \\ &\leq \frac{1}{2} ||u_{2,n}^{(0)}||^2_{L^2(\Omega)},\end{aligned} \tag{20}$$

which gives $||u_{2,n}||_{L^\infty\left(0,T;L^2(\Omega)\right)} \leq C$, hence the inequality (15).

Note that $h_\gamma(u_{1,n} + \dfrac{1}{n}, u_{2,n}) \leq \dfrac{u_{1,n}}{(u_{1,n} + \frac{1}{n})^\gamma} \leq u_{1,n}^{1-\gamma}$ and $0 < 1 - \gamma < 1$, using the L^∞-estimate of $u_{1,n}$ and (9), by plugging $\varphi = u_{1,n} \in L^2(0,T;V_1)$ as a test function in (12), we easily get

$$||u_{1,n}||_{L^\infty(0,T;L^2(\Omega))} \leq C_3,$$

where C_3 is a positive constant independent of n. Similarly, by plugging $\psi = u_{2,n} \in L^2(0,T;V_2)$ in (12), we get $||u_{2,n}||_{L^\infty\left(0,T;L^2(\Omega)\right)} \leq C_4$, hence, there exists a positive constant C_5, independent of n,

$$||u_{1,n}||_{L^2(0,T;V_1)} + ||u_{2,n}||_{L^2(0,T;V_2)} \leq C_5. \tag{21}$$

Proposition 4.2 *There exists a positive constant $C > 0$, independent of n, such that*

$$\int_{Q_T} f_{1,n}(t,x) h_\gamma(u_{1,n} + \frac{1}{n}, u_{2,n}) \varphi^2(x) \leq C \text{ for all } n \in \mathbb{N} \tag{22}$$

for every $\varphi \in C_0^\infty(Q_T)$. For $\delta > 0$, we have

$$\int_{Q_T \cap \{0 \leq u_{1,n} \leq \delta\}} f_{1,n}(t,x) h_\gamma(u_{1,n} + \frac{1}{n}, u_{2,n}) \varphi^2(x) \leq C\delta, \tag{23}$$

$$\int_{Q_T \cap \{0 \leq u_{2,n} \leq \delta\}} f_{1,n}(t,x) h_\gamma(u_{1,n} + \frac{1}{n}, u_{2,n}) \varphi^2(x) \leq \begin{cases} C\delta^{1-\gamma} & \text{if } 0 < \gamma < 1, \\ C\sqrt{\delta} & \text{if } \gamma = 1 \end{cases} \tag{24}$$

for every $\varphi \in C_0^\infty(Q_T)$ with $\varphi \geq 0$.

Proof. The proof follows the same lines as Proposition 2.20 in [7], see also [12], with slight modifications since the growth of $a(t,x,\nabla u)$ with embedding in Lemma 3.1, we examine only the estimate (22) for the convenience. Multiplying the first equation of problem (12) by the test function $\varphi^2(x)$, we get

$$\int_0^T \left\langle (u_{1,n})_t, \varphi^2(x) \right\rangle + 2\int_{Q_T} a(t,x,\nabla u_{1,n}).\varphi \nabla \varphi = \int_{Q_T} f_{1,n}(t,x) h_\gamma(u_{1,n} + \frac{1}{n}, u_{2,n}) \varphi^2(x),$$

which gives

$$\int_{Q_T} f_{1,n}(t,x) h_\gamma(u_{1,n} + \frac{1}{n}, u_{2,n}) \varphi^2(x) \leq 2\int_{Q_T} |a(t,x,\nabla u_{1,n})||\varphi||\nabla\varphi| + C,$$

this gives, by applying Hölder's inequality and the previous proposition,

$$\int_{Q_T} f_{1,n}(t,x) h_\gamma(u_{1,n} + \frac{1}{n}, u_{2,n}) \varphi^2(x) \leq C + 2\left(\int_{Q_T} |a(t,x,\nabla u_{1,n})|^2 \varphi^2\right)^{\frac{1}{2}} . \left(\int_{Q_T} |\nabla(\varphi)|^2\right)^{\frac{1}{2}}$$
$$\leq C_2,$$

which proves the inequality (22).

A similar estimate is in the following Proposition 4.3, by multiplying problem (12) by the test function $\psi^2(x)$.

Proposition 4.3 *For $\delta > 0$, we have*

$$\int_{Q_T} |f_{2,n}(t,x)| h_\gamma(u_{1,n} + \frac{1}{n}, u_{2,n}) \psi^2(x) \leq C \text{ , for all } n \in \mathbb{N}, \tag{25}$$

$$\int_{Q_T \cap \{0 \leq u_{2,n} \leq \delta\}} \big| f_{2,n}(t,x)| h_\gamma(u_{1,n} + \frac{1}{n}, u_{2,n}) \varphi^2(x) \leq C\delta, \tag{26}$$

$$\int_{Q_T \cap \{0 \leq u_{1,n} \leq \delta\}} \big| f_{2,n}(t,x)| h_\gamma(u_{1,n} + \frac{1}{n}, u_{2,n}) \varphi^2(x) \leq \begin{cases} C\delta^{1-\gamma} & \text{if } 0 < \gamma < 1 \\ C\sqrt{\delta} & \text{if } \gamma = 1. \end{cases}, \tag{27}$$

4.3 Step 3: Convergence and compactness results

To pass to the limit as $n \to \infty$ in (14) and (15), we need strongly convergent subsequences, which is ensured by the following proposition.

Proposition 4.4 *There exists a couple*

$$(u_1, u_2) \in \Big[L^2(0,T;V_1) \cap L^\infty(Q_T) \Big] \times \Big[L^2(0,T;V_2) \cap L^\infty(Q_T) \Big]$$

such that, as $n \to \infty$, we have, up to a subsequence,

$$u_{n,i} \rightharpoonup u_i \quad \text{weakly in} \quad L^2(0,T;V_i) \quad \text{for} \quad i = 1,2, \tag{28}$$

$$u_{n,i} \rightharpoonup u_i \quad \text{weakly in} \quad L^\infty(Q_T) \quad \text{for} \quad i = 1,2, \tag{29}$$

$$u_{n,i} \to u_i \quad \text{strongly in} \quad L^1(Q_T) \quad \text{for} \quad i = 1,2, \tag{30}$$

$$u_{n,i} \to u_i \quad \text{a.e.in} \quad Q_T \quad \text{for} \quad i = 1,2, \tag{31}$$

$$\lim_{n \to +\infty} \int_{Q_T} \big| \nabla(u_{n,i} - u_i) \big|^2 = 0 \quad \text{for} \quad i = 1,2. \tag{32}$$

Therefore,

$$\nabla u_{n,i} \to \nabla u_i \text{ a.e. in } Q_T \quad \text{for} \quad i = 1,2. \tag{33}$$

Proof. Convergences (28) are direct consequences of (21). The same thing applies to convergences (29). To prove (30) , we observe that the estimate (22) leads to

$$f_{1,n}(t,x) h_\gamma(u_{1,n} + \frac{1}{n}, u_{2,n}) \varphi^2(x) \in L^1(Q_T) \quad , \quad \forall \varphi \in C_0^\infty(\Omega). \tag{34}$$

In addition, we have

$$\frac{\partial(u_{1,n}\varphi^2)}{\partial t} \quad \text{is bounded in} \quad L^2(0,T;V_1^*) + L^1(Q_T). \tag{35}$$

By (35), choosing s such that $s > \frac{N}{2} + 1$ and using the same argument as in Lemma 2.3 from [17], we deduce that $\frac{\partial(u_{1,n}\varphi)}{\partial t}$ is bounded in $L^2(0,T;H^{-s})$, consequently, since $s > \frac{N}{2}$, we find that $V_1 \subset L^p(\Omega) \subset H^{-s}(\Omega)$ and the embedding $V_1 \hookrightarrow L^p(\Omega)$ is compact. Applying now Corollary 4 from [17], by (35) and the compactness results, we deduce that $u_{1,n}\varphi$ is relatively compact in $L^2(Q_T)$. Hence, up to a subsequence, convergences (30) and (31) are satisfied.

(32) and (33) can be obtained as a particular case of Proposition 3.14 from [7].

4.4 Step 4: Uniform estimate near the singularity

We consider the set $\{(t,x) \in Q_T : u_1(t,x) = 0\}$. As a consequence of the uniform estimate near the singularity (23), we have the following proposition.

Proposition 4.5 *The couple (u_1, u_2) as a solution to (2) and (3), in the sense of Definition 2.1, satisfies*

$$\int_{Q_T \cap \{u_1=0\}} f_1(t,x) h_\gamma(u_1,u_2)\varphi = 0 \tag{36}$$

$$\int_{Q_T \cap \{u_1=0\}} f_2(t,x) h_\gamma(u_1,u_2)\psi = 0 \tag{37}$$

for all $\varphi, \psi \in C_0^\infty\big(\Omega \times [0,T)\big)$ with $\varphi, \psi \geq 0$. Moreover,

$$\int_{Q_T} f_1(t,x) h_\gamma(u_1,u_2)\varphi = \int_{Q_T \cap \{u>0\}} f_1(t,x) h_\gamma(u_1,u_2)\varphi \tag{38}$$

$$\int_{Q_T} f_2(t,x) h_\gamma(u_1,u_2)\psi = \int_{Q_T \cap \{u>0\}} f_2(t,x) h_\gamma(u_1,u_2)\psi. \tag{39}$$

Proof.

1. Let $\psi \in C_0^\infty\big(\Omega \times [0,T)\big), \psi \geq 0$, with $\text{supp}\psi = Y \times [0,T_1],\ T_1 < T,\ \ Y \subset\subset E \subset\subset \Omega$ and $\varphi \in C_0^1\big(\Omega\big)$ with $\varphi(x) = 1$ over Y , $\varphi \geq 0$ with supp $\varphi = E$, by the uniform estimate (23), we obtain

$$\begin{aligned}
&\int_{Q_T \cap \{u_{1,n}<\delta\}} f_{1,n}(t,x) h_\gamma\left(u_{1,n} + \frac{1}{n}, u_{2,n}\right)\psi(t,x) \\
&\leq ||\psi||_\infty \int_{[0,T]\times Y} f_{1,n}(t,x) h_\gamma(u_{1,n} + \frac{1}{n}, u_{2,n})\chi_{\{u_{1,n}<\delta\}} \\
&\leq ||\psi||_\infty \int_{Q_T} f_{1,n}(t,x) h_\gamma\left(u_{1,n} + \frac{1}{n}, u_{2,n}\right)\varphi^2(x)\chi_{\{u_{1,n}<\delta\}}.
\end{aligned}$$

On the other hand,

$$\begin{aligned}
&\int_{Q_T} f_{1,n}(t,x) h_\gamma\left(u_{1,n} + \frac{1}{n}, u_{2,n}\right)\chi_{\{u_{1,n}<\delta\}}\psi(t,x) \\
&= \int_{Q_T} f_{1,n}(t,x) h_\gamma\left(u_{1,n} + \frac{1}{n}, u_{2,n}\right)\chi_{\{u_{1,n}<\delta\}}\chi_{\{u_1=\delta\}}\psi(t,x) \\
&+ \int_{Q_T} f_{1,n}(t,x) h_\gamma\left(u_{1,n} + \frac{1}{n}, u_{2,n}\right)\chi_{\{u_{1,n}<\delta\}}\chi_{\{u_1\neq\delta\}}\psi(t,x) \\
&\leq C\delta.
\end{aligned} \tag{40}$$

We observe that there exists at most a countable set D_1 such that meas$\{(t,x) : u_1(t,x) = \delta\} > 0$. We choose δ outside of this set D_1 so that, in (40),

$$\int_{Q_T} f_{1,n}(t,x) h_\gamma\left(u_{1,n} + \frac{1}{n}, u_{2,n}\right)\chi_{\{u_{1,n}<\delta\}}\chi_{\{u_1=\delta\}}\psi(t,x) = 0.$$

So, we have

$$\begin{aligned}&\int_{Q_T} f_{1,n}(t,x)h_\gamma\left(u_{1,n}+\frac{1}{n},u_{2,n}\right)\chi_{\{u_{1,n}<\delta\}}\psi(t,x)\\&=\int_{Q_T} f_{1,n}(t,x)h_\gamma\left(u_{1,n}+\frac{1}{n},u_{2,n}\right)\chi_{\{u_{1,n}<\delta\}}\chi_{\{u_1\neq\delta\}}\psi(t,x)\leq C\delta.\end{aligned}\tag{41}$$

By (31), we have $\chi_{\{u_{1,n}<\delta\}}\chi_{\{u_1\neq\delta\}}\to\chi_{\{u_1<\delta\}}$ a.e. in Q_T.
Fix δ, in (41), by Fatou's lemma, we get

$$\int_{Q_T} f_1(t,x)h_\gamma(u_1,u_2)\chi_{\{u<\delta\}}\psi(t,x)\leq C\delta.$$

Let δ to 0, Fatou's lemma leads to

$$\int_{Q_T} f_1(t,x)h_\gamma(u_1,u_2)\chi_{\{u=0\}}\psi(t,x)=\int_{Q_T\cap\{u_1=0\}} f_1(t,x)h_\gamma(u_1,u_2)\psi(t,x)=0,\tag{42}$$

this leads to

$$\int_{Q_T} f_1(t,x)h_\gamma(u_1,u_2)\psi(t,x)=\int_{Q_T\cap\{u_1>0\}} f_1(t,x)\psi(t,x).\tag{43}$$

These are the identities we are aiming to establish.

2. Similarly, with some simplifications, we establish the validity of (37) and (39). By plugging a test function $\phi\in C_0^\infty([0,T)\times\Omega),\phi\geq 0$ with supp $\phi=Y\times[0,T_2],T_2<T,\bar{Y}\subset\subset E\subset\subset\Omega$ and $\varphi\in C_0^1(\Omega)$ with $\varphi(x)=1$ over $\bar{Y}$, $\varphi\geq 0$ with supp $\varphi=E$. By the uniform estimate (27), we obtain

$$\begin{aligned}&\int_{Q_T\cap\{u_{1,n}\leq\delta\}}|f_{2,n}(t,x)|h_\gamma\left(u_{1,n}+\frac{1}{n},u_{2,n}\right)\phi(t,x)\\&\leq||\phi||_\infty\int_{[0,T]\times Y}\left|f_{2,n}(t,x)\right|h_\gamma\left(u_{1,n}+\frac{1}{n},u_{2,n}\right)\chi_{\{u_{1,n}<\delta\}}\\&\leq||\phi||_\infty\int_{[0,T]\times Y}\left|f_{2,n}(t,x)\right|h_\gamma\left(u_{1,n}+\frac{1}{n},u_{2,n}\right)\varphi^2(x)\chi_{\{u_{1,n}<\delta\}},\\&\leq\begin{cases}C\delta^{1-\gamma} & \text{if } 0<\gamma<1\\ C\sqrt{\delta} & \text{if } \gamma=1.\end{cases}\end{aligned}$$

On the other hand,

$$\begin{aligned}&\int_{Q_T}\left|f_{2,n}(t,x)\right|h_\gamma\left(u_{1,n}+\frac{1}{n},u_{2,n}\right)\chi_{\{u_{1,n}<\delta\}}\phi(t,x)\\&=\int_{Q_T}\left|f_{2,n}(t,x)\right|h_\gamma\left(u_{1,n}+\frac{1}{n},u_{2,n}\right)\chi_{\{u_{1,n}<\delta\}}\chi_{\{u_1=\delta\}}\phi(t,x)\\&+\int_{Q_T}\left|f_{2,n}(t,x)\right|h_\gamma\left(u_{1,n}+\frac{1}{n},u_{2,n}\right)\chi_{\{u_{1,n}<\delta\}}\chi_{\{u_1\neq\delta\}}\phi(t,x),\\&\leq\begin{cases}C\delta^{1-\gamma} & \text{if } 0<\gamma<1\\ C\sqrt{\delta} & \text{if } \gamma=1.\end{cases}\end{aligned}\tag{44}$$

Note that there exists at most a countable set $\bar{D}_2$: meas $\{(t,x) : u_1(t,x) = \delta\} > 0$. Select $\delta \notin \bar{D}_2$, so, in (44), the integral

$$\int_{Q_T} \big|f_{2,n}(t,x)\big| h_\gamma\left(u_{1,n} + \frac{1}{n}, u_{2,n}\right) \chi_{\{u_{1,n}<\delta\}} \chi_{\{u_1=\delta\}} \phi(t,x) = 0.$$

So, we have

$$\begin{aligned} &\int_{Q_T} \big|f_{2,n}(t,x)\big| h_\gamma\left(u_{1,n} + \frac{1}{n}, u_{2,n}\right) \chi_{\{u_{1,n}<\delta\}} \phi(t,x) \\ &= \int_{Q_T} \big|f_{2,n}(t,x)\big| h_\gamma\left(u_{1,n} + \frac{1}{n}, u_{2,n}\right) \chi_{\{u_{1,n}<\delta\}} \chi_{\{u_1\neq\delta\}} \phi(t,x), \qquad (45) \\ &\leq \begin{cases} C\delta^{1-\gamma} & \text{if } 0<\gamma<1 \\ C\sqrt{\delta} & \text{if } \gamma = 1. \end{cases} \end{aligned}$$

By (31), we have $\chi_{\{u_{1,n}<\delta\}} \chi_{\{u_1\neq\delta\}} \to \chi_{\{u_1<\delta\}}$ a.e. in Q_T.
For δ fixed, Fatou's lemma in (45) leads to

$$\int_{Q_T} f_2(t,x) h_\gamma(u_1,u_2) \chi_{\{u_1<\delta\}} \phi(t,x) \leq \begin{cases} C\delta^{1-\gamma} & \text{if } 0<\gamma<1 \\ C\sqrt{\delta} & \text{if } \gamma = 1. \end{cases}$$

Again, by Fatou's lemma, we get for $\delta \to 0$,

$$\int_{Q_T} \big|f_2(t,x)\big| h_\gamma(u_1,u_2) \chi_{\{u_1=0\}} \phi(t,x) = \int_{Q_T \cap \{u_1=0\}} \big|f_2(t,x)\big| h_\gamma(u_1,u_2) \phi(t,x) = 0, \qquad (46)$$

this leads to

$$\int_{Q_T} \big|f_2(t,x)\big| h_\gamma(u_1,u_2) \chi_{\{u_1=0\}} \phi(t,x) = \int_{Q_T \cap \{u>0\}} \big|f_2(t,x)\big| h_\gamma(u_1,u_2) \phi(t,x), \qquad (47)$$

which also means

$$\int_{Q_T} f_2(t,x) h_\gamma(u_1,u_2) \chi_{\{u_1=0\}} \phi(t,x) = \int_{Q_T \cap \{u_1>0\}} f_2(t,x) h_\gamma(u_1,u_2) \phi(t,x),$$

this is the desired result.

4.5 Step 5: Proof of main theorem

Now, we present the proof of the primary result in this paper. Since $u_{1,n}, u_{2,n} \geq 0$ a.e. in Q_T , thanks to (29), we obtain $u_1, u_2 \geq 0$. Thanks to (30), we can proceed to take the limit in the sections related to the time derivatives of (14) and (15). By (14), $(\nabla u_{1,n})$ and $(\nabla u_{2,n})$ are equi-integrable. By (31) and (33), Vitali's theorem (see Theorem 1.0.16 in [11]) leads to

$$\nabla u_{1,n} \to \nabla u_1 \quad \text{in} \quad L^2(Q_T), \qquad (48)$$

$$\nabla u_{2,n} \to \nabla u_2 \quad \text{in} \quad L^2(Q_T). \qquad (49)$$

We deal now with the singular lower-order terms. Let $D = K \times [0, T_1], T_1 < T$ such that $K \subset\subset E \subset\subset \Omega$ and $\psi \in C_0^\infty(\Omega)$ with supp$\psi = D$. Let ϕ be a function such that

$\phi(x) = 1$ on the set K, $0 \leq \phi \leq 1$ and supp $\phi = E$.

Let $\delta > 0$, we have

$$\begin{cases} \displaystyle\int_{Q_T} f_{1,n}(t,x)h_\gamma(u_{1,n} + \frac{1}{n}, u_{2,n})\psi = \int_{Q_T \cap \{0 \leq u_{1,n} < \delta\}} f_{1,n}(t,x)h_\gamma(u_{1,n} + \frac{1}{n}, u_{2,n})\psi \\ \displaystyle + \int_{Q_T \cap \{u_{1,n} \geq \delta\}} f_{1,n}(t,x)h_\gamma(u_{1,n} + \frac{1}{n}, u_{2,n})\psi = \Delta_1 + \Delta_2. \end{cases}$$

Concerning the term Δ_1, we proceed as

$$\begin{aligned} \Delta_1 &\leq ||\psi||_\infty \int_{D \cap \{0 \leq u_{1,n} < \delta\}} f_{1,n}(t,x)h_\gamma\left(u_{1,n} + \frac{1}{n}, u_{2,n}\right)\varphi^2(x) \\ &\leq ||\psi||_\infty \int_{Q_T \cap \{0 \leq u_{1,n} < \delta\}} f_{1,n}(t,x)h_\gamma\left(u_{1,n} + \frac{1}{n}, u_{2,n}\right)\varphi^2(x). \end{aligned}$$

By (23), we get to

$$\Delta_1 \leq C\delta, \tag{50}$$

where C is a constant independent of n. For Δ_2, we have

$$\begin{aligned} \Delta_2 &= \int_{Q_T} f_{1,n}(t,x)h_\gamma\left(u_{1,n} + \frac{1}{n}, u_{2,n}\right)\psi(t,x)\chi_{\{u_{1,n} \geq \delta\}}\chi_{\{u_1 \neq \delta\}} \\ &+ \int_{Q_T} f_{1,n}(t,x)h_\gamma\left(u_{1,n} + \frac{1}{n}, u_{2,n}\right)\psi(t,x)\chi_{\{u_{1,n} \geq \delta\}}\chi_{\{u_1 = \delta\}} \\ &= \Delta_3 + \Delta_4. \end{aligned}$$

Note that there is at most a countable set Θ_1 such that meas$\{(t,x) : u_1(t,x) = \delta\} > 0$. Choose $\delta \notin \Theta_1$, so $\Delta_4 = 0$. Since (31) holds, for Δ_3, we have that $\chi_{\{u_{1,n} \geq \delta\}}\chi_{\{u_1 \neq \delta\}} \to \chi_{\{u_1 > \delta\}}$ a.e. in Q_T. $f_{1,n}(t,x)h_\gamma\left(u_{1,n} + \frac{1}{n}, u_{2,n}\right)\chi_{\{u_{1,n} \geq \delta\}}\chi_{\{u_1 \neq \delta\}}\psi(t,x) \leq f_1(t,x)h_\gamma(\delta, u_{2,n})\psi(t,x) \in L^1(Q_T)$. By (31) and the Lebesgue theorem, we have

$$\begin{aligned} &\lim_{n \to +\infty} \int_{Q_T} f_{1,n}(t,x)h_\gamma\left(u_{1,n} + \frac{1}{n}, u_{2,n}\right)\chi_{\{u_{1,n} \geq \delta\}}\chi_{\{u_1 \neq \delta\}}\psi(t,x) \\ &\qquad = \int_{Q_T} f_1(t,x)h_\gamma(u_1, u_2)\chi_{\{u_1 \geq \delta\}}\psi(t,x). \end{aligned}$$

Then

$$\lim_{n \to +\infty} \Delta_2 = \int_{Q_T} f_1(t,x)h_\gamma(\delta, u_1)\chi_{\{u_1 \geq \delta\}}\psi(t,x). \tag{51}$$

By (4.5), (50), (51) and (43), we get

$$\begin{aligned} &\lim_{n \to +\infty} \int_{Q_T} f_{1,n}(t,x)h_\gamma\left(u_{1,n} + \frac{1}{n}, u_{2,n}\right)\psi(t,x) \\ &= \lim_{n \to +\infty} \int_{Q_T} f_{1,n}(t,x)h_\gamma\left(u_{1,n} + \frac{1}{n}, u_{2,n}\right)\psi(t,x)\chi_{\{u_{1,n} \geq \delta\}} = \int_{Q_T} f_1(t,x)h_\gamma(\delta, u_2)\psi(t,x). \end{aligned}$$

Similarly, for any $\delta > 0$,

$$\begin{aligned}\int_{Q_T} f_{2,n}(t,x)h_\gamma(u_{1,n}+\frac{1}{n},u_{2,n})\psi(t,x) &= \int_{Q_T\cap\{0\le u_{1,n}<\delta\}} f_{2,n}(t,x)h_\gamma(u_{1,n}+\frac{1}{n},u_{2,n})\psi(t,x)\\ &+\int_{Q_T\cap\{u_{1,n}\ge\delta\}} f_{2,n}(t,x)h_\gamma(u_{1,n}+\frac{1}{n},u_{2,n})\psi(t,x)\\ &= I_1+I_2.\end{aligned} \tag{52}$$

Concerning the term I_1, we have

$$\big|I_1\big| \le ||\psi||_\infty \int_{Q_T\cap\{0\le u_{1,n}<\delta\}} f_{2,n}(t,x)h_\gamma(u_{1,n}+\frac{1}{n},u_{2,n})\varphi^2(x).$$

By (27), we get to

$$|I_1| \le ||\psi||_\infty \begin{cases} C\delta^{1-\gamma} & \text{if } 0<\gamma<1,\\ C\sqrt{\delta} & \text{if } \gamma=1.\end{cases} \tag{53}$$

Hence, $\lim\limits_{\delta\to 0}\big|I_1\big| = 0$. Concerning I_2, we see that

$$\begin{aligned} I_2 &= \lim_{n\to+\infty}\int_{Q_T} f_{2,n}(t,x)h_\gamma\left(u_{1,n}+\frac{1}{n},u_{2,n}\right)\chi_{\{u_{1,n}\ge\delta\}}\chi_{\{u_1\ne\delta\}}\psi(t,x)\\ &+\int_{Q_T} f_{2,n}(t,x)h_\gamma\left(u_{1,n}+\frac{1}{n},u_{2,n}\right)\chi_{\{u_{1,n}\ge\delta\}}\chi_{\{u_1=\delta\}}\psi(t,x) = J_1+J_2.\end{aligned}$$

We note that there exists, at most, a countable set Θ_2 such that meas$\{(t,x) : u_1(t,x) = \delta\} > 0$. Choose $\delta \notin \Theta_2$, so $J_1 = 0$, since (31) holds, for B_1, we have

$$\begin{aligned} &\chi_{\{u_{1,n}\ge\delta\}}\chi_{\{u_1\ne\delta\}} \to \chi_{\{u_1>\delta\}} \quad \text{a.e. in } Q_T\\ &\big|f_{2,n}(t,x)\big|h_\gamma\left(u_{1,n}+\frac{1}{n},u_{1,n}\right)\chi_{\{u_{1,n}\ge\delta\}}\chi_{\{u_1\ne\delta\}}\psi(t,x)\\ &\le \big|f_2(t,x)\big|h_\gamma(\delta,u_{2,n})\psi(t,x)\in L^1(Q_T).\end{aligned}$$

The Lebesgue theorem combined with (31) leads to

$$\lim_{n\to\infty} I_2 = \int_{Q_T} f_2(t,x)h_\gamma(u_1,u_2)\chi_{\{u_1>\delta\}}\psi(t,x). \tag{54}$$

By (52), (53), (54) and (47), we can get

$$\begin{aligned} &\lim_{n\to+\infty}\int_{Q_T} f_{2,n}(t,x)h_\gamma\left(u_{1,n}+\frac{1}{n},u_{2,n}\right)\psi(t,x)\\ &= \lim_{n\to+\infty}\int_{Q_T} f_{2,n}(t,x)h_\gamma\left(u_{1,n}+\frac{1}{n},u_{2,n}\right)\chi_{\{u_{1,n}\ge\delta\}}\psi(t,x)\\ &= \int_{Q_T} f_2(t,x)h_\gamma(u_1,u_2)\psi(t,x).\end{aligned}$$

Applying a similar argument to $u_{1,n}$ to address the case of $u_{1,n}$, but this time utilizing (24) and (26), we conclude the proof of our main result, Theorem 2.2.

References

[1] A. Aberqi, J. Bennouna and M. Elmassoudi. Existence and uniqueness of renormalized solution for nonlinear parabolic equations in Musielak Orlicz spaces. *Boletim da Sociedade Paranaense de Matemática* **40** (2022) 1–22.

[2] A. Aberqi, J. Bennouna and M. Hammoumi. *Existence results for nonlinear degenerated parabolic systems. Nonlinear Dyn. Syst. Theory* **17** (3) (2017) 217–229.

[3] M. A. Beauregard and Q. Sheng. A fully adaptive approximation for quenching-type reaction-diffusion equations over circular domains. *Numerical methods in PDE* **30** (2) (2013) 472–489.

[4] A. Benkirane and M. Sidi El Vally. Some approximation properties in Musielak-Orlicz-Sobolev spaces. *Thai. J. Math.* (2012) 371–381.

[5] T. Bouali and R. Guefaifiai. Weak Solutions for a Class of (p,q) Laplacian quasilinear Elliptic System with Different Weights. *International Journal of Partial Differential Equations and Applications* **2** (5) (2014) 86–90.

[6] A. Dall'Aglio, D. Giachetti and J. P. Puel. Nonlinear parabolic equations with natural growth in general domains. *Boll. Unione Mat. Ital. Serie* **8-B** (3) (2005) 653–683.

[7] I. De Bonis D. and Giachetti. Nonnegative solutions for a class of singular parabolic problems involving p-laplacian. *Asymptot. Anal.* **91** (2015) 147–183.

[8] J. P. Gossez. Some approximation properties in Orlicz-Sobolev spaces. *Studia Mathematica.* T. LXXIV (1982).

[9] A. Gurusamy and H. E. Andre. Existence and uniqueness of weak solutions to parabolic problems with nonstandard growth and cross diffusion. **2020** (123) (2020) 1–13.

[10] H. Kawarada. On solutions of the initial boundary value problem for $u_t = u_{xx} + 1$. *RIMS Kyoto* **10** (1975) 729–736.

[11] O. Levenspiel. *Chemical Reaction Engineering.* John Wiley and Sons, New York, 1962.

[12] S. Mesbahi. On the existence of weak solutions for a class of singular reaction diffusion systems. *Hacettepe Journal of Mathematics and Statistics* **51** (3) (2022) 757–774.

[13] P. T. Marion. Quenching Phenomena Due to a Concentrated Nonlinear Source in an Infinitely Long Cylinder. *Journal of Applied Mathematics and Physics* **7** (2019) 2015–2025.

[14] J. Musielak. *Modular Spaces and Orlicz Spaces.* Lecture Notes in Math., 1983.

[15] T. Salin. Quenching-rate estimate for a reaction-diffusion equation with weakly singular reaction term. *Dyn. Contin. Discrete Impuls. Syst. Ser. A Math. Anal.* **11** (4) (2004).

[16] B. Selçuk. Quenching behavior of a semilinear reaction-diffusion system with singular boundary condition. *Turk J. Math.* **40** (2016) 166–180.

[17] J. Simon. Compact sets in the space $L^p(0, T, B)$. *Ann. Mat. Pura Appl.* **146** (1987) 65–96.

[18] G. Stampacchia. Le problème de Dirichlet pour les équations elliptiques du second ordre à coefficients discontinus. *Ann. Inst. Fourier* (Grenoble) **15** (1965) 189–258.

Nonlinear Dynamics and Systems Theory, **25** (1) (2025) 53–58

Existence and Uniqueness of Solution for Stochastic Nonlocal Random Functional Integral Equation

A. Ferrag [1*], A. Aoufi [2] and M. Tadjine [3]

[1] *Laboratory of Physical Chemistry and Biology of Materials, Higher Normal School of Technological Education (ENSET), Skikda 21000, Algeria.*
[2] *Higher Normal School of Technological Education, Skikda, Algeria.*
[3] *Higher Normal School of Technological Education, Skikda, Algeria.*

Received: September 30, 2024; Revised: February 4, 2025

Abstract: In this paper, we use Banach's fixed point theorem to establish sufficient conditions which guarantee the existence and uniqueness of the solution for a stochastic nonlocal random functional integral equation. As applications, an example is presented to illustrate our obtained results.

Keywords: *stochastic differential equation; existence; uniqueness; stochastic integral equations; fixed point theorem*

Mathematics Subject Classification (2020): 70K55, 93-10.

1 Introduction

Stochastic differential equations (SDEs) play an important role in characterizing many social, physical, biological, and engineering problems. The theory of SDEs has developed quickly, the investigation of SDEs has attracted considerable attention of researchers, and many qualitative theories of SDEs have been obtained (see [2, 4, 8]).

In the last two decades, the existence and uniqueness of solution for SDEs have been considered in many publications such as [1, 5, 7, 9, 10].

When random fluctuations have great effects on the parameters and evolution in the mathematical model which describes a certain phenomenon, a stochastic differential equation should be the starting point for deriving the suitable model. Recently, nonlocal stochastic models were introduced by many authors to describe the evolution of the

* Corresponding author: mailto:a.ferrag@enset-skikda.dz

© 2025 InforMath Publishing Group/1562-8353 (print)/1813-7385 (online)/http://e-ndst.kiev.ua

studied phenomena. Motivated by the papers [3,6], we study the existence and uniqueness solution of the following nonlocal functional stochastic differential equation:

$$\begin{aligned} dx(t) =& f(t, x(t), A(t)x(t))dt + g(t, x(t), C(t)x(t))dB(t),\ t \in [0, T], \\ x(0) + \sum_{k=1}^{p} c_k x(t_k) =& x_0, \end{aligned} \tag{1}$$

which is equivalent to the following stochastic functional integral equation:

$$\begin{aligned} x(t) = x(0) &+ \int_0^t f(s, x(s), A(s)x(s))ds \\ &+ \int_0^t g(s, x(s), C(s)x(s))dB(s), \end{aligned} \tag{2}$$

where the first integral is a mean square Riemann integral and the second is an Ito integral.

This paper consists of four sections. In Section 2, we review some concepts, introduce some notation and state our main result, which shows the existence and uniqueness of solution for the stochastic nonlocal random functional integral equation (2). In Section 3, we give the proof of the main result. In Section 4, one example is given to illustrate the theoretical result.

2 Preliminaries and Main Result

Throughout this paper, we assume that $(\Omega, \mathcal{F}, \mathbb{P})$ is a complete probability space with a filtration $\{\mathcal{F}_t\}_{t\in[0,T]}$ satisfying the usual conditions (i.e., it is right continuous and $\mathcal{F}_0$ contains all P-null sets). Let $\mathcal{L}^2(\Omega, \mathcal{F}, \mathbb{P})$ stand for the space of all $\mathbb{R}$-valued random variables $\{X(t),\ t \in [0, T]\}$ such that

$$\mathbf{E}|X|^2 = \int_\Omega |X|^2 \, d\mathbb{P} < \infty.$$

For $X \in \mathcal{L}_2(\Omega, \mathcal{F}, \mathbb{P})$, we let

$$\|X\|_2 := \Big(\int_\Omega |X|^2 \, d\mathbb{P} \Big)^{1/2}.$$

Then $\mathcal{L}_2(\Omega, \mathcal{F}, \mathbb{P})$ is a Hilbert space equipped with the norm $\|\cdot\|_2$. We consider the following nonlocal functional stochastic differential equation:

$$\begin{aligned} dx(t) =& f(t, x(t), A(t)x(t))dt + g(t, x(t), C(t)x(t))dB(t),\ t \in [0, T], \\ x(0) + \sum_{k=1}^{p} c_k x(t_k) =& x_0, \end{aligned}$$

where $0 = t_0 < t_1 < ... < t_p \leq T$, c_k are constants $(k = 1, ..., p)$, $p \in \mathbb{N}$, $\{B_t\}$ is a standard Brownian motion defined on the complete probability space $(\Omega, \mathcal{F}, \mathbb{P})$ adapted to the filtration $\{\mathcal{F}_t\}_{t\in[0,T]}$. $x(0)$ is an $\mathcal{F}_0$-mesurable random variable independent of B with finite second moment.

$A(t), t \in [0,T]$, and $C(t), t \in [0,T]$, are the families of linear bounded operators defined on $Y := \mathcal{C}([0,T], \mathcal{L}_2(\Omega, \mathcal{F}, \mathbb{P}))$, the space of all continuous stochastic processes defined from $[0,T]$ into $\mathcal{L}_2(\Omega, \mathcal{F}, \mathbb{P})$ with values in Y. The measurable real random functions f and g are defined on $[0,T] \times Y \times Y$ with values in the space $\mathcal{L}_2(\Omega, \mathcal{F}, \mathbb{P})$.

$A(t)$ and $C(t)$ are the families of bounded operators. So, there exist a function $\alpha(t) : [0,T] \to \mathbb{R}^+$ and a function $\gamma(t) : [0,T] \to \mathbb{R}^+$ such that $\|A(t)x\|_Y \leq \alpha(t)\|x\|_Y$ and $\|C(t)x\|_Y \leq \gamma(t)\|x\|_Y$.

For the nonlocal stochastic differential equation (1), we have the following result. It shows that under some sufficient conditions, there exists a unique solution.

Theorem 2.1 *Assume that the following conditions hold:*

(i) For all $x, y \in Y$ and $t \in [0,T]$, there exists a constant $l > 0$ such that

$$|f(t,x,y)| \leq l\sqrt{1 + |x|^2 + |y|^2},$$
$$|g(t,x,y)| \leq l\sqrt{1 + |x|^2 + |y|^2};$$

(ii) For all $x, y, x', y' \in Y$ and $t \in [0,T]$, there exists a constant $a > 0$ such that

$$|f(t,x,y) - f(t,x',y')| \leq a\sqrt{|x - x'|^2 + |y - y'|^2},$$
$$|g(t,x,y) - g(t,x',y')| \leq a\sqrt{|x - x'|^2 + |y - y'|^2};$$

(iii) There exists a real continuous monotone nondecreasing mapping F defined on $[0,T]$ such that $s < t$ implies

$$\mathbf{E}[|B(t) - B(s)|^2] = \mathbf{E}[\|B(t) - B(s)\|^2 \backslash \mathcal{F}_s] = F(t) - F(s);$$

(iv) $\sum_{k=1}^{p} c_k \neq -1$;

(v) a satisfies $4a^2 \left(1 + \frac{\sum_{k=1}^{p} c_k^2}{\left(1 + \sum_{k=1}^{p} c_k\right)^2} \right) [(1 + \theta^2)(T^2 + F(T) - F(0)] < 1.$

Then nonlocal functional stochastic integral equation (2) has a unique continuous solution $X_t(\omega)$ belonging to $\mathcal{L}_2(\Omega, \mathcal{F}, \mathbb{P})$, and $X_t(\omega)$ is adapted to the filtration $\{\mathcal{F}_t\}_{t \geq 0}$.

3 Proof of the Theorem

Assume that $\sum_{k=1}^{p} c_k \neq -1$. Integrating the equation (1) yields

$$x(t) = x(0) + \int_0^t f(s, x(s), A(s)x(s))ds + \int_0^t g(s, x(s), C(s)x(s))dB(s).$$

So we have

$$\begin{aligned} x(t_k) = x(0) &+ \int_0^{t_k} f(s, x(s), A(s)x(s))ds \\ &+ \int_0^{t_k} g(s, x(s), C(s)x(s))dB(s) \quad (k = 1, ..., p). \end{aligned} \tag{3}$$

By (1) and (3),

$$\begin{aligned} x(0) + \sum_{k=1}^{p} c_k \Big[x(0) &+ \int_0^{t_k} f(s, x(s), A(s)x(s))ds \\ &+ \int_0^{t_k} g(s, x(s), C(s)x(s))dB(s) \Big] = x_0. \end{aligned} \tag{4}$$

Since $\sum_{k=1}^{p} c_k \neq -1$, then (4) implies

$$\begin{aligned} x(0) = \Big(x_0 - \sum_{k=1}^{p} c_k \Big[&\int_0^{t_k} f(s, x(s), A(s)x(s))ds \\ &+ \int_0^{t_k} g(s, x(s), C(s)x(s))dB(s) \Big] \Big) \Big/ \Big(1 + \sum_{k=1}^{p} c_k \Big). \end{aligned}$$

Then

$$\begin{aligned} x(t) = &\frac{x_0 - \sum_{k=1}^{p} c_k \Big[\int_0^{t_k} f(s, x(s), A(s)x(s))ds + \int_0^{t_k} g(s, x(s), C(s)x(s))dB(s) \Big]}{1 + \sum_{k=1}^{p} c_k} \\ &+ \int_0^{t} f(s, x(s), A(s)x(s))ds + \int_0^{t} g(s, x(s), C(s)x(s))dB(s) \end{aligned}$$

Let us define the integral operator G by

$$\begin{aligned} Gx(t) = &\frac{x_0 - \sum_{k=1}^{p} c_k \Big[\int_0^{t_k} f(s, x(s), A(s)x(s))ds + \int_0^{t_k} g(s, x(s), C(s)x(s))dB(s) \Big]}{1 + \sum_{k=1}^{p} c_k} \\ &+ \int_0^{t} f(s, x(s), A(s)x(s))ds + \int_0^{t} g(s, x(s), C(s)x(s))dB(s). \end{aligned}$$

Lemma 3.1 *The operator G sends the space $\mathcal{C}([0,T], \mathcal{L}_2(\Omega, \mathcal{F}, \mathbb{P}))$ into itself.*

Proof. Let $0 \leq t_1 \leq t_2 \leq T$ and $x \in \mathcal{C}([0,T], \mathcal{L}_2(\Omega, \mathcal{F}, \mathbb{P}))$. By applying the Cauchy-Schwarz inequality and the condition (iii), we obtain

$$\begin{aligned} \mathbf{E}|Gx(t_2) - Gx(t_1)|^2 \leq 2(t_2 - t_1) &\int_{t_1}^{t_2} \mathbf{E}|f(s, x(s), A(s)x(s))|^2 ds \\ &+ 2 \int_{t_1}^{t_2} \mathbf{E}|g(s, x(s), C(s)x(s))|^2 dF(s). \end{aligned}$$

Let $\theta = \max\{\max_{t\in[0,T]} \alpha(t), \max_{t\in[0,T]} \gamma(t)\}$. Applying the growth condition yields

$$\mathbf{E}|Gx(t_2) - Gx(t_1)|^2 \leq 2l^2[(t_2 - t_1)^2 + F(t_2) - F(t_1)][1 + (1 + \theta^2)\|x\|_Y^2].$$

$F(t)$ is continuous, then

$$\lim_{t_1 \mapsto t_2} \|F(t_2) - F(t_1)\| = 0.$$

Therefore,

$$\lim_{t_1 \mapsto t_2} \mathbf{E}|Gx(t_2) - Gx(t_1)|^2 = 0.$$

Consequently, Gx is continuous in mean square on $[0, T]$.

But the function Gx is square integrable with respect to measure probability, has a finite second moment, and is adapted to the filtration $\{\mathcal{F}_t\}_{t\in[0,T]}$. This implies that G maps Y into itself.

Now, we will show that G is a contraction on Y.

Let x and y in Y. Applying the Cauchy-Schwarz inequality and the above conditions, we have

$$\begin{aligned}
&\mathbf{E}|Gx(t) - Gy(t)|^2 \leq 4\int_0^t \mathbf{E}|f(s, x(s), A(s)x(s)) - f(s, y(s), A(s)y(s))|^2 ds \\
&+ 4\int_0^t \mathbf{E}|g(s, x(s), C(s)x(s)) - g(s, y(s), C(s)y(s))|^2 dF(s) \\
&+ 4\mathbf{E}\left|\frac{\sum_{k=1}^{p} c_k \left[\int_0^{t_k} f(s, x(s), A(s)x(s)) - f(s, y(s), A(s)y(s))ds\right]}{1 + \sum_{k=1}^{p} c_k}\right|^2 \\
&+ 4\mathbf{E}\left|\frac{\sum_{k=1}^{p} c_k \left[\int_0^{t_k} g(s, x(s), C(s)x(s)) - g(s, y(s), C(s)y(s))dB(s)\right]}{1 + \sum_{k=1}^{p} c_k}\right|^2 \\
&\leq 4a^2 \left(1 + \frac{\sum_{k=1}^{p} c_k^2}{\left(1 + \sum_{k=1}^{p} c_k\right)^2}\right) \left[(1 + \theta^2)(T^2 + F(T) - F(0)\right] \mathbf{E}|x - y|^2.
\end{aligned}$$

4 Illustrative Example

For simplicity, let $X(0) = x_0$. The process $X_t = e^{0.36845t + 0.87B_t}$ starting from $X(0) = 1$ solves the stochastic differential equation (SDE)

$$\begin{aligned}
dX_t &= 1.01X_t dt + 0.87X_t dB_t, \\
x_0 &= 1.
\end{aligned}$$

5 Conclusion

The main goal of this paper is to discuss the existence and uniqueness of solutions for a kind of stochastic integral equations with nonlocal conditions. We obtained a sufficient condition of the existence and uniqueness of solution for stochastic integral equation with nonlocal condition.

6 Acknowledgments

The authors would like to thank the anonymous referee for the careful reading of the manuscript and pertinent comments; the constructive suggestions substantially improved the quality of this work.

References

[1] S. Azizicovici and Y. Gao. Functional differential equations with nonlocal initial conditions. *Journal of Applied Mathematics and Stochastic Analysis* **10** (2) (1997) 145–156.

[2] E. Allen. *Modeling with Ito Stochastic Differential Equations.* Springer Science and Business Media, Dordrecht, The Netherlands, 2007.

[3] L. Byszewski. Existence and uniqueness of a classical solution to a functional-differential abstract nonlocal Cauchy problem. *Journal of Applied Mathematics and Stochastic Analysis* **12** (1) (1999) 91–97.

[4] S. Cyganowski and O. Kloeden and J. Ombach. *From Elementary Probability to Stochastic Differential Equations with MAPLE.* Springer Science and Business Media, New York, 2002.

[5] M. M. Elborai and M. A. Abdou and M. I. Youssef. On the existence, uniqueness, and stability behavior of a random solution to a non local perturbed stochastic fractional integro-differential equation. *Life Science Journal* **10** (4)(2013) 3368–3376

[6] M. M. Elborai and M. I. Youssef. On stochastic solutions of nonlocal random functional integral equations. *Arab Journal of Mathematical Sciences* **25** (2) (2019) 180–188.

[7] D. D. Huan. A Note on the Controllability of Stochastic Partial Differential Equations Driven by Levy Noise. *Nonlinear Dynamics and Systems Theory* **23** (1) (2023) 34–45.

[8] B. Oksendal. *Stochastic Differential Equations: An Introduction with Applications.* Springer Science and Business Media, Berlin, 2013.

[9] P. Qi. Existence and Uniqueness of Solutions for Some Basic Stochastic Differential Equations. *In Journal of Physics: Conference Series* **1802** (4) (2021) 042094, IOP Publishing.

[10] M. K. Von Renesse and M. Scheutzow. Existence and uniqueness of solutions of stochastic functional differential equations. *Random Operators and Stochastic Equations* **18** (2010) 267–284.

Nonlinear Dynamics and Systems Theory, **25** (1) (2025) 59–67

Estimation of Amphibious Aircraft Trajectory Using Particle Filter and Square Root Ensemble Kalman Filter

T. Herlambang [1], S. Syamsuar [2], R. S. Marjianto [3*], N. I. Gutami [2], H. Arof [4], F. S. Puriningsih [2], A. Roschyntawati [2], H. Hendrato [2], M. Muhammad [2], I. Ansori [2], Y. F. Kusuma [5] and K. Oktafianto [6]

[1] *Department of Information Systems, Universitas Nahdlatul Ulama Surabaya, Indonesia*
[2] *Research Center for Transportation Technology, National Research and Innovation Agency, KST B.J Habibie, Setu, South Tangerang, Banten 15314, Indonesia*
[3*] *Departement of Engineering, Faculty of Vocational Studies, Universitas Airlangga, Indonesia*
[4] *Department of Electrical Engineering, University of Malaya, Malaysia*
[5] *Research Center for Hydrodynamics Technology, National Research and Innovation Agency, KS Said Djauharsjah Jenie, Sukolilo, Surabaya, East Java 60112, Indonesia*
[6] *Department of Mathematics, University of PGRI Ronggolawe, Indonesia*

Received: August 12, 2024; Revised: February 5, 2025

Abstract: An amphibious aircraft is a type of aircraft able to take off and land on water. Amphibious aircraft play an important role in air transportation, especially in areas having a lot of water. Amphibious aircraft perform many functions including passenger and freight transportation, medical rescue, tourism and maritime surveillance. Amphibious aircraft require navigation and guidance systems so as to steadily follow a predetermined trajectory. Several navigation guidance system algorithms in the aerospace field can be used, one of which is for amphibious aircraft trajectory estimation. The accuracy of aircraft position estimation is very important to ensure that the amphibious aircraft follows a predetermined trajectory. For this, the navigation and guidance system algorithm requires modeling the motion system of the amphibious aircraft. In this study, the Particle Filter and Square Root Ensemble Kalman Filter methods were used to estimate the trajectory to be followed by the amphibious aircraft. The main purpose of the study was to compare the performance of the two methods to find out which one proved to have a higher accuracy. Based on the simulation results, both methods had a high accuracy, that is, the Particle Filter method had an accuracy of about 98.2%, and the EnKF-SR method had an accuracy of 99.3%.

Keywords: *amphibious aircraft; trajectory estimation; particle filter method; EnKF-SR method.*

Mathematics Subject Classification (2020): 93E10, 62F10.

* Corresponding author: mailto:rachmansinatriya@vokasi.unair.ac.id

© 2025 InforMath Publishing Group/1562-8353 (print)/1813-7385 (online)/http://e-ndst.kiev.ua

1 Introduction

An amphibious aircraft is a type of aircraft designed to operate both in the air and on the water. Amphibious aircraft have multiple functions including passenger and freight transportation, medical rescue, tourism, and maritime surveillance. The amphibious aircraft ability is to take off and to land both on airstrips and on water surfaces such as wide lakes or rivers [1]. Amphibious aircraft have an important role in the field of air transportation and defence of the Homeland, as well as strategic purposes such as military operations or humanitarian assistance in emergency situations. They enable fast and targeted delivery in hard-to-reach places [2].

In addition to defence and military purpose, amphibious aircraft are needed in remote and outermost areas of the Republic of Indonesia because these remote areas are often difficult to reach by land transport, and the airstrips there are inadequate. With amphibious aircraft, logistics and supplies can be transported directly to the site via the large and accessible watersways. So, in view of the many benefits provided by amphibious aircraft, especially for logistics distribution, the technology related to amphibious aircraft needs to be developed and researched so that it can be utilized by a wider community [1].

The development of amphibious aircraft, which can take off and land on either land or water, requires advanced and reliable navigation systems to ensure operational safety and efficiency. When landing on water or land, the navigation system helps the aircraft to land safely in a pre-selected area, avoiding obstacles such as rocks or floating objects. A good navigation and control system helps the aircraft avoid obstacles such as islets or uneven terrain in the water, and can increase efficiency and reduce risk. Navigation and control systems on seaplanes play a crucial role in the operational safety and efficiency as well as their mission effectiveness [3]. Navigation system is a system that directs the position of an amphibious aircraft to follow a predetermined trajectory with a high degree of accuracy [4]. This amphibious aircraft can operate in the air and land on the water. Several navigation guidance methods in the field of robotics can also be used, one of which is to estimate the position of an amphibious aircraft. The precision and accuracy of the aircraft trajectory estimation is very important to ensure the amphibious aircraft follows the specified trajectory accurately [5].

One of the algorithms that gives a small error in estimation is the Particle Filter and Square Root Ensemble Kalman Filter, in which the EnK-SR method is a development of the EnKF method frequently used for motion and position estimation in the field of robotics, for example, for ASV [6], AUV trajectory [7], and arm robot motion [8]. Given that the EnKF method is a very reliable estimation method, in this study, two methods are used, that is, the EnKF-SR and Particle Filter methods for estimating the trajectory of unmanned amphibious aircraft. And, in this study, the focus is on comparing the numerical simulation results of the two methods, the EnKF-SR and Particle Filter methods by generating 300 and 500 ensembles.

2 Amphibious Aircraft Model

In this study, we used an amphibious aircraft model with the ability to operate in the shallow water areas of Indonesia. The forces acting on an unmanned seaplane can be categorized into the aircraft mass, hydrodynamic forces, aerodynamic forces, and engine thrust as shown in Figure 1.

We consider the Earth coordinate system $X_e; Y_e; Z_e$, then the aircraft body coordinate

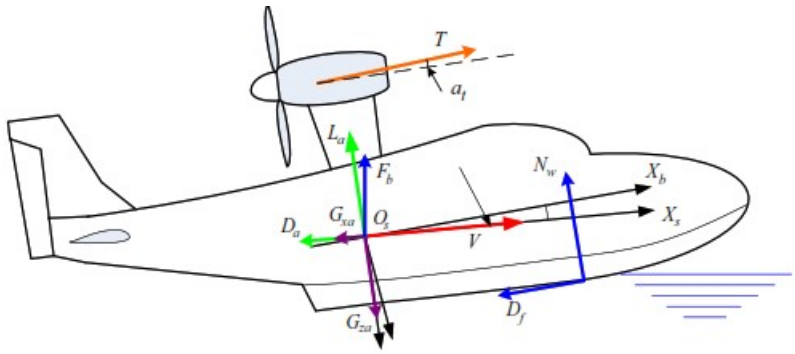

Figure 1: Forces working on amphibious aircraft [9].

system $X_b; Y_b; Z_b$ and the steady-translation coordinate system $X_s; Y_s; Z_s$.

The nonlinear longitudinal dynamic motion model of unmanned seaplanes is represented by the following equations [9]:

$$m\dot{V} = T\cos(\alpha+\alpha_t) - D_a - N_w \sin\alpha - D_f\cos\alpha + G_{xa}, \tag{1}$$

$$mV\dot{\alpha} = mVq - T\sin(\alpha+\alpha_t) - L_a - N_w\cos\alpha + D_f\sin\alpha + G_{za}, \tag{2}$$

$$I_y\dot{q} = M_a + M_w + M_T, \tag{3}$$

$$\dot{\theta} = q \tag{4}$$

$$\dot{x}_g = u\cos\theta + w\sin\theta, \tag{5}$$

$$\dot{z}_g = -u\sin\theta + w\cos\theta. \tag{6}$$

3 Particle Filter Algorithm

The Particle Filter algorithm is shown in Figure 2 [10].

4 Ensemble Kalman Filter Square Root Algorithm

The EnKF-SR algorithm, see Figure 3, is applied to the modeling of the amphibious aircraft motion system [11].

5 Result Simulation

In this study, the researchers simulated two methods at once, that is, the Particle Filter and EnKF-SR methods, and compared the accuracy achieved by the two methods. The study compared the accuracy of the two methods. The EnKF-SR method used a combination of 300 and 500 ensembles. The algorithms in Figures 2 and 3 were implemented on the motion system equations of the unmanned amphibious aircraft. The simulation results, after applying the Particle Filter and EnKF-SR algorithms to the unmanned amphibian motion system modeling, were obtained as shown in Figures 4-7.

α	Angle of attack	m	Amphibious aircraft mass
θ	Angle of pitch	D_a	Airodynamic drag force
V	Velocity	G_{xa}	gravity along X_s
α_t	Angle between engine force and X_b	G_{za}	gravity along Z_s
M_a	Total pitching moment of Air	X_g	aircraft position along X_e
M_w	Total pitching moment of Air	Z_g	aircraft position along Z_e
M_T	Total pitching moment of Engine	u	velocity component of aircraft velocity along X_b
T	Engine thrust	w	velocity component of aircraft along Z_b
N_w	Normal directional water pressure at the bottom of the aircraft	q	Pitch angular rate
D_f	Frictional force of water along the bottom of the aircraft	I_y	moment of Inertia of amphibious aircraft against Y_b
L_a	Aerodynamic lifting force	$\dot{\theta}$	Increase/decrease in angle of pitch
$\dot{V}$	Increase/decrease in velocity	$\dot{\alpha}$	Increase/decrease in angle of attack

Table 1: Description of amphibious aircraft model [4].

In Figure 4 a and b, it can be seen that the red line is the real value of the horizontal position determined to fly at a certain distance from the place of the amphibious aircraft so that the amphibious aircraft flies as high as 1180 m from the surface and advances about 2500 meters from the original place, so the position will always advance to 2500 m at the 100th iteration either by the EnKF-SR method (blue line) or the Particle Filter one (green line). Figure 4a shows the results of estimating the horizontal position of the unmanned amphibious aircraft. Figure 4b represents the position estimation results for the height reached by the amphibious aircraft. In Figure 4a and 4b, it can also be seen that the difference in distance or error between the EnKF-SR and Particle Filter methods with real values is quite small with a fairly high level of accuracy, this can be seen in Table 2. The resulting error for horizontal estimation is around 0.046% and the error in altitude estimation is around 0.2%.

Figure 5 represents an unmanned amphibious aircraft taking off and flying at an altitude of 1200 meters. It can be seen that the red line in Figure 4 is the real data of the horizontal position and altitude predetermined to be passed by the amphibious aircraft flying at a certain height and distance. The resulting error for the motion in the XY plane is about 0.253% for the EnKF-SR method and 0.254% for the Particle Filter method. In this case, the height of the unmanned amphibious aircraft represents the maximum height that can be passed by the amphibious aircraft. In this case, this simulation is only made for flying amphibious aircraft and not for landing on the ground

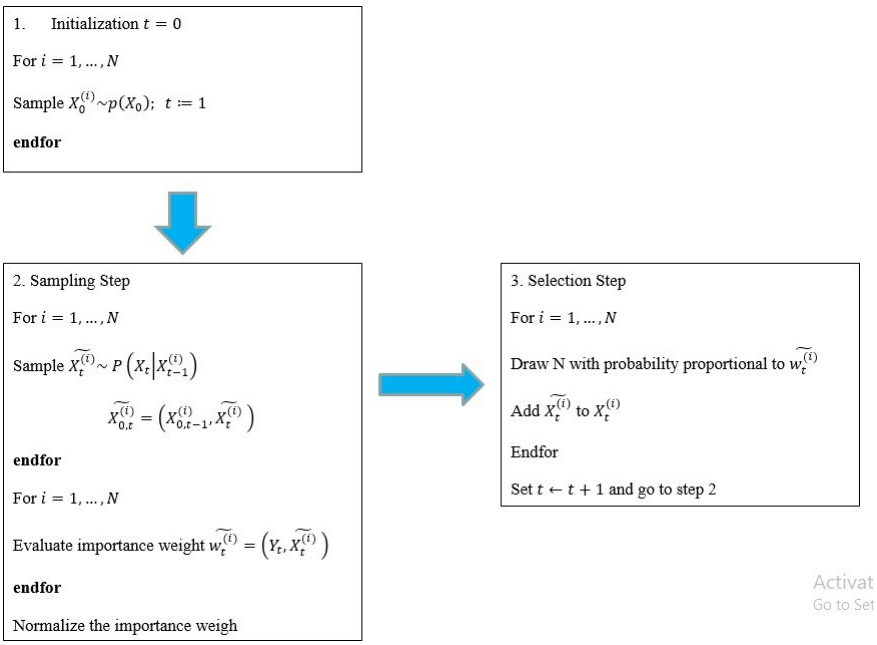

Figure 2: Particle Filter Algorithm

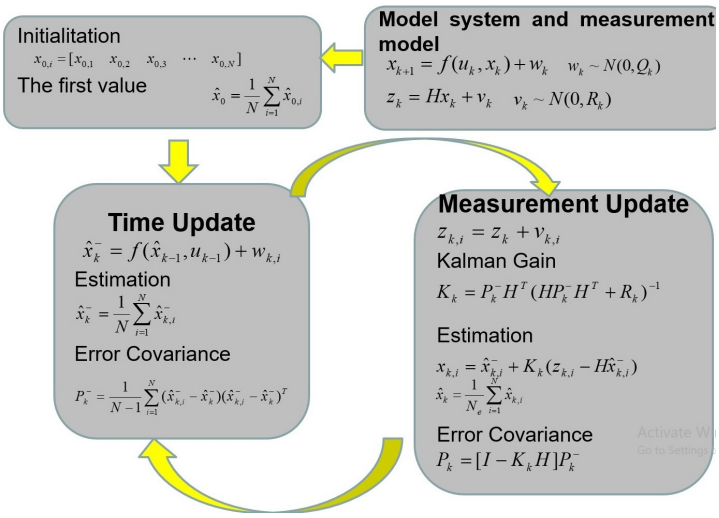

Figure 3: Square Root Ensemble Kalman Filter Algorithm.

again. Figure 4a shows a better accuracy than Figure 4b with 300 ensembles. In Figure 5, the amphibious aircraft follows the specified trajectory from the start of takeoff and flies at a certain height. Table 2 also shows that the EnKF-SR method has a smaller error of 0.001% than the Particle Filter method.

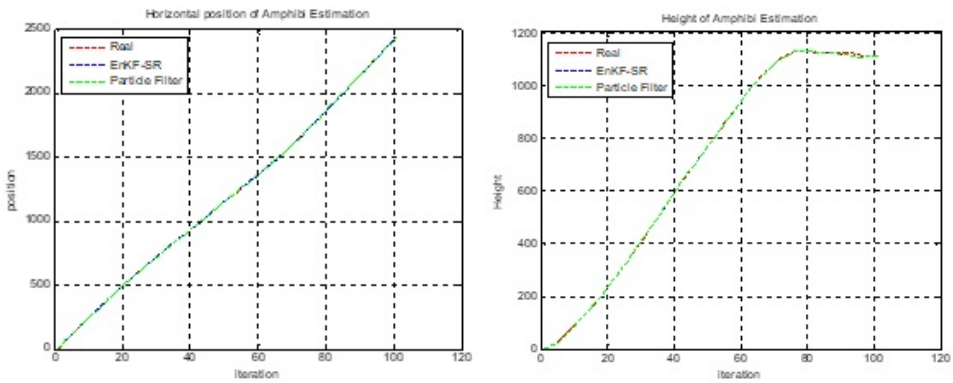

Figure 4: Numerical Simulation Results by the Particle Filter and EnKF-SR methods (500 ensembles), a) estimation of horizontal position of amphibious aircraft and b) estimation of altitude of amphibious aircraft.

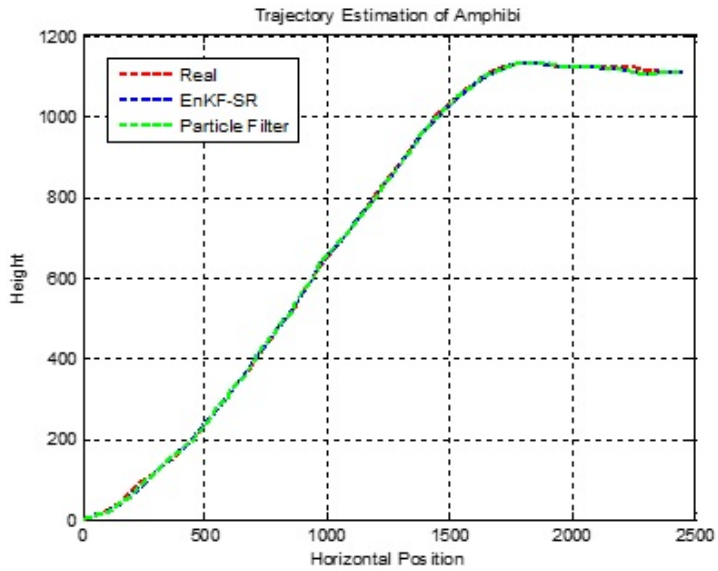

Figure 5: Amphibious aircraft position estimation by the EnKF-SR and Particle Filter methods with 500 ensembles.

In Figure 6 a and b, it can be seen that the red line is the real value of the horizontal position determined to fly at a certain distance from the place of the amphibious aircraft so that the amphibious aircraft flies as high as 1400 m from the surface and advances about 2000 meters from the original place, so the position will always advance to 2000 m at the 100th iteration either by the EnKF-SR method (blue colored line) or by the Particle Filter one (green colored line). In Figure 6a and 6b, it can also be seen that the difference in distance or error between the EnKF-SR and Particle Filter real values is quite small with a fairly high level of accuracy, as seen in Table 2. The resulting error

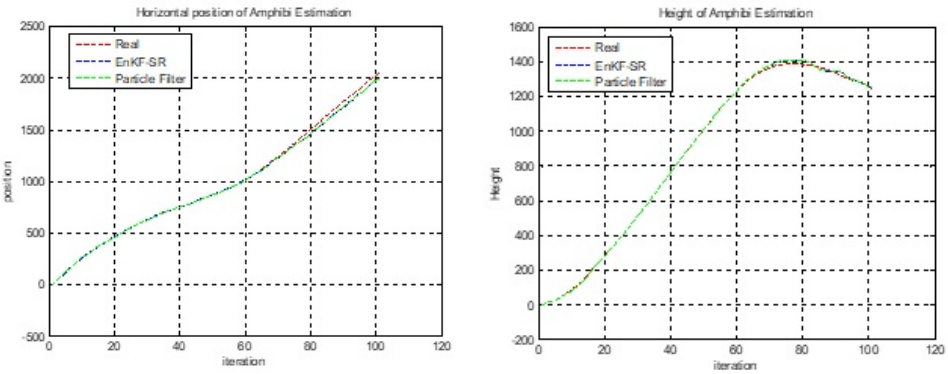

Figure 6: Numerical Simulation Results by the Particle Filter and EnKF-SR methods (300 ensembles), a) estimation of horizontal position of amphibious aircraft and b) estimation of altitude of amphibious aircraft.

for the horizontal estimation is around 0.095%, and the error in altitude estimation is around 0.5%.

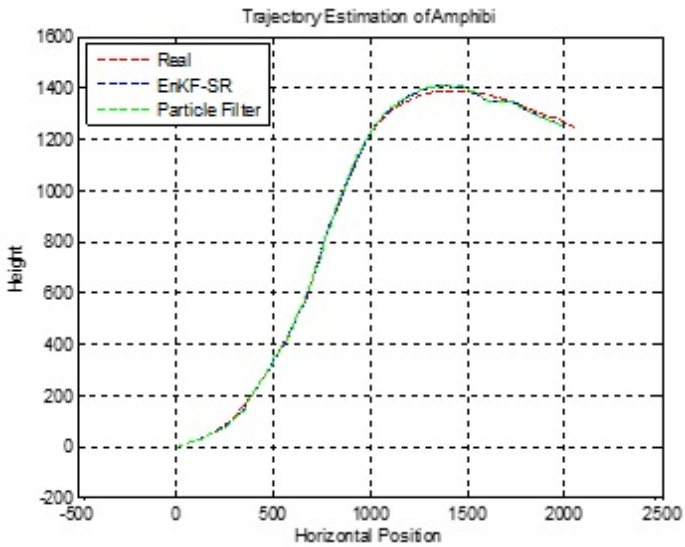

Figure 7: Amphibious aircraft position estimation by the EnKF-SR and Particle Filter methods with 300 ensembles.

Figure 7 represents an unmanned amphibious aircraft taking off and flying at an altitude of 1400 meters and traveling about 2 kilometers. It can be seen that the red line in Figure 4 is the real data of the horizontal position and altitude predetermined to be passed by the amphibious aircraft flying at a certain altitude and distance. The resulting error for the motion in the XY plane is about 0.522% for the EnKF-SR method and 0.523% for the Particle Filter method. In this case, the height of the unmanned

amphibious aircraft represents the maximum height that can be passed by the amphibious aircraft, also, in this case, this simulation is only made for the flying amphibious aircraft and not for landing on the ground again. Figure 6a has better accuracy than Figure 6b when using 300 ensembles. In Figure 7, the amphibious aircraft follows the specified trajectory from the start of takeoff and flying at a certain height. Table 2 also shows that the EnKF-SR method has a smaller error of 0.001% than the Particle Filter method.

	EnKF with 300 ensembles	Particle Filter	EnKF with 500 ensembles	Particle Filter
RMSE XY Motion	8.3604	8.3742	3.0422	3.0575
Error XY Motion	0,522%	0,523%	0,253%	0,254%
Time Simulation	3,125 s	2,546 s	7,046 s	5,187 s

Table 2: Comparison of amphibious aircreft trajectory estimation error using the Particle Filter and EnKF-SR methods.

Overall, based on the simulation results listed in Table 2, some of these simulation results can be compared to each other. As regards the comparison of the accuracy of the methods, the EnKF-SR method has a higher accuracy than the Particle Filter one, but it has a longer simulation time. If we consider the comparison in terms of the number of ensembles, then generating 500 ensembles has a higher accuracy than 300 ensembles. Overall, the EnKF-SR method by generating 500 ensembles has the highest accuracy. In this case, both estimation methods, the Particle filter and EnKF-SR ones, have an accuracy of above 98%, so the estimation methods can be effectively used to estimate the motion of unmanned amphibious aircraft.

6 Conclusion

Based on the results of analyzing the two simulations presented in Figures 4-7, it can be concluded that the EnKF-SR method by generating 500 ensembles has the highest accuracy. If we consider the comparison in terms of the number of ensembles, then 500 ensembles produced a better accuracy than 300 ensembles. In this case, both estimation methods, the EnKF-SR and the Particle Filter ones, have an accuracy of above 98%, so the estimation methods can be effectively used to estimate the motion of unmanned amphibious aircraft.

Acknowledgment

Our deep gratitude goes to Prof. Dr. Cuk Supriyadi Ali Nandar as Head of the Energy and Manufacturing Research Organization, BRIN as the person in charge of the Indonesia Maju Research and Innovation Program with contract number 60/II/HK/2022 and 8/III.3/HK/2024, and also many thanks to LPPM Universitas Nahdlatul Ulama Surabaya (UNUSA) for supporting and facilitating the writing of this publication.

References

[1] T. Herlambang, S. Syamsuar, F. Yudianto, A. BAsuki, G. Wijiatmoko, A. Roschyntawati, H. Hendrato, K. Oktafianto and R. S. Marjianto. Trajectory Estimation of Amphibious Aircraft Using H-Infinity and Ensemble Kalman Filter Methods. *Nonlinear Dynamics and Systems Theory* **24** (3) (2024) 259–266.

[2] K. Ito, T. Dhaene, Y. Hirakawa, T. Hirayama and T. Sakurai. Longitudinal Stability Augmentation of Seaplanes in Planing. *Journal of Aircraft* (2016) 1–19.

[3] T. Herlambang, F. A. Susanto, D. Adzkiya, A. Suryowinoto and K. Oktafianto. Design of Navigation and Guidance Control System of Mobile Robot with Position Estimation Using Ensemble Kalman Filter (EnKF) and Square Root Ensemble Kalman Filter (SR-EnKF). *Nonlinear Dynamics and Systems Theory* **22** (4) (2022) 390–399.

[4] S. Subchan, T. Herlambang and H. Nurhadi. UNUSAITS AUV Navigation and Guidance System with Nonlinear Modeling Motion Using Ensemble Kalman Filter. In: *Proc. International Conference on Advanced Mechatronics, Intelligent Manufacture, and Industrial Automation (ICAMIMIA)* Malang, Indonesia, 2019.

[5] T. Herlambang, D. Rahmalia, H. Nurhadi, A. Suryowinoto and A. Muhith. Estimation of Remote Operated Vehicle Motion in XY Plane using Unscented Kalman Filter. In: *Proc. 1st International Conference on Neuroscience and Learning Technology (ICONSATIN)* Jember, Indonesia, 2021.

[6] H. Nurhadi, T. Herlambang and D. Adzkiya. Position Estimation of Touristant ASV Using Ensemble Kalman Filter. In: *Proc. International Conference on Mechanical Engineering.* Indonesia, 2019.

[7] H. Nurhadi, E. Apriliani, T. Herlambang and D. Adzkiya. Sliding Mode Control Design for Autonomous Underwater Vehicle motion under The Influence of Environmental Factor. *International Journal of Electrical and Computer Engineering* **10** (5) (2020) 4789–4797.

[8] T. Herlambang, H. Nurhadi, M. Adinugroho and F. Yudianto. Estimation of Middle Finger Motion Using Extended Kalman Filter. In: *Proceedings of the 7th International Conference on Combinatorics, Graph Theory, and Network Topology (ICCGANT 2023)* AIP Conf. Proc. 3176, 010001, Indonesia, 2023.

[9] H. Du, G. Fan and J. Yi. Autonomous Takeoff Control System Design for Unmanned Seaplanes. *Ocean Engineering* **85** (2014) 21–31.

[10] A. Suryowinoto, T. Herlambang, A. A. Firdaus and M. S. Baital. Trajectory Estimation of Remote Operated Vehicle Using Particle Filter for Circular Motion. In: *Proceedings of the 7th International Conference on Combinatorics, Graph Theory, and Network Topology (ICCGANT 2023)* AIP Conf. Proc. 3176, 010001, Indonesia, 2024.

[11] T. Herlambang, F. A. Susanto, H. Nurhadi, K. Oktafianto, H. Arof and R. S. Marjianto. Square Root Ensemble Kalman Filter for Forefinger Motion Estimation as Post-Stroke Patients Medical Rehabilitation. *Nonlinear Dynamics and Systems Theory* **24** (4) (2024) 392–399.

Nonlinear Dynamics and Systems Theory, **25** (1) (2025) 68–77

Study of the Existence of Extremal Solutions for Differential Inclusions with Nonlocal Integral Boundary Conditions

Y. Khouni [1*] and M. Denche [2]

[1] *Faculty of Nature and Life Sciences, University of Batna 2, 53 Road of Constantine, Fesdis, Batna - 05078, Algeria.*
[2] *Differential Equations Laboratory, Faculty of Exact Sciences, Brothers Mentouri University, Constantine 1, 25000 Constantine, Algeria.*

Received: April 27, 2024; Revised: February 4, 2025

Abstract: In the present paper, we have studied some existence results for extremal solutions for differential inclusions with nonlocal integral boundary conditions, under certain monotonicity assumption. The existence of solutions is obtained via some well known fixed point theorems. An illustrative example is given at the end of this paper.

Keywords: *differential inclusions; fixed point theorems; minimal and maximal solutions; nonlocal integral conditions.*

Mathematics Subject Classification (2020): 34A60, 34K09, 70K75, 70K99.

1 Introduction

There are many problems in applied mathematics, control theory, nonlinear dynamics, as well as economical systems, Hamiltonian systems and mechanical problems, in which one needs to study the differential inclusions

$$x'(t) \in F(t, x(t)),$$

where $F(.,.)$ is a multivalued function, see for instance [6, 20].

In recent years, many authors have investigated the existence of absolutely continuous solutions for the initial value problems of multivalued differential equations, under

* Corresponding author: mailto:y.khouni@univ-batna2.dz

© 2025 InforMath Publishing Group/1562-8353 (print)/1813-7385 (online)/http://e-ndst.kiev.ua

lower or upper semicontinuous assumptions, for more detail, see for instance [10], and the references therein. Also, the existence of continuous, and absolutely continuous solutions for differential inclusions with nonlocal conditions, under the upper semicontinuous assumption, has been extensively studied by several authors, see for instance [11,17] and the references therein.

The study of integral boundary conditions has a great importance due to their various applications in many scientific fields such as population dynamics [9] and cellular systems [1]. Moreover, the existence of continuous, absolutely continuous, and bounded variation solutions of boundary value problems with integral boundary conditions has been studied by some authors such as Arara and Benchohra [4], Benchohra et al. [11], A. Boucherif [2], Infante [18], see also the references therein.

The existence of minimal and maximal solutions for a single-valued case, i.e., differential equations, is discused by many authors, see for instance [7,22].

In [3], the authors have proved the existence of the minimal and maximal solutions for the following initial value problem:

$$\begin{cases} x^n(t) \in F(t, x(t)), \quad a.e.\ t \in I = [0, a], \\ x^i(0) = x_i \in \Re, \quad i = 1, 2, ..., n-1. \end{cases} \tag{1}$$

And in [14], the author discuses the existence of the minimal and maximal solutions of the following periodic boundary value problem:

$$\begin{cases} x'(t) \in F(t, x(t)), \quad a.e.\ t \in I = [0, T], \\ x(0) = x(T). \end{cases} \tag{2}$$

Also, the author in [13], has proved the existence of the minimal and maximal solutions of the following integral inclusions:

$$x(t) - q(t) \in \int_0^{\sigma(t)} k(t, s) F(s, x(\eta(s)))ds \tag{3}$$

for $t \in [0, 1]$, where $\sigma, \eta : [0, 1] \to [0, 1], q : [0, 1] \to [0, 1]$,
and $k : [0, 1] \times [0, 1] \to \Re$.
For more detail about the extremal solutions of differential inclusions, see [21].
The main purpose of this paper is to demonstrate the existence of extremal absolutely continuous solutions, by using a lattice fixed point theorem [15], without the convexity condition of the following problem:

$$x'(t) \in F(t, x(t)), \quad a.e.\ t \in I = [0, T], \tag{4}$$

with the integral condition

$$x(0) = \int_0^T g(s, x(s))ds, \tag{5}$$

where $F : I \times \Re \to P(\Re)$ is a multivalued function, when F is isotone increasing in the second variable, $P(\Re)$ is the family of all nonempty subsets of $\Re$ and $g : I \times \Re \to \Re$ is a given function.

The problem (4)-(7) has been studied recently by Boucherif [3], for the existence of a bounded variation solution, under the bounded variation condition.

This work is organized as follows: in addition to the Introduction, we have two main sections. In Section 2, we give some preliminary tools that we will use later. In Section 3, we present our main results obtained. Finally, as an application, we provide an example to demonstrate the validity of our results.

2 Preliminaries

In this section, we present the necessary notations, definitions, and some basic facts that are used in this paper, for more detail, we refer the reader to [3, 5, 8, 12, 14–16, 19].
Let $(X, \|.\|_X)$ be a normed space.
$P(X)$ is the set of all nonempty subsets of X.
$P_{cl}(X) = \{Y \in P(X) : \ Y \ is \ closed\}$.
$P_{cv}(X) = \{Y \in P(X) : \ Y \ is \ convex\}$.
$P_{bd}(X) = \{Y \in P(X) : \ Y \ is \ bounded\}$.
$P_{cl,cv}(X) = \{Y \in P(X) : \ Y \ is \ closed \ and \ convex\}$.
$P_{cp,cv}(X) = \{Y \in P(X) : \ Y \ is \ compact \ and \ convex\}$.

Definition 2.1 A set-valued function $F : X \to P(X)$ is called convex (closed) valued if $F(x)$ is convex (closed) for all $x \in X$.

Definition 2.2 A set-valued function $F : X \to P(X)$ is called bounded valued on the bounded sets B if $F(B) = \bigcup_{x \in B} F(x)$ is bounded in X for all $B \in P_{bd}(X)$ or, equivalently, $\sup_{x \in B}\{sup\{|u| : \ u \in F(x)\}\} < \infty$.

Definition 2.3 A set-valued function $F : X \to P(X)$ is called upper semicontinuous (u.s.c) on X if for each $x_0 \in X$, the set $F(x_0)$ is a nonempty closed subset of X, and if for each open set N of X containing $F(x_0)$, there exists an open neighborhood N_0 of x_0 such that $F(N_0) \subseteq N$. In other words, F is u.s.c if the set $F^{-1}(A) = \{x \in X : \ F(x) \subset A\}$ is open in X for every open set A in X. Or for every closed subset A of X, the set $F^{+}(A) = \{x \in X : \ A \bigcap F(x) \neq \emptyset\}$ is closed in X.

Definition 2.4 A multivalued map $N : I \to P_{cl}(\Re)$ is said to be measurable if for every $y \in \Re$, the function

$$t \mapsto d(y, N(t)) = inf\{|y - z|; \quad z \in N(t)\}$$

is measurable.

Definition 2.5 A multivalued map $F : I \times \Re \to P(\Re)$ is said to be Carathéodory if

(i) $t \mapsto F(t, x)$ is measurable for each $x \in \Re$,

(ii) $u \mapsto F(t, u)$ is upper semicontinuous for almost all $t \in I$.

For each $x \in C(I, \Re)$, we denote by $S^1_{F,x}$ the set of Lebesgue integrable selections of F, i.e.,

$$S^1_{F,x} = \{v \in L^1(I, \Re); \quad v(t) \in F(t, x(t)) \ \ a.e. \ \ t \in I\},$$

and $AC(I, \Re)$ is the space of all absolutely continuous real-valued functions on I, and it is a Banach space with respect to the norm

$$\|x\| = sup\{|x(t)|, t \in I\},$$

where $|.|$ is the norm on $\Re$.

Theorem 2.1 *Assume that the multivalued function*

$$F : I \times \Re \to P(\Re)$$

satisfies the following assumptions:

(1) F is a Carathéodory multivalued function,

(2) for each $r > 0, \exists h_r \in L^1(I, \Re_+)$ such that

$$|F(t,x)| = \sup\{|v|, v \in F(t,x)\} \leq h_r(t), \forall |x| \leq r, \text{ and for a.e. } t \in I.$$

Then the set $S^1_{F,x}$ is nonempty.

Definition 2.6 A partially ordered set $(N, \leq)$ is called a lattice if for any $x, y \in N$, $x \wedge y = inf\{x, y\}$ and $x \vee y = sup\{x, y\}$ exist.

Let A be any subset of N, by $\wedge A$ we mean an element $a_* \in N$ such that $x \wedge a_* = a_*$ for all $x \in A$. Similarly, by $\vee A$ we mean an element a^* such that $x \vee a^* = a^*$ for all $x \in A$. The elements a_* and a^* are respectively called the infimum and supremum of A.

Definition 2.7 A lattice $(N, \leq)$ is called a complete lattice if every subset of N has the infimum and supremum in N.

Definition 2.8 A function $f : N \to N$ is called isotone increasing if for any $x, y \in N$, $x \leq y$, we have $f(x) \leq f(y)$.

Definition 2.9 *A multivalued function $T : N \to P(N)$ is called isotone increasing if for any $x, y \in N$, $x \leq y$ implies $T(x) \leq T(y)$.*

Definition 2.10 A function $\alpha \in AC(I, \Re)$ is called the lower solution of the problem (4)-(7) if for any $v \in S^1_{F,\alpha}$, we have $\alpha^{'}(t) \leq v(t)$, *a.e* $t \in I$ and $\alpha(0) \leq \int_0^T g(s, \alpha(s))ds$.

Definition 2.11 A function $\beta \in AC(I, \Re)$ is called the upper solution of the problem (4)-(7) if for any $v \in S^1_{F,\beta}$, we have $\beta^{'}(t) \geq v(t)$, *a.e* $t \in I$ and $\beta(0) \geq \int_0^T g(s, \beta(s))ds$.

Definition 2.12 A function $u \in AC(I, \Re)$ is said to be a maximal solution of (4)-(7) if it satisfies (4)-(7) on I, and for any other solution $x \in AC(I, \Re)$ of (4)-(7) on I, we have $x(t) \leq u(t)$ for $t \in I$. Similarly, we can define a minimal solution $y \in AC(I, \Re)$ of (4)-(7).

Theorem 2.2 *Let $F : [0, T] \times \Re \to P(\Re)$ be a multivalued function, assume that the multivalued function F satisfies the following assumptions:*

(1) $F(t, x)$ is nonempty closed for all $(t, x) \in I \times \Re$,

(2) $F(t, .)$ is lower semicontinuous from $\Re$ into $P(\Re)$,

(3) $F(., .)$ is measurable.

Then there exists a measurable selection of F.

Theorem 2.3 *Let $(N, \leq)$ be a complete lattice, and $T : N \to P(N)$ be a multivalued map. Suppose the following conditions hold:*

(i) T is isotone increasing on N,

(ii) $infTx \in Tx$, $supTx \in Tx$ for each $x \in N$.

Then the set $P = \{u \in N : \ u \in Tu\}$ *is nonempty, and there exists* $u_1, u_2 \in N$ *with* $u_1 \in Tu_1, \ u_2 \in Tu_2$ *with*

$$u_1 \leq u \leq u_2$$

for all $u \in N$ *with* $u \in Tu$.

Theorem 2.4 *Let* X *be a Banach space, and let* $(X, \leq)$ *be a complete lattice. Suppose that* $T : X \to P(X)$ *is a multivalued function such that*

(i) T *is isotone increasing, and*

(ii) $T(x)$ *is closed for each* $x \in X$.

Then the set of fixed points of T *is non-empty, and has the minimal and maximal elements.*

3 Existence Results

In this section, we state and prove our main results.

Theorem 3.1 *Suppose that the following conditions hold:*

(H1) $F(t, x)$ *is closed for each* $(t, x) \in I \times \Re$,

(H2) F *is isotone increasing in* x *almost everywhere for* $t \in I$,

(H3) F *is Caratheodory,*

(H4) $\exists h_F \in L^1(I, \Re_+)$ *such that*

$$|F(t, x)| \leq h_F(t), \quad a.e. \ t \in I,$$

for all $x \in \Re$,

(H5) $t \mapsto g(t, x)$ *is measurable for each* $x \in \Re$ *and* $x \mapsto g(t, x)$ *is continuous for a.e.* $t \in I$,

(H6) $\exists h_g \in L^1(I, \Re_+)$ *such that*

$$|g(t, x)| \leq h_g(t), \quad a.e. \ t \in I,$$

for all $x \in \Re$,

(H7) g *is isotone increasing in* x *almost everywhere for* $t \in I$.

Then the problem (4)-(7) has the minimal and maximal solutions on I.

Proof. We have from the assumption (H3), there exists a measurable selection v of F (i.e., $v(t) \in F(t, x)$), and from the assumption (H4), this selection is integrable, i.e., $v(.) \in L^1(I, \Re)$ (by Theorem 2.1). Now we define the multivalued function T by

$$\begin{aligned} Tx(t) = \{h \in C(I, \Re) \ s.t; h(t) = \int_0^T g(s, x(s))ds \\ + \int_0^t v(s)ds, v(t) \in F(t, x(t)), a.e. \ \ t \in I\}, \end{aligned} \tag{6}$$

let

$$N = \{x \in AC(I, \Re); \|x\| \leq M\},$$

where $M = \|h_g\|_1 + \|h_F\|_1$, we have N is a closed and bounded subset of the complete lattice $(AC(I, \Re), \leq)$ and so $(N, \leq)$ is complete.
Now, we show that T maps N into $P(N)$, to see this, let $x \in N$, and for each $u \in Tx$, $\exists v \in L^1$ such that $v(t) \in F(t, x(t))$ *a.e.* $t \in I$ with

$$u(t) = \int_0^T g(s, x(s))ds + \int_0^t v(s)ds,$$

and therefore

$$|u(t)| \leq \int_0^T |g(s, x(s))|ds + \int_0^t |v(s)|ds \leq \|h_g\|_1 + \|h_F\|_1,$$

and hence $T : N \to P(N)$.

Next, we show that Tx is a closed subset of N for each $x \in N$, to see this, it is enough to show that the values of the operator Q defined by $Qx = \{v \in L^1(I, \Re); v \in S^1_{F,x}\}$ are closed, let $(v)_n$ be a sequence in $L^1(I, \Re)$ such that $v_n \to v$, then $v_n \to v$ in measure so there exists a subsequence $(v)_{kn}$ (we take $(v)_n$) such that $v_n \to v$ a.e. and from the assumption (H1), we have that the values of Q are closed in $L_1(I, \Re)$, therefore for each $x \in N$, Tx is a closed and bounded subset of N.

Now, we show that T is isotone increasing on N, to see this, let $x, y \in N$ such that $x \leq y$, let $u_1 \in Tx$, then $\exists v_1 \in S^1_{F,x}$ such that $u_1(t) = \int_0^T g(s, x(s))ds + \int_0^t v_1(s)ds$, and since $F(t, .)$ and $g(t, .)$ are isotone increasing, we have $\exists v_2 \in S^1_{F,y}$ such that $v_1(t) \leq v_2(t), \forall t \in I$, and hence

$$u_1(t) = \int_0^T g(s, x(s))ds + \int_0^t v_1(s)ds \leq \int_0^T g(s, y(s))ds + \int_0^t v_2(s)ds = u_2(t)$$

for all $t \in I, u_2 \in Ty$. Similarly, let $u_2 \in Ty$, then $\exists v_2 \in S^1_{F,y}$ such that

$$u_2(t) = \int_0^T g(s, y(s))ds + \int_0^t v_2(s)ds$$

by the fact that F and g are isotone increasing, $\exists v_1 \in S^1_{F,x}$ such that $v_1(t) \leq v_2(t)$ for $t \in I$, hence we have

$$u_2(t) = \int_0^T g(s, y(s))ds + \int_0^t v_2(s)ds \geq \int_0^T g(s, x(s))ds + \int_0^t v_1(s)ds = u_1(t)$$

for all $t \in I$, therefore $u_1 \in Tx$, hence

$$Tx \leq Ty,$$

i.e., T is isotone increasing on N. Therefore, all conditions of Theorem 2.4 are satisfied, and hence T has a fixed point, and the set of fixed points has the minimal and maximal elements, and therefore the problem (4)-(7) has the minimal and maximal solutions on I.

Now, we give another existence theorem for the minimal and maximal solutions of the problem (4)-(7).

Theorem 3.2 *Assume that the following assumptions hold:*

(A1) $F(t,x)$ *is nonempty and closed for all* $(t,x) \in I \times \Re$,

(A2) $F(t,x)$ *is isotone increasing in* x *for a.e.* $t \in I$,

(A3) g *is measurable in the first variable and continuous in the second variable,*

(A4) $\exists h_g \in L^1(I, \Re_+)$ *such that* $|g(t,x)| \leq h_g(t), a.e. \ \ t \in I$,

(A5) $F(t,.)$ *is lower semicontinuous from* $\Re$ *into* $\Re$,

(A6) $F(.,.)$ *is measurable,*

(A7) $\exists q \in L^1(I, \Re_+)$ *and there exists a continuous nondecreasing* $\psi : [0, +\infty) \to [0, +\infty)$ *such that*

$$|F(t,x)| \leq q(t)\psi(|x|) \ for \ a.e. \ \ t \in I, \forall x \in \Re,$$

and

$$\int_0^a q(t)dt \leq \int_{\|h\|_1}^{+\infty} \frac{du}{\psi(u)},$$

(A8) g *is isotone increasing in* x *for a.e.* $t \in I$.

Then the problem (4)-(7) has the minimal and maximal solutions in I.

Proof. We have from the assumptions (A1),(A5), and (A6) that there exists a measurable selection v of F (i.e., $v(t) \in F(t,x)$), and from the assumption (A7), this selection is integrable, i.e., $v(.) \in L^1(I, \Re)$ (by Theorem 2.2). Now we define the multivalued function T by

$$Tx(t) = \{h \in C(I, \Re) s.t; h(t) = \int_0^T g(s, x(s))ds + \int_0^t v(s)ds, v(t) \in F(t, x(t)), a.e \ t \in I.\}$$

Let

$$N = \{x \in AC(I, \Re); \alpha(t) \leq x(t) \leq \beta(t), \quad for \ t \in I\},$$

where

$$\alpha(t) = -J^{-1}(\int_0^t q(s)ds)$$

and

$$\beta(t) = J^{-1}(\int_0^t q(s)ds)$$

with

$$J(z) = \int_{h_g}^z \frac{du}{\psi(u)}.$$

Firstly, we show that α is a lower solution of (4)-(7), and β is an upper solution of (4)-(7), we have for each $t \in I$, $\beta^{'}(t) = \frac{1}{J'(\beta(t))} q(t) = \psi(\beta(t)) \times q(t)$ and $-\alpha(t) = q(t)\psi(-\alpha(t))$. Also, we have $\beta(0) = \|h_g\|_1 \geq \int_0^T g(s, \beta(s))ds$ and $\alpha(0) = -\|h_g\|_1 \leq \int_0^T g(s, \alpha(s))ds$.

Now, let $v \in S^1_{F,\beta}$, then by (A7), we have $|v(t)| \leq q(t)\psi(\beta(t)) = \beta^{'}(t)$ $a.e \ t \in I$, as a result we have

$$v(t) \leq |v(t)| \leq \beta^{'}(t) \ \ a.e \ t \in I,$$

thus β is an upper solution of the problem (4)-(7).

Now, let $v \in S^1_{F,\alpha}$, and from (A7), we have

$$-v(t) \leq |v(t)| \leq q(t)\psi(|\alpha(t)|) = q(t)\psi(-\alpha(t)) = -\alpha^{'}(t) \ a.e \ t \in I,$$

therefore

$$\alpha^{'}(t) \leq v(t) \ a.e \ t \in I.$$

Thus α is a lower solution of the problem (4)-(7).
Now, we prove that T is isotone increasing, to see this, let $x, y \in N$ such that $x \leq y$, let $u_1 \in Tx$, then $\exists v_1 \in S^1_{F,x}$ such that $u_1(t) = \int_0^T g(s, x(s))ds + \int_0^t v_1(s)ds$ and since $F(t, .)$ and $g(t, .)$ are isotone increasing, we have $\exists v_2 \in S^1_{F,y}$ such that $v_1(t) \leq v_2(t), \forall t \in I$, and hence

$$u_1(t) = \int_0^T g(s, x(s))ds + \int_0^t v_1(s)ds \leq \int_0^T g(s, y(s))ds + \int_0^t v_2(s)ds = u_2(t)$$

for all $t \in I, u_2 \in Ty$. Similarly, let $u_2 \in Ty$, then $\exists v_2 \in S^1_{F,y}$ such that

$$u_2(t) = \int_0^T g(s, y(s))ds + \int_0^t v_2(s)ds$$

by the fact that F and g are isotone increasing, $\exists v_1 \in S^1_{F,x}$ such that $v_1(t) \leq v_2(t)$ for $t \in I$, hence we have

$$u_2(t) = \int_0^T g(s, y(s))ds + \int_0^t v_2(s)ds \geq \int_0^T g(s, x(s))ds + \int_0^t v_1(s)ds = u_1(t)$$

for all $t \in I$. Therefore $u_1 \in Tx$ and hence

$$Tx \leq Ty,$$

i.e., T is isotone increasing on N.
Next, we show that $T : N \to P(N)$, to see this let $x \in N$ $(\alpha(t) \leq x(t) \leq \beta(t))$, so for each $u \in T\beta, \exists v \in S^1_{F,\beta}(i.e., \ \ v(t) \in F(t, \beta(t)) \ t \in I \ )$ with

$$u(t) = \int_0^T g(s, \beta(s))ds + \int^t v(s)ds,$$

and since β is an upper solution of the problem (4)-(7), we have $v(s) \leq \beta^{'}(s) \ a.e \ s \in I$.

As a result, for each $t \in I$, we have

$$u(t) = \int_0^T g(s, \beta(s))ds + \int_0^t v(s)ds$$

$$\leq \int_0^T g(s, \beta(s))ds + \int_0^t \beta^{'}(s)ds$$

$$= \int_0^T g(s, \beta(s))ds + \beta(t) - \beta(0) \leq \beta(t) \ \ (\beta(0) \geq \int_0^T g(s, \beta(s))ds).$$

Consequently, $T\beta \leq \beta$. A similar argument guarantees that $\alpha \leq T\alpha$, and since T is isotone increasing on N and $\alpha \leq x \leq \beta$, we have $\alpha \leq T\alpha \leq Tx \leq T\beta \leq \beta$, so $T : N \to P(N)$.

As in the proof of Theorem 3.1, we deduce that Tx is closed for each $x \in N$, thus for each $x \in N$, we have Tx is a nonempty closed and bounded subset of N, so as a result we have that $supTx \in Tx$ (also $infTx \in Tx$), and by Theorem 2.3, we have that T has the minimal and maximal elements, therefore the problem (4)-(7) has the minimal and maximal solutions in N.

4 Example

As an example of our result, we consider the following boundary value problem with integral condition:

$$\begin{cases} x'(t) \in \frac{1}{3e^{t+2}}[1, 1 + |x(t)|], \quad t \in I = [0, T], \\ x(0) = \int_0^T \frac{1}{2e^{s+4}}(1 + x(s))ds. \end{cases} \tag{7}$$

Set

$$F(t, x) = \frac{1}{3e^{t+2}}[1, 1 + |x|], \quad t \in I.$$

For each $x \in \Re$, and $t \in I$, we have

$$\|F(t, x)\| = \sup\{|v| : \ v \in F(t, x)\} \leq \frac{1}{3e^{t+2}}(1 + |x|).$$

Hence for each $r > 0$, $\exists h_{F,r} \in L^1(I, \Re_+)$ such that

$$h_{F,r}(t) = \frac{1 + r}{3e^{t+2}} \quad |x| \leq r$$

and

$$g(t, x(t)) = \frac{1}{2e^{t+4}}(1 + x(t)),$$

we have also

$$|g(t, x)| \leq \frac{1 + r}{2e^{t+4}} = h_g(t)$$

for each $|x| \leq r$.

References

[1] G. Adomian and G. E. Adomian. Cellular systems and aging models. *Comput. Math. App.* **11** (1985) 283–291.

[2] R. Agarwal and A. Boucherif. Nonlocal conditions for differential inclusions in the space of functions of bounded variations. *Advences in defference equations* **2011** (17) (2011) 1–12.

[3] R. P. Agarwal and B. C. Dhage and D. O'Regan. The upper and lower solution method fro differential inclusios vie a lattice fixed point theorem. Dynamic Sys. App. **12** (2003) 1–7.

[4] A. Arara and M. Benchohra. Fuzzy solutions for boundary value problems with integral-boundary conditions. Acta Math. Univ. Comenianae LXXV (2006) 119–126.

[5] J. P. Aubin and A. Cellina. *Differential Inclusions.* Springer, Berlin, 1984.

[6] J. Bastien. Study of a driven and braked wheel using maximal monotone differential inclusions: applications to the nonlinear dynamics of wheeled vehicles. Arch. Appl. Mech. **84** (2014) 851-880.

[7] M. Benyoub and S. G. Özyurt. On extremal solutions of weighted fractional hybrid differential equations. *Faculty of Sciences and Mathematics, University of Niš, Serbia* **38** (6) (2024) 2091–2107.

[8] G. Birkhoff. *Lattice theory.* Amer. Math. Soc. Coll. Publ. V. **25** New York, 1967.

[9] K. W. Blayneh. Analysis of age structured host-parasitoid model. *FAR; East. J. Dyn. Syst.* **4** (2002) 125–145.

[10] A. Boucherif. First-order differential inclusions with nonlocal initial conditions. *Applied Mathematics Letters.* **15** (2002) 409–414.

[11] A. Boucherif. Nonlocal Cauchy problems for first-order multivalued differential equations. *Electronic Journal of Differential Equations* **2002** (47) (2002) 1–9.

[12] M. Cichon. Multivalued perturbations of m-accretive differential inclusions in a nonseparable Banach space. *Commentationes Math.* **32** (1992) 11–17.

[13] B. C. Dhage. A functional integral inclusion involving discontinuous. *Fixed Point Theory* **5** (1) (2004) 53–64.

[14] B. C. Dhage. Fixed-point theorem for discntinuous multivalued operators on ordered spaces with applications. *Com. Math. App.* **51** (2006) 589–604.

[15] B. C. Dhage. A lattice fixed point theorem and multivalued differential equations. *Functional Diff. Equ.* **9** (2002) 109–115.

[16] B. C. Dhage. A lattice fixed point theorem for multivalued mappings with application . *Chinese J. Math.* **19** (1991) 11–22.

[17] A. M. A. El-Sayed and E. M. Hamadallah, and KH. W. El Kadeky. Solutions of class of nonlocal problems for differential inclusion $x^{'}(t) \in F(t, x(t))$. *Applied Mathematics and Information Sciences.* **5** (2) (2011) 413–421.

[18] G. Infante. Eigenvalues and positive solutions of ODEs involving integral boundary conditions. *Discrete Contin. Dyn. Syst.* (2005) 436–442.

[19] A. Lasota and Z. Opial. An application of the Kakutani-Ky-Fan theorem in the theory of ordinary differential equations. *Bull. Acad. Polon. Sci. Ser. Sci. Math. Astronom. Phys.* **13** (1965) 781–786.

[20] M. D. P. M. Marques. *Differential inclusions in nonsmooth mechanical problems.* Birkhäuser Basel, 1993.

[21] A. S. P. More and B. D. Karande. *Integral and differential inclusions.* LAP Lambert Academic Publishing, 2023.

[22] R. L. Pouso and L. M. Albés. Existence of extremal solutions for discontinuous Stieljes differential equations. *J. Ineq. App.* **2020** (47) (2020) 1–21.

Nonlinear Dynamics and Systems Theory, **25** (1) (2025) 78–90

General Stability Result for a Nonlinear Viscoelastic Wave Equation With Boundary Dissipation

B. Madjour * and A. Boudiaf

Applied Mathematics Laboratory, Sétif 1 University, SETIF, 19000, Algeria.

Received: April 13, 2024; Revised: January 17, 2025

Abstract: In this paper, we consider a model of a dynamic viscoelastic wave equation with a nonlinear source and boundary dissipation. Our fundamental goal is to establish the general decay rates of the energy solutions under a class of generality of the relaxation function $g : \mathbb{R}^+ \to \mathbb{R}^+$ satisfying the inequality $g'(t) \leq -H(g(t))$ for all $t \geq 0$, where H is a function satisfying some specific properties. This work extends the previous works with a viscoelastic wave equation and improves earlier results in the literature.

Keywords: *viscoelastic wave equation; relaxation function; general decay; convexity.*

Mathematics Subject Classification (2020): 35B37, 93D15, 93D20, 74D05, 35L55.

1 Introduction

In this paper, we are concerned with the following nonlinear viscoelastic wave equations:

$$\begin{cases} u_{tt} - k_0 \Delta u + \int_0^t g\,(t-s)\, div(a(x)\nabla u\,(s))ds + b\,(x)\, u_t = |u|^{p-2}\, u & \text{in } \Omega \times \mathbb{R}^+, \\ k_0 \frac{\partial u}{\partial \nu} - \int_0^t g\,(t-s)\,(a\,(x)\,\nabla u\,(s))\,\nu ds + h\,(u_t) = 0 & \text{on } \Gamma_1 \times \mathbb{R}^+, \\ u\,(x,0) = u_0\,(x)\,, u_t\,(x,0) = u_1\,(x)\,, & x \in \Omega, \\ u = 0 & \text{on } \Gamma_0 \times \mathbb{R}^+, \end{cases} \tag{1}$$

where $k_0 > 0$, and Ω is a bounded domain in $\mathbb{R}^n$ $(n \geq 1)$ with a smooth boundary $\Gamma = \Gamma_0 \cup \Gamma_1$. Hence Γ_0 and Γ_1 are closed and disjoint with $mes\,(\Gamma_0) > 0$ and ν is the unit outward normal to Γ. $b : \Omega \to \mathbb{R}^+$ is a function, and

$$2 < p \leq \frac{2n}{(n-2)}, \quad n \geq 3, \tag{2}$$

* Corresponding author: bilel.madjour@univ-setif.dz

© 2025 InforMath Publishing Group/1562-8353 (print)/1813-7385 (online)/http://e-ndst.kiev.ua

$$p > 2, \quad n = 1, 2.$$

We consider the following hypotheses.
$(G1)$ $g : \mathbb{R}^+ \to \mathbb{R}^+$ is a C^1 function satisfying

$$g(0) > 0, \quad k_0 - \int_0^\infty g(s)\, ds = l > 0. \tag{3}$$

$(G2)$ $H : \mathbb{R}^+ \to \mathbb{R}^+$ is a $C^1(\mathbb{R}^+)$ function with $H(0) = 0$, and H is a linear or strictly increasing and strictly convex C^2 function on $(0, r]$, $r < 1$, such that

$$g'(t) \leq -H(g(t)), \quad \forall t \geq 0. \tag{4}$$

$(G3)$ $h : \mathbb{R} \to \mathbb{R}$ is a nondecreasing function with

$$h(s)\, s \geq \alpha |s|^2, \quad \forall s \in \mathbb{R}, \tag{5}$$

$$|h(s)| \leq \gamma |s|, \quad \forall s \in \mathbb{R}, \tag{6}$$

where α, γ are positive constants.
$(G4)$ $a : \Omega \to \mathbb{R}$ is a non negative function and $a \in C^1(\overline{\Omega})$ such that

$$a(x) \geq a_0 > 0, \tag{7}$$

$$|\nabla a(x)|^2 \leq a_1^2 |a(x)|, \quad \forall s \in \mathbb{R},$$

for some positive constant a_1.

This type of problems has been considered by many authors and several results concerning existence, nonexistence, and asymptotic behavior have been established. In this regard, Messaoudi [4, 5] considered

$$u_{tt} - \Delta u + \int_0^t g(t-s)\, \Delta u(s)\, ds = b |u|^{p-2} u \tag{8}$$

for $p \geq 2$ and $b = 0$ or 1, and the relaxation function satisfies a relation of the form

$$g'(t) \leq -\xi(t)\, g(t), \tag{9}$$

where ξ is a differentiable nonincreasing positive function. He established a more general decay result, from which the usual exponential and polynomial decay rates are the only special cases. Also, Messaoudi and Mustafa [1] treated the following system:

$$\begin{cases} u_{tt} - \Delta u + \int_0^t g(t-s)\, \Delta u(s)\, ds = 0 & \text{in } \Omega \times \mathbb{R}^+, \\ \frac{\partial u}{\partial \nu} - \int_0^t g(t-s)\, \frac{\partial u}{\partial \nu}(s)\, \nu ds + h(u_t) = 0 & \text{on } \Gamma_1 \times \mathbb{R}^+, \\ u = 0 & \text{on } \Gamma_0 \times \mathbb{R}^+, \end{cases} \tag{10}$$

where g satisfies (9) and h satisfies weaker conditions than those in [2], and obtained an explicit and general formula for the decay rate of the energy. In [9], Mustafa considered the nonlinear abstract equation subject to a competing effect of viscoelastic and frictional dampings:

$$\begin{cases} u_{tt} - \Delta u + \int_0^t g(t-s)\, Au(s)\, ds + h(u_t) = j(u), \qquad t > 0 \\ u(0) = u_0, u_t(0) = u_1, \end{cases} \tag{11}$$

and studied the simultaneous effect of viscoelastic and frictional dampings on the energy decay rates, with minimal conditions on both h and g, where g satisfies

$$g'(t) \leq -\xi(t) H(g(t)), \tag{12}$$

and H is an increasing and convex function. In this context, we refer to the work [6] by Alabu-Boussouria and Cannarsa, in which they considered the following viscoelastic problem:

$$\begin{cases} u_{tt} - \triangle u + \int_0^t g(t-s) \triangle u(s)\, ds = 0 & \text{in } \Omega \times \mathbb{R}^+, \\ u = 0 & \text{on } \Gamma \times \mathbb{R}^+, \\ u(x,0) = u_0, u_t(x,0) = u_1, & x \in \Omega, \end{cases} \tag{13}$$

and g is a positive function satisfying

$$g'(t) \leq -\chi(g(t)), \tag{14}$$

where χ is a nonnegative function with $\chi(0) = \chi'(0) = 0$, and χ is strictly increasing and strictly convex on $(0, k_0]$ for some $k_0 > 0$. They also required that

$$\int_0^{k_0} \frac{dx}{\chi(x)} = +\infty, \quad \int_0^{k_0} \frac{x}{\chi(x)} dx < 1, \quad \liminf_{s \to 0^+} \frac{\frac{\chi(s)}{s}}{\chi'(s)} > \frac{1}{2},$$

in this case, an explicit rate of decay is given.

In this work, we present an explicit formula for energy decay, which extends the class of functions g beyond that in [6].

2 Preliminaries

We use the standard Lebesgue and Sobolev spaces with their usual scalar products and norms, we set

$$H^1_{\Gamma_0} = \{u \in H^2(\Omega) : u = 0 \text{ on } \Gamma_0\}.$$

We first have the embedding $H^1_{\Gamma_0} \hookrightarrow L^{2(p+1)}(\Omega)$. Let $B > 0$ be the optimal constant of the Sobolev embedding which satisfies the following inequality:

$$\|u\|_{2(p+1)} \leq B \|\nabla u\|_2, \quad \forall u \in H^1_{\Gamma_0}. \tag{15}$$

Use the trace-Sobolev embedding $H^1_{\Gamma_0} \hookrightarrow L^k(\Gamma_1)$, $1 \leq k \leq \frac{2(n-1)}{n-2}$, in this case, the embedding constant is denoted by B_1, that is,

$$\|u\|_{k,\Gamma_1} \leq B_1 \|\nabla u\|_2. \tag{16}$$

Now, we introduce the following functionals:

$$\begin{aligned} J(t) &= \frac{1}{2}\left(k_0 - a(x)\int_0^t g(s)\, ds\right)\|\nabla u\|_2^2 + \frac{1}{2}(g \circ \nabla u)(t) - \frac{1}{p}\|u\|_p^p, \\ E(t) &= \frac{1}{2}\|u_t\|_2^2 + J(u(t)) \quad \text{for } t \in [0,T), \\ I(t) &= I(u(t)) = \left(k_0 - \int_0^t g(s)\, ds\right)\|\nabla u\|_2^2 + (g \circ \nabla u)(t) - \|u\|_p^p, \end{aligned} \tag{17}$$

where

$$(g \circ v)(t) = \int_0^t g(t-s) \|v(t) - v(s)\|_2^2 \, ds.$$

Lemma 2.1 *Let u be the solution of* (1)*, then, under assumptions* $(G1)$-$(G3)$*,* $E(t)$ *is a nonincreasing function on* $[0,T)$ *and*

$$E'(t) = -\frac{1}{2}\int_\Omega a(x) g(t) |\nabla u(t)|^2 \, dx + \frac{1}{2}(g' \circ \nabla u)(t) - \int_\Omega b(x) |u_t(t)|^2 \, dx \leq 0. \quad (18)$$

Proof. Multiplying the first equation in (1) by u_t and integrating over Ω and using integration by parts and the boundary condition, and hypotheses $(G1)$, $(G2)$, we obtain (18).

By using the Galerkin method and procedure similar to that from [3, 7], we can have the following local existence result for problem (1).

Theorem 2.1 *Assume that $u_0 \in H^1_{\Gamma_0} \cap H^2(\Omega)$ and $u_1 \in H^1_{\Gamma_0}$. Then there exists a strong solution u of* (1) *satisfying*

$$u \in L^\infty\left([0,T); H^1_{\Gamma_0} \cap H^2(\Omega)\right), u_t \in L^\infty\left([0,T); H^1_{\Gamma_0}\right), u_{tt} \in L^\infty\left([0,T); L^2(\Omega)\right)$$

for some $T > 0$.

Lemma 2.2 *Suppose that* $(G1)$*,* $(G3)$ *and* (2) *hold. Assume further that* $(u_0, u_1) \in H^1_{\Gamma_0} \times L^2(\Omega)$ *such that*

$$\beta = \frac{B^p}{l}\left(\frac{2p}{(p-2)l} E(0)\right)^{(p-2)/2} < 1 \quad (19)$$

and $I(u_0) > 0$, then $I(u(t)) > 0$, $\forall t > 0$, where B is the best Poincaré constant, and $E(0) = E(u_0, u_1)$.

Proof. Since $I(u_0) > 0$, there exists (by continuity) $T_i < T$ such that

$$I(u(t)) \geq 0, \quad \forall t \in [0, T_i],$$

this gives

$$\begin{aligned} J(t) &= \frac{1}{2}\left(k_0 - \int_0^t g(s)\, ds\right)\|\nabla u\|_2^2 + \frac{1}{2}(g \circ \nabla u)(t) - \frac{1}{p}\|u\|_p^p \\ &= \left(\frac{p-2}{2p}\right)\left(\left(k_0 - \int_0^t g(s)\, ds\right)\|\nabla u(t)\|_2^2 + (g \circ \nabla u)(t)\right) + \frac{1}{p} I(t) \\ &\geq \left(\frac{p-2}{2p}\right)\left(\left(k_0 - \int_0^t g(s)\, ds\right)\|\nabla u(t)\|_2^2 + (g \circ \nabla u)(t)\right). \end{aligned} \quad (20)$$

By using $(G1)$, (17), (18) and (20), we easily have

$$l\|\nabla u\|_2^2 \leq \left(\frac{2p}{p-2}\right) J(t) \leq \left(\frac{2p}{p-2}\right) E(0), \quad \forall t \in [0, T_i]. \quad (21)$$

We then exploit $(G1)$, (15), (19) and (21) to obtain

$$\begin{aligned} \|u\|_p^p &\leq B^p \|\nabla u(t)\|_2^p \leq \frac{B^p}{l} \|\nabla u(t)\|_2^{p-2} l \|\nabla u(t)\|_2^2 \leq \beta l \|\nabla u(t)\|_2^2 \\ &< \left(k_0 - \int_0^t g(s)\, ds\right) \|\nabla u(t)\|_2^2, \quad \forall t \in [0, T_i]. \end{aligned} \tag{22}$$

Therefore

$$I(t) = \left(k_0 - \int_0^t g(s)\, ds\right) \|\nabla u\|_2^2 + (g \circ \nabla u)(t) - \|u\|_p^p > 0$$

for all $t \in [0, T_i]$. By repeating this procedure, and using the fact that

$$\lim_{t \to T_i} \frac{B^p}{l} \left(\frac{2p}{(p-2)\, l} E(0)\right)^{(p-2)/2} \leq \beta < 1,$$

T_i is extended to T.

3 Global Existence

In this section, we give some lemmas and the result on the existence of the global solution.

Lemma 3.1 *For any $u \in C^1\left(0, T; H^1(\Omega)\right)$, we have*

$$\begin{aligned} &\int_\Omega \int_0^t g(t-s) \nabla u(s) \nabla u_t(t)\, ds dx \\ &= -\frac{1}{2} \int_\Omega g(t) |\nabla u(t)|^2 dx + \frac{1}{2} (g' \circ \nabla u)(t) \\ &\quad -\frac{1}{2} \frac{d}{dt} \left[(g \circ \nabla u)(t) - \int_\Omega \int_0^t g(s)\, ds |\nabla u(t)|^2 dx\right]. \end{aligned} \tag{23}$$

Proof. See [3].

Lemma 3.2 *There exist positive constants d and t_1 such that*

$$g'(t) \leq -d g(t), \quad \forall t \in [0, t_1]. \tag{24}$$

Proof. By $(G1)$ and $(G2)$, we easily deduce that $\lim_{t \to +\infty} g(t) = 0$. Hence, there is $t_1 \geq 0$ large enough such that

$$g(t_1) = r_1$$

and

$$g(t) \leq r_1, \quad \forall t \geq t_1. \tag{25}$$

As g is non increasing, $g(0) > 0$ and $g(t_1) > 0$, then $g(t) > 0$ for any $t \in [0, t_1]$ and

$$0 < g(t_1) \leq g(t) \leq g(0), \quad \forall t \in [0, t_1].$$

Therefore, since H is a positive continuous function, we get

$$a \leq H(g(t)) \leq b, \quad \forall t \in [0, t_1],$$

for some positive constants a and b.
Consequently, for all $t \in [0, t_1]$,

$$g'(t) \leq -H(g(t)) \leq -a = -\frac{a}{g(0)} g(0) \leq -\frac{a}{g(0)} g(t),$$

which gives

$$g'(t) \leq -dg(t), \quad \forall t \in [0, t_1].$$

Remark 3.1 By $(G1)$ and $(G2)$, we easily deduce that $lim_{t \to +\infty} g(t) = 0$ and

$$max\{g(t), -g'(t)\} < min\{r, H(r), H_0(r)\}, \forall t \geq t_1. \tag{26}$$

Theorem 3.1 *Suppose that* $(G1)$, $(G2)$ *and* (2) *hold. If* $(u_0, u_1) \in H^1_{\Gamma_0} \times L^2(\Omega)$ *and satisfies* (19)*, then the solution is global and bounded.*

4 Decay of Solution

In this section, we state and prove the main result of our work. First, we define some functionals. Let

$$\mathcal{L}(t) = E(t) + \varepsilon_1 \Phi(t) + \varepsilon_2 \Psi(t), \tag{27}$$

where

$$\Phi(t) = \int_\Omega u.u_t \, dx, \tag{28}$$

$$\Psi(t) = \int_\Omega a(x) u_t \int_0^t g(t-s)(u(s) - u(t)) \, ds \, dx, \tag{29}$$

and ε_1, ε_2 are some positive constants to be specified later.

Lemma 4.1 *There exist two positive constants* β_1 *and* β_2 *such that the relation*

$$\beta_1 E(t) \leq \mathcal{L}(t) \leq \beta_2 E(t) \tag{30}$$

holds for ε_1, $\varepsilon_2 > 0$ *small enough.*

Lemma 4.2 *Assume that* $(G1)$-$(G4)$ *hold, then the functional*

$$\Phi(t) = \int_\Omega u u_t \, dx$$

satisfies, along the solution of (1),

$$\begin{aligned} \Phi'(t) \quad \leq \quad & -\frac{1}{4} \int_\Omega |\nabla u|^2 \, dx + \int_\Omega |u_t|^2 \, dx + \frac{(k_0 - l)}{2l} (g \circ \nabla u)(t) \\ & + \frac{2\beta^2 B_*^2}{l} \int_{\Gamma_1} u_t^2 d\Gamma + \frac{2B^2 \|b\|_\infty}{l} \int_\Omega b(x) u_t^2 dx + \|u\|_p^p. \end{aligned} \tag{31}$$

Proof. We estimate the derivative of $\Phi(t)$. From (28) and using (1), we have

$$\begin{aligned}\Phi'(t) &= \int_\Omega u_t^2 dx - k_0 \int_\Omega |\nabla u|^2 dx + \int_\Omega \nabla u(t) a(x) \int_0^t g(t-s) \nabla u(s) ds\, dx \\ &\quad - \int_{\Gamma_1} h(u_t) u\, d\Gamma - \int_\Omega b(x) u u_t dx + \int_\Omega |u|^p dx. \end{aligned} \tag{32}$$

The third, and the fourth, and the fifth terms on the right-hand side of (32) can be estimated as follows. From Hölder's inequality, Young's inequality and (23), for $\eta > 0$, we have

$$\begin{aligned} &\int_\Omega \nabla u(t) a(x) \int_0^t g(t-s) \nabla u(s) ds dx \\ \leq\ & \frac{k_0}{2} \int_\Omega |\nabla u|^2 dx + \frac{1}{2k_0} \int_\Omega a(x) \left(\int_0^t g(t-s) (\nabla u(s) - \nabla u(t) + \nabla u(t)) ds \right)^2 dx \\ \leq\ & \left[\frac{k_0}{2} + \frac{1}{2k_0} (1+\eta)(k_0 - l)^2 \right] \|\nabla u\|_2^2 + \frac{1}{2k_0} \left(1 + \frac{1}{\eta}\right) (k_0 - l)(g \circ \nabla u)(t). \end{aligned} \tag{33}$$

Employing Hölder's inequality, Young's inequality, $(G1)$ and (15), for δ_1, $\delta_2 > 0$, we see that

$$\left| \int_{\Gamma_1} h(u_t) u\, d\Gamma \right| \leq \delta_1 B_*^2 \|\nabla u\|_2^2 + \frac{\beta^2}{4\delta_1} \int_{\Gamma_1} u_t^2 d\Gamma, \tag{34}$$

and

$$\int_\Omega b(x) u u_t dx \leq \delta_2 B^2 \|\nabla u\|_2^2 + \frac{1}{4\delta_2} \int_\Omega b(x) u_t^2\, dx. \tag{35}$$

A substitution of (33) - (34) into (32) yields

$$\begin{aligned}\Phi'(t) &\leq -\left(\frac{k_0}{2} - \frac{1}{2k_0}(1+\eta)(k_0-l)^2 - \delta_1 B_*^2 - B^2 \|b\|_\infty \delta_2 \right) \int_\Omega |\nabla u|^2 dx \\ &\quad + \frac{1}{2k_0}\left(1 + \frac{1}{\eta}\right)(k_0 - l)(g \circ \nabla u)(t) + \frac{\beta^2}{4\delta_1} \int_{\Gamma_1} u_t^2 d\Gamma \\ &\quad + \int_\Omega u_t^2 dx + \frac{1}{4\delta_2} \int_\Omega b(x) u_t^2 dx + \int_\Omega |u|^p dx. \end{aligned}$$

Letting $\eta = l/(k_0 - l) > 0$, $\delta_1 = l/8B_*^2$ and $\delta_2 = l/8\beta^2 \|b\|_\infty$ in the above inequality, we obtain

$$\begin{aligned}\Phi'(t) &\leq -\frac{1}{4} \int_\Omega |\nabla u|^2 dx + \int_\Omega u_t^2 dx + \frac{(k_0 - l)}{2l} (g \circ \nabla u)(t) + \frac{2\beta^2 B_*^2}{l} \int_{\Gamma_1} u_t^2 d\Gamma_1 \\ &\quad + \frac{2B^2 \|b\|_\infty}{4\delta_2} \int_\Omega b(x) u_t^2 dx + \int_\Omega |u|^p dx. \end{aligned} \tag{36}$$

Then (31) is established.

Lemma 4.3 *Assume that* $(G1)$-$(G4)$ *hold. Then the functional*

$$\Psi(t) = -\int_\Omega a(x) u_t \int_0^t g(t-s)(u(t) - u(s))\, ds\, dx$$

satisfies, for some positive constants c_5, c_6,

$$\begin{aligned}\Psi'(t) \;\leq\; & -\left(a_0\int_0^t g(s)\,ds-\delta\right)\|u_t\|_2^2+\delta c_5\|\nabla u\|_2^2+c_6\left(g\circ\nabla u\right)(t)+\delta\|b\|_\infty\int_\Omega b(x)u_t^2\,dx\\ & -\frac{g(0)\|b\|_\infty^2 B^2}{4a_0\delta}\left(g'\circ\nabla u\right)(t)+\beta^2\delta\int_{\Gamma_1}u_t^2 d\Gamma_1. \end{aligned}\tag{37}$$

Proof. The proof is similar to the proof of Lemma 4.2.

Theorem 4.1 *Let* $(u_0,u_1)\in H^1_{\Gamma_0}\times L^2(\Omega)$ *be given, satisfying* (19). *Assume that* $(G1)$ *and* $(G2)$ *hold. Then there exist positive constants* c_1,c_2,c_3 *and* ε_0 *such that the following statements hold:*
(**A**) *In the special case,* $H(t)=ct^p$ *with* $1\leq p<\frac{3}{2}$, *the solution energy of* (1) *satisfies*

$$E(t)\leq c_1e^{-c_2t}\qquad \text{if}\quad p=1,\tag{38}$$

$$E(t)\leq\frac{c_3}{(c_1t+c_2)^{\frac{1}{2(p-1)}}}\qquad \text{if}\quad 1<p<\frac{3}{2}.\tag{39}$$

(**B**) *In the general case, the solution energy of* (1) *satisfies*

$$E(t)\leq c_3H_1^{-1}(c_1t+c_2),\quad \forall t\geq 0,\tag{40}$$

where

$$H_1(t)=\int_t^1\frac{1}{sH_0'(\varepsilon_0 s)}ds\quad \text{and}\quad H_0(t)=H(S(t)),$$

provided that S *is a positive* C^1 *function and that* H_0 *is a strictly increasing and strictly convex* C^2 *function on* $(0,r]$ *with* $S(0)=0$.

$$\int_0^{+\infty}\frac{g(s)}{H_0^{-1}(-g'(s))}ds<+\infty.\tag{41}$$

Proof. By using (18), (27), (31) and (37), we obtain

$$\begin{aligned}\mathcal{L}'(t) \;\leq\; & -\left(\varepsilon_2\left(a_0g_0-\delta\right)-\varepsilon_1\right)\|u_t\|_2^2-\left(\frac{\varepsilon_1 l}{4}-\varepsilon_2\delta c_5\right)\|\nabla u\|_2^2\\ & +\left(\varepsilon_2c_6+\frac{(k_0-l)\varepsilon_1}{2l}\right)(g\circ\nabla u)(t)+\varepsilon_1\int_\Omega|u|^p\,dx\\ & -\left(1-\frac{2\varepsilon_1B^2\|b\|_\infty}{l}-\varepsilon_2\delta\|b\|_\infty\right)\int_\Omega b(x)\,u_t^2dx\\ & -\left(\frac{1}{2}-\varepsilon_2\frac{g(0)\|a\|_\infty^2B^2}{4\delta a_0}\right)(-g\circ\nabla u)(t)\\ & -\left(\alpha-\frac{2B_*^2\varepsilon_1\beta^2}{l}-\varepsilon_2\delta\beta^2\right)\int_{\Gamma_1}|u_t|^2\,d\Gamma,\quad \forall t\geq t_1.\end{aligned}$$

We have used the fact that for any $t_1>0$,

$$\int_0^t g(s)\,ds\geq\int_0^{t_1}g(s)\,ds=g_0\quad\forall t\geq t_1.\tag{42}$$

At this point, we choose δ small enough so that

$$\frac{4\delta c_5}{l} < \frac{a_0 g_0}{2} < a_0 g_0 - \delta, \tag{43}$$

where δ is fixed, the choice of any two positive constants ε_1 and ε_2 satisfying

$$\frac{4\delta c_5 \varepsilon_2}{l} < \varepsilon_1 < \frac{a_0 g_0}{2}\varepsilon_2 \tag{44}$$

will make

$$k_1 = \frac{\varepsilon_1 l}{4} - \varepsilon_2 \delta c_5 > 0 \tag{45}$$

and

$$k_2 = \varepsilon_2 \left(a_0 g_0 - \delta\right) - \varepsilon_1 > 0. \tag{46}$$

Then we choose δ, ε_1 and ε_2 small so that (30) and (43) remain valid, further

$$k_3 = 1 - \frac{2\varepsilon_1 B^2 \|b\|_\infty}{l} - \varepsilon_2 \delta \|b\|_\infty > 0 \tag{47}$$

$$k_4 = \alpha - \frac{2B_*^2 \varepsilon_1 \beta^2}{l} - \varepsilon_2 \delta \beta^2 > 0 \tag{48}$$

$$k_5 = \frac{1}{2} - \varepsilon_2 \frac{g(0) \|a\|_\infty^2 B^2}{4\delta a_0} > 0. \tag{49}$$

Hence, for all $t_1 > 0$, we arrive at

$$\begin{aligned} \mathcal{L}'(t) \quad \leq \quad & -k_1 \|\nabla u\|_2^2 - k_2 \|u_t\|_2^2 + c_7 \left(g \circ \nabla u\right)(t) + c_8 \left(g' \circ \nabla u\right)(t) \\ & -k_3 \int_\Omega b(x) u_t^2 dx - k_4 \int_{\Gamma_1} |u_t|^2 d\Gamma + \varepsilon_1 \|u\|_p^p, \end{aligned} \tag{50}$$

which yields that if needed, one can choose ε_1 sufficiently small

$$\mathcal{L}'(t) \leq -mE(t) + C\left(g \circ \nabla u\right)(t), \tag{51}$$

where $c_i = 7, 8$ m, C are some positive constants.

Now, we use (18) and (24) to conclude that, for any $t \geq t_1$,

$$\begin{aligned} \int_0^{t_1} g(s) \int_\Omega |\nabla u(t) - \nabla u(t-s)|^2 dx ds \quad & \leq \quad -\frac{1}{d} \int_0^{t_1} g'(s) \int_\Omega |\nabla u(t) - \nabla u(t-s)|^2 dx ds \\ & \leq \quad -cE'(t). \end{aligned} \tag{52}$$

Next, we take $\mathcal{F}(t) = \mathcal{L}(t) + cE(t)$, which is clearly equivalent to $E(t)$. From (51) and (52), we get, for all $t \geq t_1$,

$$\mathcal{F}'(t) \leq -mE(t) + c \int_0^{t_1} g(s) \int_\Omega |\nabla u(t) - \nabla u(t-s)|^2 dx ds. \tag{53}$$

(I) $H(t) = ct^p$ and $1 \leq p < \frac{3}{2}$.
Case 1 $p = 1$: Estimate (53) yields

$$\mathcal{F}'(t) \leq -mE(t) + c\left(g' \circ \nabla u\right)(t) \leq -mE(t) - cE'(t), \quad \forall t \geq t_1,$$

which gives

$$(\mathcal{F}+cE)'(t) \leq -mE(t), \quad \forall t \geq t_1.$$

Hence, using the fact that $\mathcal{F}+cE \sim E$, we easily obtain (38).

Case 2 $1<p<\frac{3}{2}$: One can easily show that $\int_0^{+\infty} g^{1-\delta_0}(s)\,ds < +\infty$ for any $\delta_0 < 2-p$ (see [7]). Using this fact and (18), and choosing t_1 even larger if needed, we deduce that, for all $t \geq t_1$,

$$\eta(t) := \int_{t_1}^{t} g^{1-\delta_0}(s) \int_\Omega |\nabla u(t) - \nabla u(t-s)|^2 dxds$$

$$\leq 2\int_{t_1}^{t} g^{1-\delta_0}(s) \int_0^1 \left(|\nabla u(t)|^2 + |\nabla u(t-s)|^2\right) dxds \leq cE(0)\int_{t_1}^{t} g^{1-\delta_0}(s) < 1. \quad (54)$$

Then, Jensen's inequality, (18), hypothesis $(G1)$ and (54) lead to

$$\int_{t_1}^{t} g(s) \int_\Omega |\nabla u(t) - \nabla u(t-s)|^2 dxds = \int_{t_1}^{t} g^{\delta_0}(s)\, g^{1-\delta_0}(s) \int_\Omega |\nabla u(t) - \nabla u(t-s)|^2 dxds$$

$$= \int_{t_1}^{t} g^{(p-1+\delta_0)\left(\frac{\delta_0}{p-1+\delta_0}\right)}(s)\, g^{1-\delta_0}(s) \int_\Omega |\nabla u(t) - \nabla u(t-s)|^2 dxds$$

$$\leq c\left[\int_{t_1}^{t} -g'(s) \int_\Omega |\nabla u(t) - \nabla u(t-s)|^2 dxds\right]^{\frac{\delta_0}{p-1+\delta_0}} \leq c\left[-E'(t)\right]^{\frac{\delta_0}{p-1+\delta_0}}.$$

Then, particularly for $\delta_0 = \frac{1}{2}$, we find that (53) becomes

$$\mathcal{F}'(t) \leq -mE(t) + c\left[-E'(t)\right]^{\frac{1}{2p-1}}.$$

Now, we multiply by $E^\alpha(t)$, with $\alpha = 2p-2$, to get, using (18),

$$(\mathcal{F}E^\alpha)'(t) \leq \mathcal{F}'(t)\,E^\alpha(t) \leq -mE^{1+\alpha}(t) + cE^\alpha(t)\left[-E'(t)\right]^{\frac{1}{1+\alpha}}.$$

Then Young's inequality, with $q = 1+\alpha$ and $q' = \frac{1+\alpha}{\alpha}$, gives

$$(\mathcal{F}E^\alpha)'(t) \leq -mE^{1+\alpha}(t) + \epsilon E^{1+\alpha}(t) + C_\varepsilon\left(-E'(t)\right).$$

Consequently, picking $\varepsilon < m$, we obtain

$$F_0'(t) \leq -m'E^{1+\alpha}(t),$$

where $F_0 = \mathcal{F}E^\alpha + C_\varepsilon E \sim E$. Hence we have, for some $a_0 > 0$,

$$F_0'(t) \leq -a_0 F_0^{1+\alpha}(t),$$

from which we easily deduce that

$$E(t) \leq \frac{c_3}{(c_1 t + c_2)^{\frac{1}{2(p-1)}}}. \quad (55)$$

(II) The general case: We define $\mathcal{I}(t)$ by

$$\mathcal{I}(t) := \int_{t_1}^{t} \frac{g(s)}{H_0^{-1}(-g'(s))} \int_\Omega |\nabla u(t) - \nabla u(t-s)|^2 dxds,$$

where H_0 is such that (41) is satisfied. As in (54), we find that $\mathcal{I}(t)$ satisfies, for all $t \geq t_1$,

$$0 < \mathcal{I}(t) < 1. \tag{56}$$

We also assume, without loss of generality, that $\mathcal{I}(t) \geq \beta > 0$ for all $t \geq t_1$; otherwise (53) yields an exponential decay. In addition, we define $\lambda(t)$ by

$$\lambda(t) := -\int_{t_1}^{t} g'(s) \frac{g(s)}{H_0^{-1}(-g'(s))} \int_{\Omega} |\nabla u(t) - \nabla u(t-s)|^2 dxds$$

and infer from $(G1)$ and the properties of H_0 and S that

$$\frac{g(s)}{H_0^{-1}(-g'(s))} \leq \frac{g(s)}{H_0^{-1}(H(g(s)))} = \frac{g(s)}{S^{-1}(g(s))} \leq \sigma_0$$

for some positive constant σ_0. Then, using (18) and choosing t_1 even larger (if needed), one can easily see that $\lambda(t)$ satisfies, for all $t \geq t_1$,

$$\begin{aligned} \lambda(t) &\leq -k_0 \int_{t_1}^{t} g'(s) \int_{\Omega} |\nabla u(t) - \nabla u(t-s)|^2 dxds \\ &\leq -cE(0) \int_{t_1}^{t} g'(s)\, ds \leq cg(t_1) E(0) < \min\{r, H(r), H_0(r)\}. \end{aligned}$$

Since H_0 is strictly convex on $(0, r]$ and $H_0(0) = 0$, one has $H_0(\theta x) \leq \theta H_0(x)$, provided $0 \leq \theta < 1$ and $x \in (0, r]$. The use of hypothesis $(G1)$, (26), (56), (57) and Jensen's inequality leads to

$$\begin{aligned} \lambda(t) &= \frac{1}{\mathcal{I}(t)} \int_{t_1}^{t} \mathcal{I}(t) H_0[H_0^{-1}(-g'(s))] \frac{g(s)}{H_0^{-1}(-g'(s))} \int_{\Omega} |\nabla u(t) - \nabla u(t-s)|^2 dxds \\ &\geq \frac{1}{\mathcal{I}(t)} \int_{t_1}^{t} H_0[\mathcal{I}(t) H_0^{-1}(-g'(s))] \frac{g(s)}{H_0^{-1}(-g'(s))} \int_{\Omega} |\nabla u(t) - \nabla u(t-s)|^2 dxds \\ &= H_0\left(\int_{t_1}^{t} g(s) \int_{\Omega} |\nabla u(t) - \nabla u(t-s)|^2 dxds\right). \end{aligned}$$

This implies that

$$\int_{t_1}^{t} g(s) \int_{\Omega} |\nabla u(t) - \nabla u(t-s)|^2 dxds \leq H_0^{-1}(\lambda(t)),$$

then (53) becomes

$$\mathcal{F}'(t) \leq -mE(t) + cH_0^{-1}(\lambda(t)), \forall t \geq t_1. \tag{57}$$

Now, for $\varepsilon_0 < r$ and $c_0 > 0$, using (57) and the fact that $E' \leq 0$, $H_0' > 0$, $H_0'' > 0$ on $(0, r]$, we find that the functional F_1 defined by

$$F_1(t) := H_0'\left(\varepsilon_0 \frac{E(t)}{E(0)}\right) \mathcal{F}(t) + c_0 E(t)$$

satisfies, for some $\alpha_1, \alpha_2 > 0$,

$$\alpha_1 F_1(t) \leq E(t) \leq \alpha_2 F_1(t) \tag{58}$$

and

$$F_1'(t) = \varepsilon_0 \frac{E'(t)}{E(0)} H_0''\left(\varepsilon_0 \frac{E(t)}{E(0)}\right) \mathcal{F}(t) + H_0'\left(\varepsilon_0 \frac{E(t)}{E(0)}\right) \mathcal{F}'(t) + c_0 E'(t)$$
$$\leq -mE(t) H_0'\left(\varepsilon_0 \frac{E(t)}{E(0)}\right) + cH_0'\left(\varepsilon_0 \frac{E(t)}{E(0)}\right) H_0^{-1}(\lambda(t)) + c_0 E'(t). \tag{59}$$

Let H_0^* be the convex conjugate of H_0 in the sense of Young (see [8], p.61-64), then

$$H_0^*(s) = s(H_0')^{-1}(s) - H_0\left[(H_0')^{-1}(s)\right] \quad if\ s \in (0, H_0'(r)] \tag{60}$$

and H_0^* satisfies the following Young's inequality:

$$AB \leq H_0^*(A) + H_0(B) \quad if\ A \in (0, H_0'(r)], B \in (0, r]. \tag{61}$$

With $A = H_0'\left(\varepsilon_0 \frac{E(t)}{E(0)}\right)$ and $B = H_0^{-1}(\lambda(t))$, using (18), (53) and (59)-(61), we arrive at

$$F_1'(t) \leq -mE(t) H_0'\left(\varepsilon_0 \frac{E(t)}{E(0)}\right) + cH_0^*\left(H_0'\left(\varepsilon_0 \frac{E(t)}{E(0)}\right)\right) + c\lambda(t) + c_0 E'(t)$$
$$\leq -mE(t) H_0'\left(\varepsilon_0 \frac{E(t)}{E(0)}\right) + c\varepsilon_0 \left(\frac{E(t)}{E(0)}\right) H_0'\left(\varepsilon_0 \frac{E(t)}{E(0)}\right) - cE'(t) + c_0 E'(t) \tag{62}$$

Consequently, with a suitable choice of ε_0 and c_0, we obtain, for all $t \geq t_1$,

$$F_1'(t) \leq -k\left(\frac{E(t)}{E(0)}\right) H_0'\left(\varepsilon_0 \frac{E(t)}{E(0)}\right) = -kH_2\left(\varepsilon_0 \frac{E(t)}{E(0)}\right), \tag{63}$$

where $H_2(t) = tH_0'(\varepsilon_0 t)$.

Since $H_2'(t) = H_0'(\varepsilon_0 t) + \varepsilon_0 t H_0''(\varepsilon t)$, using the strict convexity of H_0 on $(0, 1]$, we find that $H_2'(t)$, $H_2(t) > 0$ on $(0, r]$. Thus, with

$$R_0(t) = \alpha_1 \frac{\varepsilon F_1(t)}{E(0)}, \quad 0 < \varepsilon < 1,$$

taking in account (58) and (63), we have

$$R_0(t) \sim E(t) \tag{64}$$

and, for some $k_0' > 0$,

$$R_0'(t) \leq -\varepsilon k_0' H_2(R_0(t)), \quad \forall t \geq t_1.$$

Then a simple integration and a suitable choice of ε yield, for some k_1', $k_2' > 0$,

$$R_0(t) \leq H_1^{-1}(k_1' t + k_2'), \quad \forall t \geq t_1, \tag{65}$$

where $H_1(t) = \int_t^1 \frac{1}{H_2(s)} ds$.

By a combination of (64) and (65), estimate (40) is established.

5 Conclusion

In this paper, we studied the asymptotic behavior of the dynamic viscoelastic wave equation with boundary dissipation and a nonlinear source term. The existence of dissipation through boundary conditions ensures the decay of energy. By using the convexity of the relaxation function g and without imposing any restrictive growth assumption on the damping term, we establish a general decay rate. These results have potential for application in the fields of physics and nonlinear dynamics. A similar study for the models of dynamic viscoelastic wave equations with a logarithmic nonlinear source term and thermal dissipation will be the purpose for future research.

References

[1] S. A. Messaoudi and M. I. Mustafa. On the control of solutions of viscoelastic equations with boundary feedback. *Nonlinear Analysis: Real World Applications* **10** (5) (2009) 3132–3140.

[2] M. M. Cavalcanti, V. N. D. Cavalcanti and P. Martinez. General decay rate estimates for viscoelastic dissipative systems. *Nonlinear Analysis* **68** (1) (2008) 177–193.

[3] F. Li, Z. Zhao and Y. Chen. Global existence uniqueness and decay estimates for nonlinear viscoelastic wave equation with boundary dissipation. *Nonlinear Analysis: Real World Applications* **12** (3) (2011) 1759–1773.

[4] S. A. Messaoudi. General decay of solutions of a viscoelastic equation. *Journal of Mathematical Analysis and Applications* **341** (2) (2008) 1457–1467.

[5] S. A. Messaoudi. General decay of the solution energy in a viscoelastic equation with a nonlinear source. Nonlinear Anal. *Theory, Methods & Appl.* **69** (8) (2008) 2589–2598.

[6] F. B. Alabau and P. Cannarsa. A general method for proving sharp energy decay rates for memory-dissipative evolution equations. *Comptes Rendus Mathematique* **347** (15–16) (2009) 867–872.

[7] S. A. Messaoudi and W. Al-Khulaifi. General and optimal decay for a quasilinear viscoelastic equation. *Applied Mathematics Letters* **66** (4) (2017) 16–22.

[8] J. E. M. Rivera and A. P. Salvatierra. Asymptotic behavior of the energy in partially viscoelastic materials. *Quarterly of Applied Mathematics* **59** (3) (2001) 557–578.

[9] M. I. Mustafa. Optimal energy decay results for nonlinear abstract viscoelastic dissipative systems. *Zeitschrift fűr angewandte Mathematik und Physik.* **72** (2021) 1–15.

Nonlinear Dynamics and Systems Theory, **25** (1) (2025) 91–100

Efficient Descent Direction of a Conjugate Gradient Algorithm for Nonlinear Optimization

Mohamed Lamine Ouaoua * and Samia Khelladi

Laboratory of Fundamental and Numerical Mathematics,
Department of Mathematics, Faculty of Sciences,
Setif 1 University-Ferhat Abbas, 19000, Algeria.

Received: February 21, 2024; Revised: January 9, 2025

Abstract: We propose an efficient variant of the conjugate gradient method for nonlinear optimization based on a new parameter β_k. We show that the new search direction fills the sufficient descent condition and we prove the global convergence of the corresponding algorithm using the strong Wolfe inexact line search. The established numerical results show that the new algorithm is more efficient in comparison with the standard Fletcher-Reeves method in terms of either the iteration number or CPU time.

Keywords: *unconstrained optimization; conjugate gradient method; descent direction; inexact line search; global convergence.*

Mathematics Subject Classification (2020): 65K05, 90C26, 90C30, 93A30.

1 Introduction

Consider the following unconstrained nonlinear optimization problem:

$$\begin{cases} \min \ f(x), \\ x \in \mathbb{R}^n, \end{cases} \tag{1}$$

where $f : \mathbb{R}^n \longrightarrow \mathbb{R}$ is a continuously differentiable function.

Conjugate gradient methods are efficient to solve unconstrained optimization problem (1), especially for large scale problems. These methods generate the following sequence:

$$x_{k+1} = x_k + \alpha_k d_k, \tag{2}$$

* Corresponding author: mailto:mohamedlamine.ouaoua@univ-setif.dz

© 2025 InforMath Publishing Group/1562-8353 (print)/1813-7385 (online)/http://e-ndst.kiev.ua

where x_k is the current iterate point, $\alpha_k > 0$ is the step size which can be found by one of the line search methods, and d_k is the search direction defined by

$$d_k = \begin{cases} -g_k & \text{for } k = 1, \\ -g_k + \beta_k d_{k-1} & \text{for } k \geq 2, \end{cases} \tag{3}$$

where $g_k = \nabla f(x_k)$ is the gradient of f at x_k, and β_k is a scalar conjugacy coefficient.

Different conjugate gradient methods correspond to different values of the coefficient β_k, a survey of these methods was given by Hager an Zhang in [11].

Recently, a great contribution in the area of conjugate gradient methods and their application has been done by Andrei in [1].

Among the well known formulas of β_k, we can cite Hestenes-Stiefel (HS) [13], Fletcher-Reeves (FR) [10], Polak-Ribière-Polyak (PRP) [15,16], Conjugate Descent-Fletcher (CD) [9], Liu-Story (LS) [14] and Dai-Yuan (DY) [4], which are given as follows:

$$\beta_k^{HS} = \frac{g_k^T y_{k-1}}{d_{k-1}^T y_{k-1}},$$

$$\beta_k^{FR} = \frac{\| g_k \|^2}{\| g_{k-1} \|^2},$$

$$\beta_k^{PRP} = \frac{g_k^T y_{k-1}}{\| g_{k-1} \|^2},$$

$$\beta_k^{CD} = -\frac{\| g_k \|^2}{g_{k-1}^T d_{k-1}},$$

$$\beta_k^{LS} = -\frac{g_k^T y_{k-1}}{g_{k-1}^T d_{k-1}},$$

$$\beta_k^{DY} = \frac{\| g_{k-1} \|^2}{d_{k-1}^T y_{k-1}},$$

where $y_{k-1} = g_k - g_{k-1}$.

If f is a strongly convex quadratic function and the line search is exact, then all the above formulas of β_k are the same.

In the general case, where f is non-quadratic, the algorithms corresponding to each β_k have different numerical performances.

There are many other conjugate gradient methods such as those where the scalar is given by parametric formulas like the β_k proposed by Sellami and Chaib in [17, 18].

Several researchers have also proposed hybrid conjugate gradient methods combining the existing β_k [3, 5–8, 12] .

There are many convergence results with some line search conditions which have been widely studied, there the method can guarantee the descent property of each direction which provided the step length α computed by carrying out a line search and it satisfies the strong Wolfe conditions such that

$$f(x_k + \alpha d_k) \leq f(x_k) + \rho \alpha g_k^T d_k, \tag{4}$$

$$\left| g_{k+1}^T d_k \right| \leq -\sigma g_k^T d_k, \tag{5}$$

where $0 < \rho < \sigma < \frac{1}{2}$.

The aim of this paper is to ameliorate the conjugate gradient method for nonlinear optimization using a new parameter which leads to a new descent direction.

The rest of the paper is organized as follows. In Section 2, we define the formula of the new conjugate gradient coefficient using the Fletcher-Reeves formula with a modification in its denominator, then we give the description of the corresponding algorithm. In the second part, we present a complete analysis of the descent condition of the obtained direction, then we show the global convergence of the corresponding algorithm. Section 3 contains numerical experiments on some examples considering the well known test functions in the literature. Finally, we end with a conclusion in Section 4.

2 Convergence Analysis of the Algorithm Based on the New Parameter β_k

In this section, we propose a new conjugate gradient coefficient using the Fletcher-Reeves formula [10] with a modification in its denominator. This coefficient is defined as follows:

$$\beta_k^{MSD} = \frac{\|g_k\|^2}{\|g_{k-1}\|^2 + \mu \left|g_k^T d_{k-1}\right|}, \tag{6}$$

where $\mu > 0$.

Recall that the case $\mu = 0$ corresponds to the Fletcher-Reeves coefficient [10].

2.1 Description of the conjugate gradient algorithm

2.1.1 Algorithm MSD

Begin algorithm

- Given a starting point $x_1 \in \mathbb{R}^n$ and a parameter $\varepsilon > 0$.
- Set $k = 1$ and compute $d_1 = -g_1$.
- While $\|g_k\| > \varepsilon$ do
- Find $\alpha_k > 0$ satisfying the strong Wolfe conditions $(4, 5)$.
- Take $x_{k+1} = x_k + \alpha_k d_k$.
- Compute β_{k+1} by the new formula (6).
- Set $d_{k+1} = -g_{k+1} + \beta_{k+1} d_k$ and $k = k + 1$.
- End while.

End algorithm.

2.2 Sufficient descent property and global convergence analysis

We make the following basic assumptions on the objective function in order to establish the global convergence results for the new algorithm.

2.2.1 Assumptions

- (i) f is a lower bounded function on the level set

$$\Omega = \{x \in \mathbb{R}^n : f(x) \leq f(x_0)\}.$$

- (ii) In some neighborhood Ω_0 of Ω, f is differentiable and its gradient $g(x)$ is Lipschitz continuous, namely, there exists a constant $L > 0$ such that

$$\|g(x) - g(y)\| \leq L\|x - y\|, \forall x, y \in \Omega_0. \tag{7}$$

Under these assumptions, there exists a constant $\varepsilon > 0$ such that

$$\|g_k\| \leq \varepsilon, \forall k. \tag{8}$$

To prove the global convergence of the nonlinear conjugate gradient methods, we use the following lemma, called the Zoutendijk condition [19].

Lemma 2.1 *[19] Suppose that the assumptions $(i), (ii)$ hold. Let the sequence $\{x_k\}$ be generated by (2) and d_k satisfy $g_k^T d_k < 0$. If α_k is determined by the Wolfe line search conditions, then we have*

$$\sum_{k\geq 1} \frac{\left(g_k^T d_k\right)^2}{\|d_k\|^2} < +\infty.$$

Lemma 2.2 *Suppose that the assumption (ii) holds, let the sequence $\{x_k\}$ be generated by (2) and the step length α_k satisfy the strong Wolfe conditions with $0 < \sigma < \frac{1}{2}$, then for any k,*

$$-\frac{1}{1-\sigma} \leq \frac{g_k^T d_k}{\|g_k\|^2} \leq \frac{2\sigma - 1}{1-\sigma}. \tag{9}$$

As soon as $g_k \neq 0$ for all k, the descent property of d_k is satisfied, i.e.,

$$g_k^T d_k < 0. \tag{10}$$

Proof. The lemma is proved by induction. For $k = 1$, since $d_1 = -g_1$, the relations (9) and (10) are true.

For some $k > 1$, we suppose that (9) and (10) are true. By using (3), we get

$$\frac{g_{k+1}^T d_{k+1}}{\|g_{k+1}\|^2} = -1 + \frac{\beta_{k+1} g_{k+1}^T d_k}{\|g_{k+1}\|^2}. \tag{11}$$

From the second strong Wolfe condition (5) and (11), we get

$$-1 + \sigma \frac{\beta_{k+1} g_k^T d_k}{\|g_{k+1}\|^2} \leq \frac{g_{k+1}^T d_{k+1}}{\|g_{k+1}\|^2} \leq -1 - \sigma \frac{\beta_{k+1} g_k^T d_k}{\|g_{k+1}\|^2}. \tag{12}$$

By using (6), we have

$$-1 + \sigma \frac{g_k^T d_k}{\|g_k\|^2 + \mu \left|g_{k+1}^T d_k\right|} \leq \frac{g_{k+1}^T d_{k+1}}{\|g_{k+1}\|^2} \leq -1 - \sigma \frac{g_k^T d_k}{\|g_k\|^2 + \mu \left|g_{k+1}^T d_k\right|}. \tag{13}$$

Observe that for all k, we have

$$\frac{1}{\|g_k\|^2 + \mu \left|g_{k+1}^T d_k\right|} \leq \frac{1}{\|g_k\|^2}. \tag{14}$$

By introducing (14) in (13), we get

$$-1 + \sigma \frac{g_k^T d_k}{\|g_k\|^2} \leq \frac{g_{k+1}^T d_{k+1}}{\|g_{k+1}\|^2} \leq -1 - \sigma \frac{g_k^T d_k}{\|g_k\|^2}. \tag{15}$$

From (9), it follows that for all k,

$$-1 - \frac{\sigma}{1-\sigma} \leq \frac{g_{k+1}^T d_{k+1}}{\|g_{k+1}\|^2} \leq -1 + \frac{\sigma}{1-\sigma},$$

which implies

$$-\frac{1}{1-\sigma} \leq \frac{g_{k+1}^T d_{k+1}}{\|g_{k+1}\|^2} \leq \frac{2\sigma - 1}{1-\sigma}.$$

This gives the formula (9).

Since $0 < \sigma < \frac{1}{2}$, it results from (9) that $g_k^T d_k < 0$.

This completes the proof of the lemma.

Theorem 2.1 *Consider the sequence $\{x_k\}$ generated by (2), where d_k is defined by (3) and satisfies $g_k^T d_k < 0$ and suppose that the assumptions (i) and (ii) hold. Then the Algorithm MSD either stops at a stationary point or converges in the sense that*

$$\lim_{k \longrightarrow \infty} \inf \|g_k\| = 0. \tag{16}$$

Proof. From the second strong Wolfe condition (5) and (9), we get

$$\left|g_k^T d_{k-1}\right| \leq -\sigma g_{k-1}^T d_{k-1} \leq \frac{\sigma}{1-\sigma} \|g_{k-1}\|^2, \tag{17}$$

using (3), (14) and (17), we obtain

$$\begin{aligned} \|d_k\|^2 &= \|g_k\|^2 - 2\beta_k g_k^T d_{k-1} + \beta_k^2 \|d_{k-1}\|^2 \\ &\leq \|g_k\|^2 + \beta_k \frac{2\sigma}{1-\sigma} \|g_{k-1}\|^2 + \beta_k^2 \|d_{k-1}\|^2 \\ &\leq \|g_k\|^2 + \frac{2\sigma}{1-\sigma} \|g_k\|^2 + \beta_k^2 \|d_{k-1}\|^2 \\ &\leq \left(\frac{1+\sigma}{1-\sigma}\right) \|g_k\|^2 + \beta_k^2 \|d_{k-1}\|^2. \end{aligned} \tag{18}$$

After defining $\tau = \frac{1+\sigma}{1-\sigma}$ and applying (18) repeatedly, and using (14), it follows that

$$\begin{aligned}
\|d_k\|^2 &\leq \tau\|g_k\|^2 + \beta_k^2 \|d_{k-1}\|^2 \\
&\leq \tau\left[\|g_k\|^2 + \beta_k^2 \|g_{k-1}\|^2 + \beta_k^2\beta_{k-1}^2 \|g_{k-2}\|^2 + \cdots + \beta_k^2\beta_{k-1}^2 \cdots \beta_3^2 \|g_2\|^2\right] \\
&\quad +\beta_k^2\beta_{k-1}^2 \cdots \beta_2^2 \|d_1\|^2 \\
&\leq \tau\left[\|g_k\|^2 + \frac{\|g_k\|^4}{\|g_{k-1}\|^2} + \frac{\|g_k\|^4}{\|g_{k-2}\|^2} + \cdots + \frac{\|g_k\|^4}{\|g_2\|^2}\right] + \frac{\|g_k\|^4}{\|g_1\|^2} \\
&\leq \tau\|g_k\|^4 \left[\sum_{i=2}^{k} \frac{1}{\|g_i\|^2}\right] + \frac{\|g_k\|^4}{\|g_1\|^2} \\
&\leq \tau\|g_k\|^4 \left[\sum_{i=1}^{k} \frac{1}{\|g_i\|^2}\right]. \qquad (19)
\end{aligned}$$

Now, if (16) is not true, then there exists a constant $\varepsilon > 0$ such that $\|g_k\| > \varepsilon$ for all k. From (19), we obtain

$$\frac{\|g_k\|^4}{\|d_k\|^2} \geq \frac{\varepsilon^2}{\tau k},$$

which implies

$$\sum_{k=1}^{\infty} \frac{\|g_k\|^4}{\|d_k\|^2} = \infty. \qquad (20)$$

By using (9), we have

$$\frac{(g_k d_k)^2}{\|d_k\|^2} \geq \left(\frac{1-2\sigma}{1-\sigma}\right)^2 \frac{\|g_k\|^4}{\|d_k\|^2}, \qquad (21)$$

which implies

$$\sum_{k=1}^{\infty} \frac{(g_k d_k)^2}{\|d_k\|^2} = \infty, \qquad (22)$$

thus contradicting the Zoutendijk condition.

This completes the proof of the theorem.

3 Numerical Experiments

In this section, we present some numerical tests on a set of test functions [1, 2] of unconstrained nonlinear optimization problems using Matlab language.

The objective of these experiments is to show the performance of our new coefficient in comparison with other class of existing classical coefficients. In numerical tests, we consider the *Algorithm MSD* based on our new coefficient β_k^{MSD} (6) compared with the FR method with β_k^{FR} [10].

In the tables of results, we designate by

- n: the size of the problem

- *iter*: the number of iterations

- *time*: the total time in seconds required to complete the evaluation process.

Test function	Size	β_k^{MSD}		β_k^{FR}	
	n	*iter*	*time*	*iter*	*time*
Raydan 1	100	8	0,000411	15	0,000535
	200	8	0,000604	15	0,000852
	500	8	0,001085	15	0,001769
	1000	8	0,002022	15	0,003233
Raydan 2	100	16	0,000421	52	0,001469
	200	16	0,000543	57	0,002259
	500	21	0,001113	3241	0,232550
	1000	21	0,001937	NAN	NAN
Diagonal 4	100	41	0,003746	63	0,005513
	200	42	0,007477	60	0,009580
	500	44	0,016702	62	0,020083
	1000	44	0,038645	99	0,081462
Extended Woods	100	369	0,062696	839	0,162356
	200	471	0,131264	782	0,233382
	500	430	0,271904	659	0,472802
	1000	430	0,029804	932	1,597367
HIMMELBC	100	30	0,004411	42	0,004066
	200	30	0,006783	43	0,007018
	500	32	0,014692	43	0,016906
	1000	32	0,054439	44	0,040352
DIXMAANC	100	14	0,005565	32	0,011920
	200	15	0,012137	23	0,016665
	500	18	0,030703	21	0,033251
	1000	16	0,054192	17	0,073482
HARKERP	100	91	0,004411	302	0,014902
	200	98	0,006783	102	0,007951
	500	108	0,014692	156	0,020768
	1000	255	0,054439	NAN	NAN
PROD1	100	26	0,020014	36	0,022772
	200	26	0,075946	37	0,099651
	500	13	0,262461	13	0,274593
	1000	13	1,105908	14	1,160563

Test function	Size	β_k^{MSD}		β_k^{FR}	
	n	$iter$	$time$	$iter$	$time$
Extended Block	100	23	0,002571	103	0,016227
Diagonal 1	200	24	0,004266	107	0,026036
	500	24	0,013149	103	0,064142
	1000	25	0,028290	114	0,144926
Extended Maratos	100	41	0,002943	42	0,005326
	200	41	0,005166	42	0,009220
	500	41	0,012851	42	0,021821
	1000	42	0,029804	43	0,045364
DIXMAANB	100	13	0,005753	19	0,007854
	200	13	0,011356	20	0,014953
	500	12	0,023140	20	0,031973
	1000	12	0,041619	22	0,066770
Extended Beale	100	66	0,033441	79	0,041068
	200	66/	0,061550	128	0,136998
	500	70	0,155799	90	0,220902
	1000	70	0,312607	132	0,665937
Extended White	100	48	0,021397	63	0,025315
and holst	200	48	0,037467	74	0,054997
	500	51	0,093806	144	0,293700
	1000	52	0,187531	78	0,279982
Quadratic Diagonal	100	102	0,005432	126	0,008635
Perturbed 1	200	155	0,009727	1073	0,065435
	500	280	0,029289	1332	0,145182
	1000	421	0,078164	1983	0,411533
DIXMAANA	100	12	0,005473	19	0,007968
	200	12	0,010762	21	0,015383
	500	13	0,025386	20	0,031282
	1000	13	0,046094	20	0,064289
DENSCHNA	100	35	0,009824	58	0,016107
	200	35	0,020065	61	0,031975
	500	35	0,041322	59	0,066094
	1000	36	0,081710	64	0,149320
Freudenstein	100	136	0,018940	265	0,038783
and Roth	200	115	0,026829	171	0,038423
	500	119	0,065969	145	0,085392
	1000	111	0,142784	112	0,143777
Nondiag	100	138	0,014461	NAN	NAN
	200	136	0,011197	NAN	NAN
	500	240	0,043510	NAN	NAN
	1000	835	0,243155	NAN	NAN

Remark 3.1 In the results tables, NAN means that the algorithm does not display the optimal solution after a maximum number of iterations k_{max}.

3.1 Commentaries

From the results obtained in the tables above, it is clear that our new algorithm based on the β_k^{MSD} parameter is more efficient than the FR method in terms of the number of iterations and computation time. There is a significant reduction in the number of iterations when using the algorithm MSD compared to FR. On the other hand, when the size of certain examples becomes large $n > 1000$, the FR algorithms fail to provide the optimal solution after the number of iterations $k_{max} = 50000$.

4 Conclusion

We proposed a new β_k, and also provided the proof of the global convergence of the new *Algorithm MSD*. We have proven the effectiveness of this algorithm based on the new β_k^{MSD}. It has a good performance compared with other conjugate gradient methods such as the FR method when considering the selected list of test problems.

References

[1] M. Andrei. *Nonlinear Conjugate Gradient Methods for Unconstrained Optimization.* Springer Optimization and its Applications, Vol. 158, 2020.

[2] M. Andrei. An unconstrained optimization test functions collection. *Adv. Model. Optim.* **10** (2008) 1–20.

[3] S. Ben Hanachi, B. Sellami and M. Belloufi. New iterative conjugate gradient method for nonlinear unconstrained optimization. *RAIRO-Oper.* **56** (2022) 2315–2327.

[4] Y. H. Dai and Y. Yuan. A nonlinear conjugate gradient method with a strong global convergence property. *SIAM J. Optim.* **10** (1) (1999) 177–182.

[5] Y. H. Dai and Y. Yuan. An efficient hybrid conjugate gradient method for unconstrained optimization. *Ann. Oper. Res.* **103** (2001) 33–47.

[6] S. Delladji, M. Belloufi and B. Sellami. New hybrid conjugate gradient method as a convex combination of FR and BA methods. *Journal of Information and Optimization Sciences.* **42** (3) (2021) 591–602.

[7] S. Djordjevic. New hybrid conjugate gradient method as a convex combination of LS and FR methods. *Acta Mathematica Scientia.* **39B** (1) (2019) 214–378.

[8] S. Djordjevic. New hybrid conjugate gradient method as a convex combination of HS and FR methods. *Journal of Applied Mathematics and Computation.* **2** (9) (2019) 366–378.

[9] R. Fletcher. *Practical Methods of Optimization.* Unconstrained optimization. Vol. 1, Wiley, New York, 1987.

[10] R. Fletcher and C. M. Reeves. Function minimization by conjugate gradients. *Comput. J.* **7** (2) (1964) 149–154.

[11] W. W. Hager and H. Zhang. A survey of nonlinear conjugate gradient methods. *Pacific Journal of Optimization* **2** (2006) 35–58.

[12] A. Hallal, M. Belloufi and B. Sellami. An efficient new hybrid CG-method as convex combination of DY and CD and HS algorithms. *RAIRO-Oper. Res.* **56** (2022) 4047–4056.

[13] M. R. Hestenes and E. Steifel. Methods of conjugate gradient for solving linear systems. *Res. Natl. Bur. Stand.* **49**(6) (1952) 409–436.

[14] Y. Liu and C. Storey. Efficient generalized conjugate gradient algorithms. *J. Optim. Theory Appl.* **69** (1) (1991) 129–137.

[15] E. Polak and G. Ribiere. Note sur la convergence des méthodes de directions conjuguées. *Rev. Française d'Informatique et de Recherche Opérationnelle.* **16** (2) (1969) 35–43.

[16] B. T. Polyak. The conjugate gradient method in extrem problems. *U.S.S.R. Comput. Math. Phys.* **9** (1969) 94–112.

[17] B. Sellami and Y. Chaib. A new family of globally convergent conjugate gradient methods. *Ann. Oper. Res. Springer.* **241** (2016) 497–513.

[18] B. Sellami and Y. Chaib. New conjugate gradient method for unconstrained optimization. *RAIRO Operations Research.* **50** (2016) 1013–1026.

[19] G. Zoutendijk. Nonlinear programming, computational methods. In: Integer and Nonlinear Programming (J. Abadie (ed.), 1970, 37–86.

Nonlinear Dynamics and Systems Theory, **25** (1) (2025) 101–111

Theoretical and Numerical Results for Nonlinear Optimization Problems

C. Souli [1*] and A. Leulmi [2]

[1] *Laboratory of Fundamental and Numerical Mathematics, Ferhat Abbas University of Setif-1, Algeria.*
[2] *Department of Mathematics, Ferhat Abbas University of Setif-1, Algeria.*

Received: August 16, 2024; Revised: January 26, 2025

Abstract: In this work, we develop a new approach for solving a large class of programming optimization problems by employing a logarithmic barrier interior point method, leveraging a vector $\rho \in \mathbb{R}^n_+$ as the penalty term based on some new minorant function. Firstly, we compute the direction by Newton's method. Then, we propose a new alternative way to determine the step length along the direction, our proposed strategy enables easy and quick computation of the step length. Finally, we illustrate the out-performance of our new minorant functions with respect to the line search one through a numerical experiment on numerous collections of test problems.

Keywords: *nonlinear optimization; logarithmic barrier method; applications; minorant function; secant technique; step length.*

Mathematics Subject Classification (2020): 90C25, 90C30, 90C51, 93C95, 70k75.

1 Introduction

We consider the nonlinear constrained optimization problem

$$\{\min f(x) : \quad x \in \mathcal{L}\}, \tag{1}$$

where f is a convex and twice continuously differentiable function on $\mathcal{L}$ and $\mathcal{L} = \{x \in \mathbb{R}^n : x \geq 0, Ax = c\}$, with $c \in \mathbb{R}^m$ and $A \in \mathbb{R}^{m\times n}$ being a matrix.
Nonlinear optimization is crucial in various fields such as engineering, economics, machine learning, and nonlinear dynamics and systems (see [3, 8]) for finding optimal solutions under complex constraints.

* Corresponding author: mailto:as_smaleulmi@yahoo.fr

© 2025 InforMath Publishing Group/1562-8353 (print)/1813-7385 (online)/http://e-ndst.kiev.ua

The paper highlights the evolution of interior point methods, a significant approach to solving such problems. These methods date back to 1955, see K. R. Frisch [6], and were significantly developed in the contributions of P. Huard [7] in 1967, and A. V. Fiacco and G. P. McCormick [5] in 1968. Notably, the development of logarithmic barrier methods, which replace non-negativity constraints with penalty terms, transforms constrained problems into unconstrained ones, allowing for the use of majorant or minorant functions. Based on this concept, various logarithmic barrier interior point methods leveraging the majorant or minorant functions have been introduced. Crouzeix and Merikhi [2] were the first to develop a logarithmic barrier algorithm based on majorant functions explicitly designed for semidefinite programming. Fellahi and Merikhi [4] introduced new majorant functions for nonlinear programming. Recently, Leulmi et al. [10] focused on devising minorant functions applicable to semidefinite programming while in [9] and [11], they explored the application of minorant functions in the contexts of linear and nonlinear programming, respectively.

Inspired by the methods mentioned above, we propose a novel approach centered on determining the step length in a straightforward manner through the utilization of a minorant function technique. The remainder of this paper is organized as follows. In the next Section 2, we present some useful inequalities that will be utilized throughout the paper. In Section 3, we replace the original problem with a perturbed problem. In Section 4, we study the existence and uniqueness of the optimal solution to the perturbed problem and analyze its convergence. In Section 5, we choose a descent direction and propose new minorant functions to calculate the step length. In Section 6, we describe the algorithm in detail. In the last section, numerical results are reported and some conclusions are drawn.

2 Some Useful Inequalities

In this section, we present some useful inequalities that will be used throughout the paper.

Proposition 2.1 *[14]*

$$\begin{aligned} \bar{z} - \sigma_z\sqrt{n-1} &\leq \min_i z_i \leq \bar{z} - \frac{\sigma_z}{\sqrt{n-1}}, \\ \bar{z} + \frac{\sigma_z}{\sqrt{n-1}} &\leq \max_i z_i \leq \bar{z} + \sigma_z\sqrt{n-1}. \end{aligned}$$

Theorem 2.1 *[2]*

$$n\ln\left(\bar{z} - \sigma_z\sqrt{n-1}\right) \leq A \leq \sum_{i=1}^{n} \ln(z_i) \leq B \leq n\ln(\bar{z}), \tag{2}$$

where

$$\begin{aligned} A &= (n-1)\ln\left(\bar{z} + \frac{\sigma_z}{\sqrt{n-1}}\right) + \ln\left(\bar{z} - \sigma_z\sqrt{n-1}\right), \\ B &= \ln\left(\bar{z} + \sigma_z\sqrt{n-1}\right) + (n-1)\ln\left(\bar{z} - \frac{\sigma_z}{\sqrt{n-1}}\right). \end{aligned}$$

$\bar{z}$ and σ_z are, respectively, the mean and the standard deviation of a statistical series of n real numbers,

$$\bar{z} = \frac{1}{n}\sum_{i=1}^{n} z_i \quad \text{and} \quad \sigma_z^2 = \frac{1}{n}\sum_{i=1}^{n} z_i^2 - \bar{z}^2 = \frac{1}{n}\sum_{i=1}^{n}(z_i - \bar{z})^2.$$

3 Penalization

In this section, we approximated the problem (1) by a perturbed problem where the parameter of penalization is a vector $\rho \in \mathbb{R}_+^n$. Let our problem (1) be considered with the following mild assumptions:

1. A is an $(m \times n)$ full-rank matrix and $c \in \mathbb{R}^m (m < n)$.
2. The optimal solution set of the problem (1) is nonempty and bounded.
3. $\exists x_0 > 0$ such that $Ax_0 = c$.

We have from the optimality conditions that x^* is an optimal solution of (1) if and only if there exists $u^* \in \mathbb{R}^m$ and $v^* \in \mathbb{R}_+^n$,

$$\nabla f(x^*) + A^t u^* - v^* = 0, \quad Ax^* = c, \quad < v^*, x >= 0. \tag{3}$$

3.1 The perturbed problem

Let us present the function $\varphi : \mathbb{R}_+^n \times \mathbb{R}^n \to \mathbb{R}^n \cup \{+\infty\}$ by

$$\varphi(\rho, x) = \begin{cases} f(x) + \vartheta(\rho, x) & \text{if } x, \rho \geq 0, Ax = c. \\ +\infty & \text{otherwise,} \end{cases}$$

where the function $\vartheta : \mathbb{R}_+^n \times \mathbb{R}^n \to \mathbb{R}^n \cup \{+\infty\}$ is given by

$$\vartheta(\rho, x) = \begin{cases} \sum_{i=1}^n \rho_i \ln(\rho_i) - \sum_{i=1}^n \rho_i \ln(x_i) & \textit{if} \quad x, \rho > 0, \\ 0 & \textit{if} \quad x \geq 0 \textit{ and } \rho = 0, \\ +\infty & \textit{otherwise.} \end{cases}$$

The two functions are convex, lower semicountinuous and proper. Let us now provide the convex function Ω defined by

$$\Omega(\rho) = \inf_x [\varphi_\rho(x) := \varphi(\rho, x) : x \in \mathbb{R}]. \tag{4}$$

Remark 3.1 The problems (1) and (4) coincide when $\|\rho\|$ tents to 0.

4 Theoretical Aspects of the Perturbed Problem

4.1 Existence and uniqueness of optimal solution

The next lemma deals with the issue of the existence and uniqueness of optimal solution of (4).

Lemma 4.1 *The perturbed problem* (4) *possesses a unique optimal solution if and only if the recession cone $C_d(\varphi_\rho)$ reduces to the origin, i.e.,*

$$C_d(\varphi_\rho) = \{d \in \mathbb{R}^n : [\varphi_\rho]_\infty(d) \leq 0, \quad Ad = 0, d \geq 0\} = \{0\}. \tag{5}$$

Proof. For the proof, see [4].

The strictly convex problem (4) possesses a unique optimal solution $x(\rho)$ in its feasible set.

4.2 The convergence analysis

We are now prepared to state the convergence result of the perturbed problem (4).

Lemma 4.2 *Let $x(\rho)$ be the optimal solution of the perturbed problem* (4)*, and x^* be the optimal solution of the the original problem* (1)*,*

$$\textit{if} \quad \|\rho\| \to 0, \quad \textit{then} \quad x_\rho \to x.$$

Proof. *For the proof, see [4]*

Note: If either the original problem (1) or its perturbed version (4) possesses an optimal solution with finite and equal objective function values, then the other problem also has an optimal solution.

5 The Numerical Aspects of the Perturbed Problem

This section focuses on numerically solving problem (4). Our study starts with computing the descent direction and determining the step length, employing an innovative technique involving minorant functions.

5.1 The descent direction

When x belongs to the feasible set $\mathcal{L}$, the Newton descent direction d is obtained by solving the following convex quadratic optimization problem:

$$\begin{cases} \min_d \left\{ \frac{1}{2}\langle \nabla^2 \varphi_\rho(x) d, d\rangle + \langle \nabla \varphi_\rho(x), d\rangle \right\}, \\ Ad = 0. \end{cases}$$

From the necessary and sufficient optimality conditions, there exists $v \in \mathbb{R}$ such that

$$\begin{cases} \nabla^2 \varphi_\rho(x) d + \nabla \varphi_\rho(x) + Av = 0, \\ Ad = 0 \end{cases}$$

is equal to

$$\begin{pmatrix} \nabla^2 f(x) + PX^{-2} & A^t \\ A & 0 \end{pmatrix} \begin{pmatrix} d \\ v \end{pmatrix} = \begin{pmatrix} X^{-1}\rho - \nabla f(x) \\ 0 \end{pmatrix},$$

where X, P are diagonal matrices with $X_{ii} = x_i$ and $P_{ii} = \rho_i, i = \overline{1,n}$. Then we obtain

$$\begin{pmatrix} d^t & 0 \end{pmatrix} \begin{pmatrix} \nabla^2 f(x) + PX^{-2} & A^t \\ A & 0 \end{pmatrix} \begin{pmatrix} d \\ v \end{pmatrix} = \begin{pmatrix} d^t & 0 \end{pmatrix} \begin{pmatrix} X^{-1}\rho - \nabla f(x) \\ 0 \end{pmatrix}.$$

Then

$$\langle \nabla^2 f(x)d, d\rangle + \langle \nabla f(x), d\rangle = \langle \rho, X^{-1}d\rangle - \langle PX^{-1}d, X^{-1}d\rangle \tag{6}$$

is equivalent to

$$\begin{pmatrix} X\nabla^2 f(x)X + P & XA^t \\ AX & 0 \end{pmatrix} \begin{pmatrix} X^{-1}d \\ v \end{pmatrix} = \begin{pmatrix} \rho - X\nabla f(x) \\ 0 \end{pmatrix}.$$

The descent direction being acquired.

5.2 The proposed calculation of the step length

Typically, the most commonly employed approaches within line search techniques involve traditional iterative methods, but these methods might involve computationally expensive procedures, especially when function evaluations are costly. Hence, Leulmi et al. [2] introduced the minorant function concept, approximating the function $G(\alpha)$, to provide a simple step length for linear semidefinite programming and linear programming, respectively. Building upon this concept, we propose in this study to approximate the function $G(\alpha)$ using a minorant function. This function offers, at each iteration k, a step length in an easy and much simpler way than the line search methods. Let the function G_0 be as

$$G_0(\alpha) = \varphi_\rho(x + \alpha d) - \varphi_\rho(x) = f(x + \alpha d) - f(x) - \sum_{i=1}^{n} \rho_i \ln(1 + \alpha y_i),$$

where $y = X^{-1}d$ and $\alpha \in]0, \widehat{\alpha}_0[$, $\widehat{\alpha}_0 = \max\{\alpha : 1 + \alpha y_i > 0\}$. From Proposition 2.1, we have $\rho_i \leq \max_i \rho_i \leq \bar{\rho} + \sigma_\rho\sqrt{n-1}$ for all $i = 1, ..., n$.

For $\tau = \bar{\rho} + \sigma_\rho\sqrt{n-1}$ and for all $\alpha \in]0, \widehat{\alpha}_0[$, we obtain

$$G(\alpha) \geq G_1(\alpha) = \frac{1}{\tau}(f(x + \alpha d) - f(x)) - \sum_{i=1}^{n} \ln(1 + \alpha y_i), \tag{7}$$

where $G(\alpha) = \frac{G_0(\alpha)}{\tau}$. It easy to show that

$$G'(\alpha) = \frac{1}{\tau}\left(\langle \nabla f(x + \alpha d), d\rangle - \sum_{i=1}^{n} \rho_i \frac{y_i}{1 + \alpha y_i}\right),$$

$$G''(\alpha) = \frac{1}{\tau}\left(\langle \nabla^2 f(x + \alpha d)d, d\rangle - \sum_{i=1}^{n} \rho_i \frac{y_i^2}{(1 + \alpha y_i)^2}\right),$$

and

$$G_1'(\alpha) = \frac{1}{\tau}\left(\langle \nabla f(x + \alpha d), d\rangle - \sum_{i=1}^{n} \frac{y_i}{1 + \alpha y_i}\right),$$

$$G_1''(\alpha) = \frac{1}{\tau}\left(\langle \nabla^2 f(x + \alpha d)d, d\rangle - \sum_{i=1}^{n} \frac{y_i^2}{(1 + \alpha y_i)^2}\right).$$

G_1 verifies the significant decrease because

(i) From(6) : $G'(0) + G''(0) = 0$ and $G''(0) \geq 0$, then we deduce that $G'(0) \leq 0$.

(ii) $G_1'(0) \leq 0$ if

1. $y_i \geq 0$.

2. $y_i < 0$, we have from (6): $G_1'(0) + G_1''(0) = 0$ and $G_1''(0) \geq 0$.

5.3 The first minorant function

This approach involves minimizing the minorant approximation, denoted as G_2, of G within the interval $[0, \widehat{\alpha}]$. For effectiveness, this approximation necessitates simplicity while maintaining a close proximity to G_1. In our case, it requires that

$$G(0) = G_1(0) = G_2(0) = 0, \quad G_1'(0) = G_2'(0), \quad G_1''(0) = G_2''(0) > 0. \tag{8}$$

In what follows, we take $x_i = 1 + \alpha y_i$, $\bar{x}_i = 1 + \alpha \bar{y}_i$ and $\sigma_x = \alpha \sigma_y$.

From Theorem 2.1, we have $\sum_{i=1}^{n} \ln(x_i) \leq B$, after a simple calculation, we obtain $G_2(\alpha) \leq G_1(\alpha)$, in which

$$G_2(\alpha) = \frac{1}{\tau}(f(x + \alpha d) - f(x)) - (n-1)\ln(1 + \alpha\gamma) - \ln(1 + \alpha\beta),$$

where $\alpha \in]0, \widehat{\alpha}[$, $\gamma = \bar{y} - \frac{\sigma_y}{\sqrt{n-1}}$, $\beta = \bar{y} + \sigma_y\sqrt{n-1}$ and $\widehat{\alpha} = \min\{\widehat{\alpha}_0, \max\{\alpha : 1 + \alpha\gamma > 0\}\}$. It is clear that

$$\begin{aligned} G_2'(\alpha) &= \frac{1}{\tau}\langle \nabla f(x + \alpha d), d\rangle - (n-1)\frac{\gamma}{1 + \alpha\gamma} - \frac{\beta}{1 + \alpha\beta}, \\ G_2''(\alpha) &= \frac{1}{\tau}\langle \nabla^2 f(x + \alpha d)d, d\rangle + (n-1)\frac{\gamma^2}{(1 + \alpha\gamma)^2} + \frac{\beta^2}{(1 + \alpha\beta)^2}. \end{aligned}$$

G_2 verifies the conditions (8), hence the strictly convex function G_2 is a good approximation of G_1 in $]0, \hat{\alpha}[$. Moreover, the unique minimum α^* of G_2 verifies

$$G_2(\alpha^*) \leq G_1(\alpha^*) \leq G(\alpha^*).$$

5.4 The auxiliary function ζ

5.4.1 If the objective function f is linear

We take $f(x) = c^t x$, where $c, x \in \mathbb{R}^n$, the auxiliary function is defined by

$$\zeta(\alpha) = n\eta\alpha - (n-1)\ln(1 + \alpha\gamma) - \ln(1 + \alpha\beta), \quad \eta = \frac{1}{\tau n} c^t d.$$

The two functions ζ and G_2 coincide. The unique solution of $\zeta'(\alpha) = 0$ is the same unique root of $G_2'(\alpha) = 0$ and the unique $\bar{\alpha}$ verifies $G_2(\bar{\alpha}) \leq G_1(\bar{\alpha}) \leq G(\bar{\alpha})$.

5.4.2 If the objective function f is only convex

Under these circumstances, the equation $G_2'(\bar{\alpha}) = 0$ no longer simplifies to a second-degree equation. To address this, we explore an alternative function better than G_2, employing the secant technique. Let $\bar{\alpha} \in]0, \widehat{\alpha}[$ for all $\alpha \in]\bar{\alpha}, \widehat{\alpha}[$, then we have

$$\frac{\alpha}{\tau\bar{\alpha}}(h(x + \bar{\alpha}d) - h(x)) \leq \frac{1}{\tau}(h(x + \alpha d) - h(x)).$$

So, the auxiliary function is given by

$$\zeta(\alpha) = n\eta\alpha - (n-1)\ln(1 + \alpha\gamma) - \ln(1 + \alpha\beta), \quad \textit{where} \quad \eta = \frac{1}{n\tau\bar{\alpha}}(f(x + \bar{\alpha}d) - f(x)),$$

then we have the following results:

(i) If $\bar{\alpha} = 1$ and $\widehat{\alpha} > 1$, then $\zeta'(\bar{\alpha}) = 0$.

(ii) If $\bar{\alpha} \neq 1$, then
1. If $\alpha^* \leq \bar{\alpha}$, we must take another $\bar{\alpha} \in]\alpha^*, \widehat{\alpha}[$, for example, we choose $\bar{\alpha} = \alpha^* + \xi(\alpha^* - \widehat{\alpha}),\ \ \xi \in [0, 1]$.
2. If $\alpha^* \geq \bar{\alpha}$, we have $\zeta(\alpha^*) \leq G_2(\alpha^*) \leq G_1(\alpha^*) \leq G(\alpha^*)$.

5.4.3 Minimization of the auxiliary function

We have

$$\zeta(\alpha) = n\eta\alpha - (n-1)\ln(1+\alpha\gamma) - \ln(1+\alpha\beta).$$

We obtain

$$\zeta'(\alpha) = n\eta - (n-1)\frac{\gamma}{1+\alpha\gamma} - \frac{\beta}{1+\alpha\beta}, \quad \zeta''(\alpha) = (n-1)\frac{\gamma^2}{(1+\alpha\gamma)^2} - \frac{\beta^2}{(1+\alpha\beta)^2}.$$

We note that $\zeta(0) = 0,\ \ \zeta'(0) = n(\eta - \bar{y}),\ \ \zeta''(0) = n(\bar{y}^2 + \sigma_y^2) = \|y\|^2$ and we impose that $\zeta'(0) \leq 0$ and $\zeta''(0) \geq 0$. $\zeta'(\alpha) = 0$ is similar to $\eta\gamma\beta\alpha^2 + (\eta(\alpha+\beta) - \gamma\beta)\alpha + \eta - \bar{y} = 0$.

We obtain

$$\alpha^* = \begin{cases} \frac{-\bar{y}}{\gamma\beta} & \text{if } \eta = 0, \\ \frac{\bar{y}-\eta}{\eta\beta} & \text{if } \gamma = 0, \\ \frac{\bar{y}-\eta}{\eta\gamma} & \text{if } \beta = 0. \end{cases} \tag{9}$$

In the case of $\eta\gamma\beta \neq 0$, we have two solutions, we choose only the root α^* that belongs to the domain of ζ, we have

$$\alpha_1^* = \frac{1}{2}\left(\frac{1}{\eta} - \frac{1}{\gamma} - \frac{1}{\beta} - \sqrt{\Delta}\right), \ \ \alpha_2^* = \frac{1}{2}\left(\frac{1}{\eta} - \frac{1}{\gamma} - \frac{1}{\beta} + \sqrt{\Delta}\right),$$

where

$$\Delta = \frac{1}{\eta^2} + \frac{1}{\gamma^2} + \frac{1}{\beta^2} - \frac{2}{\gamma\beta} - \left(\frac{2n-4}{n\eta}\right)\left(\frac{1}{\gamma} - \frac{1}{\beta}\right).$$

We take $\alpha^* \in]0, \widehat{\alpha} - \epsilon[$, where $\epsilon > 0$.

Remark 5.1 The computation of α^* is conducted using a dichotomous procedure under the conditions where α^* is not within the interval $]0, \widehat{\alpha} - \epsilon[$ and $G'(\alpha^*) > 0$.
Take $a = 0$, $b = \widehat{\alpha} - \epsilon$.
While $|b - a| > \epsilon$ do
- $c = \frac{a+b}{2}$.
- If $G'(c) < 0$, then $b = c$ else $a = c$.
This computation ensures an improved approximation of the minimum of $G(\alpha)$ while maintaining adherence to the domain of G.

5.5 The second minorant function

In this context, our aim is to discover another function simpler than G_1, hence we used the following inequality:

$$(\|y\| - n\bar{y})\alpha - \ln(1 + \alpha\|y\|) \leq -\sum_{i=1}^{n} ln(1 + \alpha y_i). \tag{10}$$

From (7) and (10), we take

$$G_3(t) = \frac{1}{\tau}(f(x+\alpha d) - f(x)) + (\|y\| - n\bar{y})\alpha - \ln(1+\alpha\|y\|),$$

where $\alpha \in [0, \widehat{\alpha}[$, it is clear that

$$G_3'(\alpha) = \frac{1}{\tau}\langle \nabla f(x+\alpha d), d\rangle + \|y\| - n\bar{y} - \frac{\|y\|}{1+\alpha\|y\|},\ G_3''(\alpha) = \frac{1}{\tau}\langle \nabla^2 f(x+\alpha d)d, d\rangle + \frac{\|y\|^2}{(1+\alpha\gamma)^2}.$$

The strictly convex function G_3 is a good approximation of G_1 in $]0, \widehat{\alpha}[$ and the unique root $\alpha^*$of $G_3'(\alpha) = 0$ verifies $G_3(\alpha^*) \leq G_2(\alpha^*) \leq G_1(\alpha^*)$.

Because we have $G(0) = G_1(0) = G_2(0) = G_3(0) = 0$, $G_3'(0) = G_1'(0) = G_2'(0) < 0$ and $G_3''(0) = G_1''(0) = G_2''(0) > 0$.

5.5.1 Minimization of an auxiliary function

Let the auxiliary function ζ_2 be defined as

$$\zeta_2(\alpha) = n\eta\alpha + (\|y\| - n\bar{y})\alpha - \ln(1+\alpha\|y\|),$$

we have

$$\zeta_2'(\alpha) = n\eta + \|y\| - n\bar{y} - \frac{\|y\|}{1+\alpha\|y\|}, \quad \zeta_2''(\alpha) = \frac{\|y\|^2}{(1+\alpha\|y\|)^2}.$$

We note that $\zeta_2(0) = 0$, $\zeta_2'(0) = n(\eta - \bar{y})$, $\zeta_2''(0) = \|y\|^2$ and we impose that $\zeta_2'(0) \leq 0$ and $\zeta_2''(0) \geq 0$. The minimum α^* is the root of $\zeta_2'(\alpha) = 0$.

We take $\alpha^* \in [0, \widehat{\alpha} - \epsilon[$, where $G_1'(\alpha^*) < 0$. We use Remark 5.1 to obtain a good approximation for the minimum of $G_1'(\alpha)$ while $\alpha^* \notin [0, \widehat{\alpha} - \epsilon[$.

6 The Algorithm

The algorithm below summarizes the main steps of the proposed method.

Algorithm.

Step 0: (Initialization) Select $x_0 \in \mathcal{L}$, $X_{ii} = (x_0)_i$ and the parameters ρ_s, $\rho \in \mathbb{R}_+^n$, $b \in [0,1]^n$ *and* $\epsilon > 0$.

Step 1: Calculate d and $y = X^{-1}d$.

Step 2:

- If $\|y\| \leq \epsilon$, then we have a good approximation of $\Omega(\rho)$, So if $\|\rho\| \leq \rho_s$, then stop; (We have a good approximation of the optimal solution), otherwise we put $\rho = b \times \rho$ with $b \times \rho = (b_1 \times \rho_1, ..., b_n \times \rho_n)$ and go to the **Step 1.**

- If $\|y\| \geq \epsilon$,

* Compute η, γ, β and calculate $\alpha^* > 0$ using the equation $\zeta'(\alpha) = 0$.

*Put $x = x + \alpha^* d$ and return to the **Step 1**.

End Algorithm.

7 Numerical Experiments

To evaluate the enhanced performance and accuracy of our algorithm, which leverages minorant functions, we conduct numerical tests to compare our new approach with the traditional line search method. In this section, we present comparative numerical tests

using various examples from the literature [12, 13]. The results were obtained by implementing the algorithm in MATLAB on an Intel Core i7-7700HQ (2.80 GHz) machine with 16 GB of RAM. In the following tables, we take $\epsilon = 10^{-4}$. We also note that

- (iter) is the number of iterations.
- (time) is the computational time in seconds (s).
- $(\text{sti})_{i=1,2}$ represents the strategy of approximate functions introduced in this paper.
- (LS) represents the classical line search method.

- **Example 1:** (Erikson's problem [13]).

We consider the following quadratic problem, with $n = 2m$:

$$\zeta = \min\left[f(x) = \sum_{i=1}^{n} x_i \ln\left(\frac{x_i}{a_i}\right) : x_i + x_{i+m} = b, x \geq 0\right],$$

where $a_i > 0$ and $b \in \mathbb{R}^m$ are fixed.

We test this example for the different values of n, a_i and b_i.

The following table resumes the obtained result in the case $(a_i = 2, \forall i = 1, ..., n, b_i = 4, \forall i = 1, ..., m)$.

ex(m,n)	st1		st2		LS	
	iter	time	iter	time	iter	time
30×60	1	0.0009	1	0.0013	3	0.023
150×300	1	0.0035	2	0.0091	4	0.0645
300×600	2	0.0035	3	0.0212	5	3.199
500×1000	2	0.1112	3	0.0987	5	5.324

Table 1: Example of Erikson's problem (with variable size (Example 1)).

- **Example 2:** Quadratic case [12].

We consider the following quadratic problem with $n = m + 2$:

$$f^* = \min\{f(x) : Ax = c, x \geq 0\},$$

with $f(x) = \frac{1}{2}\langle x, Qx\rangle$, $Q[i,j] = \begin{cases} 2 & \text{if } i = j = 1 \text{ or } i = j = m, \\ 4 & \text{if } i = j \text{ and } i \neq \{1, m\}, \\ 2 & \text{if } i = j - 1 \text{ or } i = j + 1, \\ 0 & \text{otherwise,} \end{cases}$

and $A[i,j] = \begin{cases} 1 & \text{if } i = j, \\ 2 & \text{if } i = j - 1, \\ 3 & \text{if } i = j - 2, \\ 0 & \text{otherwise.} \end{cases}$

$f_i = 1 \ \ \forall i, j = 1, .., n$. We test this example for the different values of n.

ex(n)	st1		st2		LS	
	iter	time	iter	time	iter	time
30	5	0.0041	3	0.0053	26	18.3244
400	3	0.0985	1	0.0121	35	60.1003
600	3	9.6544	1	7.0129	23	79.0024
1000	5	11.9912	3	9.0473	33	91.3358

Table 2: Example of Quadratic case (with variable size (Example 2)).

8 Conclusion

In this paper, we introduced a logarithmic barrier method for solving nonlinear programming. Based on some new minorant functions and secant technique, this method calculates the step length in a straightforward manner. The numerical simulations demonstrate the efficacy of our approach as a significant alternative, yielding promising outcomes when compared to traditional line search methods. Exploring new approximate functions presents a promising direction for future research in various classes of optimization. We plan to apply our key findings to a range of issues in nonlinear dynamics problems.

Acknowledgment

The authors extend their appreciation to The Directorate General for Scientific Research and Technological Development (DGRSDT-MESRS) under the PRFU project number C00L03UN190120220009, Algeria.

References

[1] M. F. Hassan and E. K. Boukas. Constrained linear quadratic regulator: continuous-time case. *Nonlinear Dynamics and Systems Theory* **8** (1) (2008) 35–42.

[2] J.P. Crouzeix, B. Merikhi, A logarithm barrier method for semidefinite programming. *RAIRO-Operations Research* **42** (2008) 123–139.

[3] A. Djaout, T. Hamaizia and F. Derouiche. Performance Comparison of Some Two Dimensional Chaotic Maps for Global Optimization. *Nonlinear Dynamics and Systems Theory* **22** (2) (2022) 144–154.

[4] B. Fellahi and B. Merikhi, A Logarithmic Barrier Approach Via Majorant Function for Nonlinear Programming. *Journal of Siberian Federal University, Mathematics and Physics* **16** (4) (2023) 528–539.

[5] A. V. Fiacco and G. P. Mccormick. *Nonlinear Programming.* Sequential Unconstrained Minimization Techniques, Wiley, New York, 1968.

[6] K.R. Frisch. *The Logarithmic Potential Method of Convex Programming.* Technical report, University Institute of Economics, Oslo, Norway, 1955.

[7] P. Huard, Resolution of mathematical programming with nonlinear constraints by the method of centers. *In J. Abadie, editor, Nonlinear Programming, North Holland, Amsterdam, The Netherlands*, (1967), 207-219.

[8] T. Herlambang, A.Y.P. Asih, D. Rahmalia, D. Adzkiya and N. Aini. The Effects of Pesticide as Optimal Control of Agriculture Pest Growth Dynamical Model. *Nonlinear Dynamics and Systems Theory* **22** (3) (2022) 281–290.

[9] A. Leulmi, S. Leulmi, Logarithmic barrier method via minorant function for linear programming. *Journal of Siberian Federal University, Mathematics and Physics* **12** (2019) 191–201.

[10] A. Leulmi, B. Merikhi and D. Benterki. Study of a logarithmic barrier approach for linear semidefinite programming. *Journal of Siberian Federal University, Mathematics and Physics* **11** (2018) 300–312.

[11] A. Leulmi. An efficient penalty method without a line search for nonlinear optimization. *Axioms* **13** (3) (2024) 176.

[12] M.Ouriemchi, Résolution de problèmes non linèaires par les méthodes de points intèrieurs,Théorie et algorithmes. Thèse de doctorat, Univeritè du Havre, France, 2006.

[13] E. Shannon. A mathematical theory of communication. *Bell Syst. Tech. J.* **27** (1948) 379–423, 623–656.

[14] H. Wolkowicz and G.P.H. Styan. Bounds for Eigenvalues Using Traces. *Lin. Alg. Appl.* **29** (1980) 471–506.

WORLD SCIENTIFIC PUBLISHING

Series on Advances in Mathematics for Applied Sciences - Vol 93

Mathematical Modelling
Selected Objects and Processes
by
Anatoliy A. Martynyuk *(S. P. Timoshenko Institute of Mechanics, Ukraine)* &
Boguslaw Radziszewski *(Institute of Fundamental Technological Research, Polish Academy of Sciences, Poland)*

This is the first book on the problems of mathematical modeling that combines a generalized approach to the problem of mathematical modeling processes and phenomena in the real world with developing modeling methods in relation to specific objects and processes. Some of the problems discussed here include stability and bifurcation of simplified models of supply and demand, and resultants of various approaches, such as standardization, unification and partial order, data packaging.

CONTENTS
Preface * Model and Modelling, General Remarks * Sets of Numbers and Modelling * Orders, rankings * Average rank methods * Modeling elements, first patterns * Econometric and Economic Models * Coronavirus and other models * Facts about Population Growth, Mathematical Models * Modelling errors * Principle of Comparison in Stability Theory * Stability Analysis of Nonlinear Systems via Matrix-Valued Functions * Stability of Singularly Perturbed Systems via Matrix-Valued Functions* Stability of Stochastic Systems via Matrix-Valued Functions Method * Stability in Models of Real-World Phenomena

Mathematical Modelling: Selected Objects and Processes fulfills the references' needs of pure and applied mathematics, applied physics, industrial engineers, operations researchers, and Upper-level undergraduate and graduate students studying ordinary differential equations, singularly perturbed equations and stochastic equations and its applications.

350pp	Apr 2025	
978-981-12-9065-7	US$138	£125
978-981-12-9067-1(ebook)	US$110	£100

Please send order form to: World Scientific Publishing
USA | Tel: 1-201-487-9655 | E-mail: wspc_us@wspc.com
UK | Tel: 44-20-7836-0888 | E-mail: IPSUK.Customercare@ingramcontent.com
ASIA | Tel: 65-6466-5775 | E-mail: sales@wspc.com
Or buy direct from our secure website: https://doi.org/10.1142/13772

CAMBRIDGE SCIENTIFIC PUBLISHERS

AN INTERNATIONAL BOOK SERIES
STABILITY OSCILLATIONS AND OPTIMIZATION OF SYSTEMS

Advances in Stability and Control Theory for Uncertain Dynamical Systems
Stability, Oscillations and Optimization of Systems: Volume 11
317+xxii pp., 2021 ISBN 978-1-908106-73-5 £60/$80/€67

C. Cruz-Hernández (Ed.)
Department of Electronics and Telecommunications, Scientific Research and Advanced Studies Center of Ensenada (CICESE), Ensenada, México.
A.A. Martynyuk (Ed.)
Institute of Mechanics, National Academy of Sciences of Ukraine, Kyiv, Ukraine
A.G. Mazko (Ed.)
Institute of Mathematics, National Academy of Sciences of Ukraine, Kyiv, Ukraine

This volume presents the latest investigations in stability and control theory for uncertain dynamical systems, incorporating the main engineering applications. The volume consists of 16 chapters containing the results of theoretical research and engineering applications of some uncertain systems and provides new trends for future promising researches. Some issues covered in the volume include:

- stability and control in uncertain systems: optimal design of robust control, generalization of direct Lyapunov method, robust output feedback stabilization and optimization of control systems, optimal control of nonlinear systems over an infinite horizon;
- stability and stabilization in discrete-time systems: stability conditions for discrete-time positive switched systems with delay, quadratic stabilization for nonlinear perturbed discrete time-delay systems, robust output feedback stabilization and optimization of discrete-time control systems, stability of singularly perturbed nonlinear Lur'e discrete-time systems;
- synchronization in dynamical systems: function projective dual synchronization of chaotic systems with uncertain parameters, anti-synchronization and hybrid synchronization of 3D discrete generalized Hénon map, adaptive hybrid function projective synchronization;
- engineering applications: attitude stabilization of a rigid body, adaptive control of continuous bioreactors, wavelet adaptive tracking control, adaptive fuzzy control of nonlinear systems, robust active control for structural systems with structured uncertainties.

The **Advances in Stability and Control Theory for Uncertain Dynamical Systems** may be useful for graduate students and researchers in applied mathematics and physics, control, nonlinear science, and engineering.

CONTENTS: Introduction to the series • Preface • Contributors • An Overview • Stability and Control in Uncertain Systems • Stability and Stabilization in Discrete-Time Systems • Synchronization in Dynamical Systems • Engineering applications • Index

Please send order form to:
Cambridge Scientific Publishers
45 Margett Street, Cottenham, Cambridge CB24 8QY, UK
Telephone: +44 (0) 1954 251283; Fax: +44 (0) 1954 252517
Email: janie.wardle@cambridgescientificpublishers.com
Or buy direct from our secure website: www.cambridgescientificpublishers.com

NAUKOVA DUMKA

MATRIX METHODS FOR THE ANALYSIS AND SYNTHESIS OF DYNAMICAL SYSTEMS

Kyiv: Naukova dumka, 2023, 320 pp. [Ukrainian]
ISBN 978-966-00-1892-1
https://doi.org/10.37863/6103136622-55

A. G. Mazko
Institute of Mathematics, National Academy of Sciences of Ukraine, Kyiv, Ukraine

The book outlines constructive methods for the analysis and synthesis of dynamical systems based on the application of matrix equations and inequalities. The generalizations of the Lyapunov equation are presented in the framework of stability and spectrum localization theory of linear systems. Classical methods for motion stability analysis, modern methods for robust stabilization and optimization of dynamical systems, as well as new approaches to solving generalized H_∞-control problems for continuous and discrete time systems with controllable and observable outputs are presented. Algorithms for estimating and minimizing the weighted damping level of bounded perturbations in standard and descriptor control systems are proposed. The stability theory of positive and monotone dynamical systems is developed. The book is intended for scientists, engineers, PhD students and senior students of the corresponding specialties.

CONTENTS (8 chapters):

Preface • Notation • Matrix equations and inequalities • Stability of dynamic systems • Stabilization and optimization of linear systems • Pseudo-linear control systems • Generalized output-feedback H_∞-control • Discrete-time control systems • Positive and monotone dynamic systems • Addition • Comments and bibliographic pointers • References • Subject index

For more information please check:
https://imath.kiev.ua/monographs/?id=4
https://imath.kiev.ua/monographs/4/monograph.pdf
Contents & Abstract (pdf)